MODELING OF SOIL WATER EROSION: A COMPARISON OF EMPIRICAL AND PHYSICAL APPROACHES IN MEXICO

PALMIRA BUENO HURTADO

Thesis submitted in partial fulfillment of the requirements for the
Doctor in Philosophy in Environmental Engineering

Presented to the University of Ottawa under the auspices of Ottawa Carleton Institute of Environmental Engineering (OCIENE)

University of Ottawa

Preface

No formal approvals were required to conduct this research. This study contributes to the ongoing discussion in soil erosion modeling, a field where empirical and physical approaches both bring valuable insights, yet debate persists about which approach better serves specific contexts. Despite the global use of popular models such as the Universal Soil Loss Equation (RUSLE) and Water Erosion Prediction Project (WEPP), our ability to accurately predict soil erosion is still elusive and this question remains unresolved, keeping soil erosion modeling as relevant as ever. This thesis provides a structured methodology aimed at calibrating and validating these widely used models, creating a practical framework for future research.

The novelty of this study lies in its focus on predicting erosion and sediment yield with limited local data, which contrasts with existing research that often centers on gaged sites. The approach constrained by data availability significantly augments the practical applicability of the developed methodologies, thereby providing a valuable resource for regions with similar data limitations. I acknowledge the contributions of collaborators and co-authors to this research endeavor, while my primary responsibilities encompassed securing funding, executing experiments, and conducting the analysis.

Abstract

Soil erosion is a pressing environmental issue, accelerated by agricultural practices and climate variability, and it poses significant challenges to land productivity and water quality. This thesis investigates soil erosion processes and sediment yield modeling at both hillslope and watershed scales in an arid region of north-central Mexico, using empirical and physical modeling approaches to guide conservation strategies. Three comprehensive studies were undertaken to assess the impact of tillage practices, soil moisture conditions, and the appropriateness of models for estimating erosion.

The first study assessed the impacts of tillage systems and antecedent soil moisture conditions on erosion and runoff under high intensity simulated rainfall. The findings demonstrated that conservation-oriented practices, such as crop residue cover and no-till methods, effectively mitigate erosion and runoff, particularly in conditions characterized by dry soil. The subsequent study compared the Revised Universal Soil Loss Equation (RUSLE) and the Water Erosion Prediction Project (WEPP) models to ascertain the most efficacious approach for predicting erosion on agricultural hillslopes. RUSLE exhibited superior performance compared to WEPP in capturing erosion trends across various treatments, indicating its appropriateness for regional conditions; however, WEPP yielded valuable insights in specific scenarios involving conventional tillage.

The last study expanded the modeling of sediment yield to encompass the watershed scale by employing the Modified Universal Soil Loss Equation (MUSLE) with its parameters sourced from hillslope assessments. An approach utilizing daily water balance, which integrates Actual Evapotranspiration (AET), enabled the model to account for variations in soil moisture, thereby elucidating a nonlinear association between precipitation and sediment

yield. This association demonstrated that sediment yield initially increases to a maximum before attenuating during episodes of extreme rainfall. Despite MUSLE's capability to accurately reflect sediment dynamics, it exhibited a tendency to overestimate sediment yield in the context of intense rainfall events, underscoring the necessity for advanced modeling approaches in semi-arid regions.

This research advances erosion modeling by demonstrating the importance of context-specific model calibration, conservation practices, and the integration of soil moisture dynamics to improve sediment yield predictions. These findings offer practical insights for soil and water conservation in semi-arid environments and contribute valuable data to guide erosion management in similar landscapes.

Acknowledgements

I would like to extend my gratitude to the National Institute for Forestry, Agriculture and Livestock Research (INIFAP, in its Spanish acronym), the National Council for Humanities, Sciences and Technologies (CONAHCYT, in its Spanish acronym), and the Faculty of Engineering, as well as Graduate and Postdoctoral Studies at the University of Ottawa. I appreciate the financial support provided for the research project, living expenses, and the scholarships granted to me during my PhD studies. I would also like to express my sincere thanks to my supervisor, Dr. Ousmane Seidou, for his invaluable guidance and support throughout this journey.

Table of contents

List of tables

List of figures

List of nomenclature

Symbol	Description	Units
A	Soil loss or erosion (in USLE)	Tons per hectare per year
A	Watershed area (in Rational Method)	Square kilometers
AET	Actual Evapotranspiration	Millimeters per day
a_f	Measured soil loss	Tons
a_u	Estimated soil loss for a specific *EI*	Tons per hectare
b	Coefficient of the effectiveness of surface cover	Dimensionless
B_{md}	Above-ground biomass	Kilograms per hectare
B_s	Dry weight of residue	Kilograms per square meter
B_{ur}	Mass density of roots	Kilograms per hectare
B_{us}	Mass density of incorporated residues	Kilograms per hectare
C	Cover Management Factor	Dimensionless
C_{br}	Adjustment factor for buried residue	Dimensionless
C_{br}	Adjustment factor for buried residue	Dimensionless
CC	Canopy cover (fraction of soil surface covered by vegetation)	Dimensionless (0–1)
CEC	Cation exchange capacity	Milliequivalents per 100 grams
C_f	Soil consolidation factor	Dimensionless
Ci	Runoff coefficient or intensity-related parameter	Dimensionless
CN	Curve Number	Dimensionless (0–100)
Cs	Sediment Concentration	Grams per liter
c_{uf}	Impact of soil consolidation	Dimensionless
C_{ur}	Calibration coefficient in PLU	Dimensionless
C_{us}	Calibration coefficient in PLU	Dimensionless
Dc	Detachment capacity by rill flow	Kilograms per second per square meter
Df	Rill erosion rate	Kilograms per second per square meter
Dg	Mean weighted diameter of soil particles	Millimeters
Di	Interrill sediment delivery to rill	Kilograms per second per square meter
EI_{30}	30-minute maximum rainfall intensity erosivity index	Megajoules per millimeter per hectare per hour
ET_0	Potential Evapotranspiration	Millimeters per day
FC	Field capacity	Percentage

Fc	Fraction of vegetation cover at ground level	Dimensionless (0–1)
F_{cd}	Soil fraction covered by canopy	Dimensionless
F_{nozzle}	Adjustment factor to account for sprinklers	Dimensionless
G	Sediment load	Kilograms per second per square meter
GDU	Growing degree units	Celsius
H	Height of vegetation canopy	Meters
I_a	Initial abstraction	Millimeters
I_e	Effective rainfall intensity	Meters per second
K	Soil Erodibility Factor	Tons per hectare per hour per hectare per Megajoule per millimeter
Kef	Hydraulic conductivity for fallow conditions	Millimeters per hour
Ki	Interrill erodibility	Kilograms per second per meter to the fourth power
$Kiadj$	Adjusted interrill erodibility	Kilograms per second per meter to the fourth power
K_{ib}	Baseline interrill erodibility	Kilograms per second per meter to the fourth power
K_{rb}	Baseline rill soil erodibility	Seconds per meter
Ks	Hydraulic conductivity	Millimeters per hour
LS	Topographic Factor (Slope Length and Steepness)	Dimensionless
$M_{t,j}$	Remaining residue biomass	Kilograms per square meter
NSE	Nash-Sutcliffe efficiency index	Dimensionless
OM	Organic matter	Percentage
P	Support Practice Factor	Dimensionless
$PBIAS$	Percent bias	Percentage
PET	Potential Evapotranspiration	Millimeters per day
PLU	Prior Land Use Factor	Dimensionless
Q	Runoff	Cubic meters or Millimeters
qp	Peak discharge	Cubic meters per second
R	Rainfall-Runoff erosivity factor	Megajoules per millimeter per hectare per hour per year
Ra	Solar radiation	Megajoules per square meter per day
R_c	Cumulative rainfall since tillage	Meters
RH_o	Ridge height after tillage	Meters

RH_t	Ridge height at time t	Meters
RR_0	Random roughness promoted by an implement	Meters
RR_i	Random roughness	Meters
RR_{t-1}	Random roughness of previous day	Meters
Rs	Rill spacing	Meters
R_u	Surface roughness	Dimensionless
S	Potential maximum retention	Millimeters
$SALB$	Soil albedo	Dimensionless (0-1)
SC	Surface cover	Dimensionless
SC	Surface cover subfactor	Dimensionless
SDR_{RR}	Sediment delivery ratio depending on random roughness	Dimensionless
SLR	Soil Loss Ratio	Dimensionless
SM	Soil moisture	Percentage
SOM	Soil Organic Matter	Percentage
S_p	Covered area	Dimensionless (0-1)
SR	Surface roughness	Dimensionless
Sy	Sediment yield	Tons
Tc	Sediment transport capacity	Kilograms per second per meter
T_{ds}	Fraction of disturbed soil surface	Dimensionless (0-1)
Vf	Fall velocity of sediments	Meters per second
vfs	Fraction of very fine sand	Dimensionless
w	Rill width	Meters
WP	Wilting point	Percentage
$\varnothing$	Slope angle	Radians
α	Ratio of covered area	Dimensionless
β	Rill to interrill erosion ratio	Dimensionless
γ	Nonlinearity exponent	Dimensionless
δ	Crop-specific canopy coverage factor	Dimensionless
ε	Canopy cover effectiveness factor	Dimensionless
θ	Slope angle radians	Radians
λ	Horizontal projection of the plot length	Meters
π	Constant pi	Dimensionless
ρ	Soil bulk density	Kilograms per cubic meter
σ	Interrill runoff rate	Meters per second
τ_{cb}	Critical shear stress	Pascals

ϕ	Latitude	Radians
ω_s	Sunset hour angle	Radians

CHAPTER 1. Introduction

1.1. Background

Soil water erosion is the process by which raindrops cause soil detachment and subsequent transport by runoff. It eventually promotes soil deposition elsewhere in the landscape. Soil erosion is a natural process, but it may be exacerbated by anthropogenic activities such as agriculture, construction, mining, etc.

There are negative and positive effects caused by soil erosion. The zones of long-term soil accumulation are usually the most fertile lands while the eroded zones have lower fertility and capacity for supporting life. The soil accumulation also alters fish spawning areas and promotes pollution of waterways with agrochemicals. With regard to eroded areas, the soil productivity decreases because the removal of the upper layer, which contains the highest organic matter content, and the decrement of root growth as the soil layers get thinner. Soil erosion also affects the capture and release of greenhouse gases, but the amount of gas involved is still unknown (FAO, 2019).

Globally, soil losses due to water erosion are estimated at 20-30 Gt yr^{-1}. A typical erosion rate is 10-20 t ha^{-1} yr^{-1} in hilly croplands under conventional agriculture and temperate climate, 50-100 t ha^{-1} yr^{-1} in tropical and subtropical zones (FAO and ITPS, 2015). Economic losses related to soil erosion were estimated to be around $44 billion each year in the U.S. (Pimentel et al., 1995). In the European Union, the agricultural lands with severe erosion lose 0.43% of their crop productivity annually. The annual cost of such reduction is EUR 1.25 billion (Panagos et al., 2018). These losses were calculated by summing income losses resulting from lower production and cost increments due to the replacement of nutrients lost by fertilizers (FAO, 2019).

In the United States, soil erosion investigations started in the 1930s after farmers noticed yield depletion on their most valuable crops, corn and cotton (Bennett, 1931). Fertilizer application increased rapidly in the 1940s as farmers tried to increase yields, leading with increased crop production costs (Cao et al., 2018). At that time, soil conservation practices started, but there was a lack of knowledge about which methods were most beneficial.

Systematic measurements in field plots and erosion modeling began to gain popularity as researchers tried to address that lack of knowledge. After several years of soil erosion measurements in the United States, the first mathematical relationship between soil erosion and slope was published by Zingg (1940). The earlier objectives of erosion modeling were soil detachment prediction by rainfall and runoff and soil loss estimation in certain areas.

Soil erosion models are categorized according to their spatial scale or to the erosion process simulated. Plot or field-scale models usually consider detachment and exclude transport and deposition, while catchment, province, and country scale models consider detachment, transport, and deposition (Jetten and Maneta, 2011). Soil erosion models, based on how the process is simulated, can be classified as empirical, conceptual, or physical based. Empirical models rely on statistical relationships obtained from many field observations, while physical models consider the process itself and attempt to describe the complex interactions between the components. Conceptual models take an intermediate approach between empirical and physical (Patil, 2018). Today, most erosion models use a mixture of empirical and physical approaches. Examples of physically-based models are the Water Erosion Prediction (WEPP), the European Soil Erosion Model (EUROSEM), the Limburg Soil Erosion Model (LISEM), and Pan European Soil Erosion Risk Assessment (PESERA) (Alewell et al., 2019). One of the most known empirical model is the Universal Soil Loss Equation (USLE) and its revised version (RUSLE). Some examples of models based on USLE are the Soil and Water Assessment Tool (SWAT), the Agricultural non-point source Pollution Model (AGNPS), Water and Tillage Erosion, and Sediment Model (Watem/Sedem), and the Chinese Soil Loss Equation (CSLE).

The USLE-type models are widely used because of their parsimonious parametrization, they are flexible, and their inputs are easily accessible. USLE-type models are also covered by an extensive literature that provides a comparison base for the results. However, USLE-type models have significant limitations: their application to different locations from where it was initially developed requires the generation of local values, a time-consuming process that requires data collection (Alewell et al., 2019). Physically-based models are hard to parametrize as they generally need many parameters not usually measured, one advantage is that their use is not limited to a particular region (Alewell et al., 2019).

The main criteria for selecting an erosion model are the study's scale, data availability, model uncertainty, the number of parameters required (Nearing, 2013). The scale of the study can be referred to as *onsite*, *offsite*, or both. *Onsite* refers to soil loss at the plot level, while *offsite* is related to sediment yield at the catchment level.

The current study focuses on Mexico, where 76% of the total country area is affected by water erosion. Erosion is significant on agricultural lands in semi-arid regions, where rainstorms are especially harmful due to high intensities and low soil organic matter. Additionally, long periods without rain promote the prevalence of loose soil on surfaces with a poor structure, summarizing, the area is very susceptible to soil erosion by water; in this case, modeling is useful for evaluating different tillage practices and impacts on soil erosion.

1.2. Thesis objective

The general objective is to evaluate and compare the performance of empirical and physical soil erosion models under various tillage practices and antecedent soil moisture conditions at the hillslope scale, and to apply the best-performing model to predict sediment yield at the watershed scale in an arid region of Mexico.

1.3. Hypothesis

- Soil management practices influence soil water erosion and runoff differentially.
- Physical and empirical models have different performances when predicting soil erosion by water.
- Some parameter values in both empirical and process-based models are not adequate for the Mexican context and need to be improved.

1.4. Methodology

The current research focuses on both hillslope and watershed scales. Measurements collected at the hillslope scale were used to calibrate and validate the model parameters, which were then applied to the watershed scale. The key application steps are summarized as follows:

- Perform a critical review of relevant soil erosion methods.
- Process field measurements and collect data at the hillslope scale.
- Setup and calibrate the models.
- Compare and analyse model performance.
- Propose improvements to parameter estimation and equations if needed.
- Assess the impact of different scenarios on soil erosion.
- Select appropriate scenarios and parameters for sediment yield estimation at the watershed scale.

1.5. Thesis organization

This thesis is organized to explore soil erosion research, assess the impacts of soil management on erosion, compare empirical and physical modeling approaches at the hillslope scale, and apply sediment yield modeling at the watershed scale. Chapter 2 presents the novelty of the study, outlining the unique contributions of this research. Chapter 3 provides a comprehensive literature review on soil erosion and sediment yield modeling. Chapter 4, "Impacts of soil moisture and tillage on short-term erosion under high-intensity simulated rainfall," examines the effects of different tillage systems and antecedent soil moisture conditions on runoff and erosion. Chapter 5, "Empirical and physical modeling of soil erosion in agricultural hillslopes," compares the performance of the Revised Universal Soil Loss Equation (RUSLE) and the Water Erosion Prediction Project (WEPP) models and has been published in the Journal of Hydrology and Hydromechanics (DOI: 10.2478/johh-2024-0017). Chapter 6, "Sediment yield modeling: linking hillslope and watershed analysis," applies the Modified Universal Soil Loss Equation (MUSLE) at the watershed scale using parameters derived from hillslope data. Finally, Chapter 7 presents the conclusions of this research.

CHAPTER 2. Novelty of the study

This thesis presents a novel approach to sediment yield and erosion modeling by adapting USLE-type models to the unique challenges of semi-arid, data-scarce regions. While traditional studies often rely on single-scale analysis (Prado-Hernández et al., 2017; Alberto Ramos Castillo and Orozco Medina, 2020; Gutierrez-Lopez et al., 2021), this research bridges hillslope and watershed scales, enhancing the accuracy and applicability of sediment yield predictions. In our second paper, we conducted a comparative analysis of empirical and physical erosion models on agricultural hillslopes. This analysis provides a valuable framework for model selection based on specific land management practices and environmental conditions, showcasing the performance and applicability of models like USLE and WEPP across different scales and contexts. Our third paper further builds on this work by linking hillslope data directly to watershed-scale predictions. By creating an adaptable framework for sediment yield modeling in ungauged basins, this study advances the capacity for accurate erosion prediction in data-limited areas. Additionally, by integrating daily adjustments for Potential Evapotranspiration (PET) and Actual Evapotranspiration (AET) within the MUSLE model, we refined soil moisture and runoff estimations, a novel step that enhances model precision, particularly under extreme rainfall conditions.

Overall, this research extends the application of established models to new, challenging contexts and offers essential insights for erosion control and watershed management in semi-arid environments.

CHAPTER 3. Literature review

3.1. Soil erosion in Mexico

Soil erosion is a significant problem in Mexico. SEMARNAT-CP (2003) found that 45% of the country is subject to anthropogenic soil degradation, 12% of which is soil water erosion. Avedoy (2004) reported that 37% caused by soil water erosion. González et al. (2016) used satellite maps and field observations to demonstrate that 76% of Mexico's total area is affected by water erosion, of which 6.79% presents extreme erosion, 5.79% strong erosion, 26.37% moderate erosion, and 37.06% low erosion.

Agricultural lands represent 45% of the total area affected by soil erosion, leading to a substantial crop yield reduction. For example, corn yield reduction is around three or four tonnes per hectare after three years of low soil water erosion (Contreras-Hinojosa et al., 2005; Campbell and Berry, 2008). Cotler et al. (2011) found that in Mexico, the cost of soil losses is around US$ 16.2 to US$ 32.4 per hectare, while the replacement of the lost nutrients is US$ 22.1 per hectare.

The Mexican government initiated early conservation practices in the 1940s by establishing the first two soil conservation districts. A few years later, the soil and water conservation law was promulgated to promote practices such as terracing, tree replanting, contour plowing, crop rotation, and watershed management (Simonian, 1995). Nowadays, agricultural lands' primary soil conservation practices are crop rotation, the addition of organic matter, and intercropping (Cotler and Cuevas, 2019). The area under conservation practices is estimated at around 22800 ha in 2008/09 and 41000 ha in 2013 (Friedrich et al., 2017).

3.2. Soil erosion modeling

The earlier objectives of erosion modeling were soil detachment prediction by rainfall and runoff and soil loss estimation in certain areas. Soil erosion models can be classified according to their spatial scale or according to how the erosion process is simulated. Plot or field-scale models usually consider detachment and exclude transport and deposition, while catchment, province, and country scale models consider detachment, transport, and deposition (Jetten and Maneta, 2011). Soil erosion models can also be classified as empirical, conceptual, or physical based on how the process is simulated. Empirical models rely on statistical relationships obtained from many field observations, while physical models consider the process itself and attempt to describe the complex interactions between the components. Conceptual models take an intermediate approach between empirical and physical (Patil, 2018). There are various tools available to evaluate the quantity of soil eroded, test the mitigation practices, and estimate climate change effects. Today, most erosion models use a mixture of empirical and physical approaches. Recent studies focused on physical-based models such as the Water Erosion Prediction (WEPP), the European Soil Erosion Model (EUROSEM), and the empirical Universal Soil Loss Equation (USLE) and its revised version (RUSLE). RUSLE is the most widely applied model around the world. Some examples of well-known models based on USLE are the Soil and Water Assessment Tool (SWAT), the Agricultural non-point source Pollution Model (AGNPS), Water and Tillage Erosion, and Sediment Model (Watem/Sedem), and the Chinese Soil Loss Equation (CSLE). Examples of physically-based models that do not use the USLE are the already mentioned WEPP and EUROSEM, the Limburg Soil Erosion Model (LISEM), and Pan European Soil Erosion Risk Assessment (PESERA) (Alewell et al., 2019). USLE-type models are widely used because of their parsimonious parametrization. They are flexible, and their inputs are easily accessible. USLE-type models are also covered by an extensive literature that provides a comparison base for the results. However, USLE-type models also have significant limitations: for example, their application to locations different from where it was initially developed requires the generation of local equations/parameter values, a time-consuming process that requires data collection (Alewell et al., 2019). Physically-based models are hard to parametrize as they generally need many parameters not usually measured. Their advantage is that their use is not limited to a particular region, as these kinds of models are, in principle, universal and can be applied everywhere (Alewell et al., 2019).

The main criteria for selecting an erosion model are the study's scale, data availability, model uncertainty, the number of parameters required included (Nearing, 2013). The scale of the study can be referred to as *onsite*, *offsite*, or both. *Onsite* refers to soil loss at the plot level, while *offsite* is related to sediment yield at the catchment level. Table 3-1 lists some of these criteria for popular erosion modeling methods.

Table 3-1. Description of common soil water erosion models (Nearing, 2013)

Model	Approach	Target	Scale	Output
USLE (1960)	Empirical	Conservation planning	Onsite	Average annual erosion rate (Mg ha-1 year-1)
RUSLE (1991)	Combined	Conservation planning	Onsite	Average annual erosion rate Rill Deposition (last version in 2003)
MUSLE (1975)	Empirical	Conservation planning	Offsite	Sediment yield (t)
WEPP (1995)	Mainly physical	Agricultural management practices	Onsite and Offsite	Hillslope: Rill and interrill erosion Net soil loss Net deposition Watershed: Channel erosion Deposition Deposition in impoundments
LISEM (1996)	Physical	Conservation planning	Onsite and Offsite	Splash detachment (Interrill) Flow detachment Deposition

				(Rill) Sediment yield
CREAMS (1980)	Combined	Nonpoint-source pollution Agricultural management systems	Onsite	Interill Rill Deposition Pesticide and nutrient component

The models selected in this study are USLE-type models and WEPP because there are many studies conducted with these models. Another significant advantage is that both models have routines to estimate soil erosion onsite or hillslope and sediment yield offsite or downstream.

3.2.1. USLE-type models

The USLE (Universal Soil Loss Equation) was developed in 1960 to estimate sheet and rill erosion in agricultural lands and has since been widely used worldwide. The USLE model calculates long-term average annual soil erosion (Patil, 2018). The USLE was derived from studies in field plots and small watersheds (Wischmeier and Smith, 1978).

$$A = R * K * L * S * C * P \qquad \text{Eq. 3-1}$$

In equation 3-1, A is the annual average soil erosion (Mg ha^{-1} $year^{-1}$); R is the rainfall-runoff erosivity factor (mm h^{-1} ha^{-1} $year^{-1}$); K is the soil erodibility factor (Mg h^{-1} MJ^{-1} mm^{-1}); L is the slope length factor (dimensionless); S is the slope steepness factor (dimensionless); C is the land cover and management factor (dimensionless), and finally P is the soil conservation or prevention practices factor (dimensionless).

The RUSLE equation uses the same formulation, but the methods used to calculate the factors are different. The calculation of R also considers flat slopes, ponded water, thawing, snow, and partly frozen soil. The K factor in USLE is obtained using a nomograph. In contrast, an alternative method is used in RUSLE, which considers the soil particles' diameter, the seasonal variability of the K factor, and rocks' effect. The calculation of the L factor in RUSLE uses an improved method for selecting slope length. The estimation of the slope steepness is improved too. The topographic effect is better-described thanks to a slope steepness relationship for short slopes and interill erosion. The C factor in RUSLE is calculated using an equation that considers canopy, surface cover, and surface roughness. The P factor encloses new ways to calculate contouring and terracing and now considers strip cropping (Renard et al., 1991).

The first version of RUSLE (known as RUSLE1) has evolved to RUSLE1.06c, which assumes a constant value for the K factor. The last version of RUSLE is RUSLE2, which generates daily erosion. The daily erosion is summed to obtain average annual erosion (Foster et al., 2003).

Another USLE-type model is the Modified Universal Soil Loss Equation (MUSLE), where a runoff factor replaces the rainfall factor R. The equation was developed from storm-runoff events in small watersheds (15 to 1500 ha) by Sadeghi et al. (2014)

$$S_y = a(Q'q_p)^b K * LS * C * P \qquad \text{(Eq. 3-2)}$$

S_y is the sediment yield in tons, Q is the volume of runoff in m^3, q_p is the peak flow rate in m^3 s^{-1}, and the other components of the equation are already defined in equation 3-1. a and b are location coefficients that can be optimized according to location

3.2.1.1. Rainfall and runoff factor (R)

Field data collected in agricultural lands suggest a direct relationship between soil losses and the energy of the storm (E) multiplied by the maximum intensity in 30 minutes (I_{30}). Therefore, the R factor should consider the raindrop impact and runoff rate associated with such rainfall events. The energy of a storm is a function of the amount of rain and its intensity; thus, it is function of the size of rainfall drops, which increases with greater intensities; at the same time, the larger the drop, the greater its velocity. Using the kinetic energy equation ($e=mv^2/2$), it can be demonstrated that the energy of a given mass in motion is proportional to the squared velocity and that there is a linear relation between rainfall energy and its intensity. The following relations were derived from observed data by Renard et al. (1997):

$$e_m = 0.119 + 0.0873 \log_{10} i_m \qquad i_m \leq 76 \text{ mm . h}^{-1} \quad \text{(Eq. 3-3)}$$

$$e_m = 0.283 \qquad i_m > 76 \text{ mm. h}^{-1} \quad \text{(Eq. 3-4)}$$

Where e_m is the kinetic energy (MJ ha^{-1} mm^{-1}), i_m is the intensity (mm h^{-1})

The equation of the R factor in RUSLE is presented below: (Renard et al., 1997b).

$$R = \frac{\sum_{i=I}^{j} (EI_{30})_i}{N} \quad \text{(Eq. 3-5)}$$

Where R is the rainfall erosivity (MJ mm^{-1} ha^{-1} h^{-1} $year^{-1}$); N is the number of years of observations; E is the kinetic energy (MJ ha^{-1}), and I_{30} is the maximum intensity in 30 minutes for storm i, j is the number of storms in N years.

Seasonal variations of EI should be accounted, another special consideration to take into account is that the ten-year frequency storm EI value is required to calculate the P factor for contour farming. Also, some modifications in snow or air-mass thunderstorm conditions should be considered (Renard et al., 1997b).

3.2.1.2. Soil Erodibility Factor (K)

This factor represents the effect of soil properties and soil profile on soil loss. The best way to obtain the K factor is from direct measurements on natural runoff plots, accounting for antecedent soil moisture, soil surface conditions and rainfall (Romkens et al., 1997).

An extensive database of observations (usually two years, according to Romkens et al., 1997) has to be collected to estimate the K factor under natural rainfall. The experimental plot should be tilled immediately before the observation period, and the topography of the study area should be uniform. Renards et al. (1997) attempted to relate the soil properties to the K factor. These attempts led to the soil-erodibility nomograph that considers silt, sand, organic matter, structure, and permeability. For soil containing less than 68% of silt, Keppel et al. (2002) proposed an algebraic approximation in SI (t ha^{-1} h^{-1}/ha MJ^{-1} mm^{-1}) units of such nomograph:

$$K = 2.766 \cdot M^{1.14} \cdot 10^{-7}(12 - OM) + 4.28 \cdot 10^{-3}(s - 2) + 3.28 \cdot 10^{-3}(p - 3) \quad \text{(Eq. 3-6)}$$

Where *M* (% silt + %very fine sand).(100 minus % clay), *OM* is % of organic matter, *s* is the soil-structure code in soil classification, and *p* is the profile-permeability class.

Another way to obtain the K factor using soil properties is to use the equations proposed by Tetteh et al. (2019) (Eq. 3-7) and Wang et al. (2016) (Eq. 3-8).

$$K = 0.0034 + 0.0387\exp\left[-\frac{1}{2}\left(\frac{\log_{10}(Dg)+1.533}{0.7671}\right)^2\right] \quad \text{(Eq. 3-7)}$$

$$K = 0.0667 - 0.0013\left[\ln\left(\frac{SOM}{Dg}\right) - 5.6706\right]^2 - 0.015\, exp[-28.9589((\log Dg) + 1.827)^2] \quad \text{(Eq. 3-8)}$$

$$Dg = exp(0.01 \cdot \textstyle\sum_{i=1}^{n} f_i \ln m_i) \quad \text{(Eq. 3-9)}$$

Where *Dg* is the geometric mean diameter (mm); *fi* is the weight % of the particle size fraction, *mi* is the arithmetic mean of the particle size (mm), and *n* is the number of particle size fractions; *SOM* is the soil organic matter in %.

It is also possible to calculate the K factor from measured data. The measured soil data is related to modeled soil loss for unit plot conditions (see Eq. 3-10 to 3-12) (Foster et al., 1981).

$$a_u = \frac{a_f}{L_f S_f C_f P_f} \quad \text{(Eq. 3-10)}$$

Where a_u is the estimated soil loss for a specific EI; a_f is the measured soil loss; L_f, S_f, C_f, and P_f are the other factors of USLE for a given plot.

The K factor is the slope of the next equation.

$$a_u = (EI)K \quad \text{(Eq. 3-11)}$$

A K factor could be estimated from:

$$K = \frac{\sum_{j=1}^{n}(a_u)}{\sum_{j=1}^{n}(EI)_j} \quad \text{(Eq. 3-12)}$$

Oher equations focusing on clayey soil, soils of volcanic origin, etcetera are presented in a guide of conservation planning with RUSLE developed by Romkens et al. (1997).

3.2.1.3. Slope length and steepness factors (LS)

LS factor describes the influence of topography on soil erosion, the slope length is "L" and "S" represents the steepness. Slope length is the horizontal distance from the start of overland flow to where soil deposition begins, or runoff becomes concentrated towards a defined stream; Steepness reflects the slope gradient effect on erosion. The standard USLE length and steepness are 22.1 m in length and 1.83 m in width, and a slope of 9%. In general, erosion increases as slope length is greater, but slope steepness promotes more rapid soil losses (McCool et al., 1997).

Soil erosion caused by slope length varies.

$$L = \left(\frac{\lambda}{22.1}\right)^{m} \qquad \text{(Eq. 3-13)}$$

Where 22.1 is the RUSLE unit plot length (m), and *m* is a variable slope-length exponent, λ is the horizontal projection of the plot length.The *m* exponent in equation 3-13 is obtained from the ratio β of rill and interrill erosion (McCool et al., 1997).

$$m = \frac{\beta}{1+\beta} \qquad \text{(Eq. 3-14)}$$

When the soil is moderately susceptible to rill and interrill erosion, then the next expression is used.

$$\beta = \frac{\left(\frac{\sin\theta}{0.0896}\right)}{3(\sin\theta)^{0.8}+0.56} \qquad \text{(Eq. 3-15)}$$

Where Θ is the slope angle (radians).

In agricultural lands, the *m* exponent should increase in soils with high susceptibility to rill erosion.

The slope steepness factor (S) is calculated from equations 3-16 and 3-17 (McCool et al., 1997).

$$S = 10.8\ \sin\theta + 0.03 \qquad s < 9\% \quad \text{(Eq. 3-16)}$$

$$S = 16.8\ \sin\theta - 0.50 \qquad s \geq 9\% \quad \text{(Eq. 3-17)}$$

When the slope Lengths are shorter than 4.5 meters, the following equation is used:

$$S = 3.0\ (\sin\theta)^{0.8} + 0.56 \quad \text{(Eq. 3-18)}$$

The above equations were developed using experimental data. Equation 3-17 assumes that there is no effect of slope steepness on runoff.

The RUSLE manual also explains how to calculate the LS factor in thawing conditions and non uniform slopes (McCool et al., 1997).

3.2.1.4. Cover-management factor (C)

The C factor describes how cropping and management practices influence the soil erosion process. The C factor's final value is obtained from various subfactors: land use, canopy cover, surface cover, roughness, and soil moisture. The proper calculation of the C factor should consider that cropping and management practices are temporally changing. For example, the crop's growth stage will have a specific value of C. First, a soil loss ratio (SLR) is calculated for each period, then each of these values is weighted by EI. The SLR for a particular condition is given in equation 3-19 (Yoder et al., 1997).

$$SLR = PLU \cdot CC \cdot SC \cdot SR \cdot SM \quad \text{(Eq. 3-19)}$$

PLU is the prior land use, *CC* is the canopy cover, *SC* is the surface cover, *SR* is the surface roughness, and *SM* is the soil moisture.

The *PLU* includes the subsurface residual and tillage practices effects from the previous crop.

$$PLU = C_f \cdot C_b \cdot exp\left[(-c_{ur} \cdot B_{ur}) + \left(\frac{c_{us} \cdot B_{us}}{{C_f}^{c_{uf}}}\right)\right] \quad \text{(Eq. 3-20)}$$

Where *PLU* ranges from 0 to 1, C_f is a soil consolidation factor (dimensionless), C_b the effectiveness of subsurface residue in consolidation, B_{ur} is the mass density of roots (kg ha^{-1} cm^{-1}), B_{us} is the mass density of incorporated residues (kg ha^{-1} cm^{-1}), c_{uf} is the impact of soil consolidation, C_{ur} (ha cm^{-1} kg^{-1}) and C_{us} (ha cm^{-1} kg^{-1}) are calibration coefficients.

The disturbed area determines the value of Cf: C_f is 1.0 for a freshly tilled soil and 0.45 for an undisturbed soil. B_u is the biomass density in the topsoil. RUSLE assumes that 80% of the total root biomass is in the first 10 - 20 cm. B_{ur} is obtained by dividing the entire root biomass residue by the mass of soil where such biomass is. B_{us} should be used in case there are residues on the ground that could be incorporated into the soil through tillage activities. The values that describe the relative effectiveness of surface biomass in preventing soil erosion were calculated from experiments; these values are C_b = 0.951, c_{ur} = 0.00199 acres per in per lb, c_{us} = 0.000416 acres per in per lb and c_{uf} = 0.5 (Yoder et al., 1997)

The canopy cover effect is represented by equation 3-21.

$$CC = 1 - F_c \cdot \exp(-0.1 \cdot H) \quad \text{(Eq. 3-21)}$$

Fc is the fraction of area covered by the canopy, and H is the distance that drops have to travel until it reaches the soil after striking the canopy. Default values for several crops can be found in the literature.

The surface cover subfactor SC accounts for everything on soil, such as crop residue, rocks, etc. The effect of SC is given by Eq. 3-22 (Yoder et al., 1997).

$$SC = \exp\left[-b \cdot S_p \cdot \left(\frac{0.24}{R_u}\right)^{0.08}\right] \quad \text{(Eq. 3-22)}$$

Where b is a coefficient of the effectiveness of surface cove. b varies from 0.030 to 0.070 in row crops; S_p is % of covered area, R_u is surface roughness.

The higher the b value, the more significant the rill erosion. Large values of b correspond to steep and/or long slopes. In contrast, the b value decreases if interrill erosion is more significant than rill erosion, common in flat and/or short slopes. b is also influenced by soil texture and soil cover.

The % of covered area by residue is obtained in equation 3-23.

$$S_p = [1 - exp(-\alpha \cdot B_s)] \cdot 100 \qquad \text{(Eq. 3-23)}$$

Where α is the ratio of covered area and the mass of the residue in acre lb^{-1}, B_s is the dry weight of residue on the soil in lb $acre^{-1}$.

The surface roughness is calculated using equation 3-24 (Yoder et al., 1997).

$$SR = exp[-0.66(R_u - 0.24)] \qquad \text{(Eq. 3-24)}$$

Where R_u is the roughness before the tillage operation in inches.

The soil moisture value (SM) is near 1.0 if the water content is close to field capacity. In contrast, a value of 0 indicates that soil moisture is near the wilting point. Lianes Revilla (2008) proposed the following equation for SM

$$SM = \frac{M - WP}{FC - WP} \qquad \text{(Eq. 3-25)}$$

Where M is the soil moisture (dimensionless); WP is the wilting point (%), and FC is the field capacity (%).

There are several approximations to calculate field capacity and wilting point considering the particle sizes of soil; examples are the equations proposed by Smith (1917) for field capacity (Eq. 3-26) and Silva et al. (1988) for wilting point (Eq. 3-27).

$$FC = 0.1(\%\ sands) + 0.15(\%\ silt) + 0.61(\%\ clay) \qquad \text{(Eq. 3-26)}$$

$$WP = FC * 0.74\text{-}5 \qquad \text{(Eq. 3-27)}$$

Once all the SLR's are obtained, equation 3-28 is applied to the data (Yoder et al., 1997).

$$C = \frac{(SLR_1 EI_1 + SLR_2 EI_2 + \cdots SLR_n EI_n)}{EI_t} \qquad \text{(Eq. 3-28)}$$

Where C is the average annual crop value, SLR_i is the crop value per time period, EI_j is the % of EI that occurs in a particular period, n is the number of periods, and EI_t is the sum of EI.

3.2.1.5. Support practice factor (P)

The P factor describes the impact of specific practices on soil loss. The conservation practices modify erosion by changing the amount, pattern, and direction of surface runoff. Conservation practices in agricultural lands include contouring, strip cropping, terracing, and subsurface drainage (Foster et al., 1997).

3.2.2. USLE-type models application in Mexico

Most of the studies using USLE-type models in Mexico focus on soil use and land cover management. Most at the catchment and country scales used GIS tools to estimate soil erosion. Flores-López et al. (2003) applied GIS to estimate potential erosion, current erosion, and tolerable erosion in Jalisco's state at the watershed scale using USLE. They obtained satisfactory results but concluded a need for a better calculation of factor L to avoid overestimation. They also pointed out the need to estimate the local values of the K factor. Ramírez-León (2009) estimated sediments loss using SDR (Sediment Delivery Ratio) and USLE; the Monte-Carlo method is proposed to estimate the R factor; the results were compared with sediments in dams, and the error varied from -32.03% to 235.11%. Montes-León et al. (2011) studied the potential erosion in all Mexican territory; the results showed that 64% of the total country area is affected by extreme soil water erosion with more. Pedraza-Villafaña (2015) determined potential and current soil water erosion using two methods based on USLE in the Chapingo river watershed and found that the two methods yield similar results. Prado-Hernández et al. (2017) calibrated the USLE and MUSLE on a silty clay loam soil and found that MUSLE fitted observations relatively well, but not USLE; the calibration procedure was focused on factor K, and a final value of 0.1067 was obtained. Aguirre-Salado et al. (2017) identified potential sites for ecological restoration using USLE and multi-criteria decision analysis in San Luis Potosí, México; the authors concluded that the methodology was useful for planning forest restoration. González-Morales et al. (2018) assessed soil erosion to find mitigation practices and appropriate locations for these practices in Chiapas. Bolaños-González et al. (2016) developed a soil water erosion map for all the Mexican territory and estimated soil organic carbon losses due to erosion. They found that 76% of the country is affected by soil water erosion. 6.79% of the country is affected by extreme erosion, 5.79% by strong erosion, 26.37% by moderate erosion, and 37.06% by low erosion. López-García et al. (2020) estimated soil erosion applying USLE and GIS in Puebla; the authors found four classes of soil erosion risk were identified, the most of the area was under low risk of erosion (less than 23 t ha^{-1} $year^{-1}$).

3.2.3. WEPP

The USDA (United States Department of Agriculture) developed WEPP, a process-based model focusing on erosion prediction on hillslopes and watersheds. WEPP includes stochastic weather generator and explicitly accounts for processes in hydrology, soil physics, plant science, hydraulics, and erosion mechanics. The hillslope processes include rill and interrill erosion; sediment transport and deposition; infiltration; soil consolidation; residue and canopy effects; surface sealing; rill hydraulics; surface runoff; plant growth; residue decomposition; percolation; evaporation; transpiration; snowmelt; frozen soil effects on infiltration and erodibility; climate; tillage; effects on soil properties; and finally, the impact of random soil roughness, and contour effects. The watershed model considers channel detachment, sediment transport, and deposition (Flanagan et al., 1995).

3.2.3.1. Hillslope erosion

The erosion and deposition processes on a hillslope are described in two ways: interrill erosion and rill erosion. Interill erosion is caused by raindrops and consists of soil particle detachment, transport, and deposition. Rill erosion occurs when hydraulic shear stress is greater than critical shear stress, and sediment load is less than sediment transport capacity. The WEPP hillslope erosion model calculates rill erosion by solving a steady sediment continuity equation (Eq. 3-29) (Foster et al., 1995).

$$\frac{dG}{dx} = D_f + D_i \quad \text{(Eq. 3-29)}$$

Where x is the downslope distance (m); G is the sediment load (kg s^{-1} m^{-1}); D_i is the interrill sediment delivery to rill (kg s^{-1} m^{-2}), and D_f is the rill erosion rate in (kg s^{-1} m^{-2}).

Rill erosion in a hillslope is described in WEPP by Eq. 3-30 (Foster et al., 1995).

$$D_f = D_c \left(1 - \frac{G}{T_c}\right) \quad \text{(Eq. 3-30)}$$

Dc is detachment capacity by rill flow (kg s^{-1} m^{-2}) and Tc is the sediment transport capacity (kg s^{-1} m^{-1}).

Soil deposition in a rill occurs when sediment load is greater than sediment transport capacity. The model calculates this soil deposition using Eq. 3-31 (Foster et al., 1995).

$$D_f = \frac{\beta V_f}{q}(T_c - G) \quad \text{(Eq. 3-31)}$$

Where V_f is the effective fall velocity of sediments (m.s^{-1}); q is the flow discharge per unit width (m^{2}s^{-1}) and β is a coefficient of raindrop turbulence.

The interrill delivery process is modeled using the assumption that it is proportional to the product of rainfall intensity and interrill runoff rate. Interrill delivery rate is estimated using equation 3-32 (Foster et al., 1995).

$$D_i = K_{iadj} I_e \sigma_{ir} SDR_{RR} F_{nozzle} \left[\frac{R_s}{w}\right] \quad \text{(Eq. 3-32)}$$

In the above model, K_{iadj} is the adjusted interrill erodibility; I_e is the effective rainfall intensity (m.s^{-1}); σ_{ir} is the interrill runoff rate (m.s^{-1}); SDR_{RR} is a sediment delivery ratio depending on random roughness, the row side-slope, and the interrill sediment particle size distribution; F_{nozzle} is an adjustment factor to account for sprinklers; in case irrigation is applied, R_s is the rill spacing (m) and w is the rill width (m).

3.2.3.2. Residue decomposition WEPP

The decomposition of residues is estimated for flat residues, standing material, submerged residues, and dead roots. To simulate the process of decomposition, WEPP uses equation 3-33 (Stott et al., 1995).

$$M_{t,j} = M_{t-1,j} e^{ENVIND_j \cdot ORATE_j \cdot PSZIND_j \cdot FERIND_j} \quad \text{(Eq. 3-33)}$$

Where $M_{t,j}$ is the remaining residue biomass per unit area (kg m^{-2}) and $M_{t-1,j}$ is the residue biomass remaining the previous day (kg m^{-2}), both for the type of residue j, ENVIND is an environmental factor, ORATE is a decomposition constant for a specific type of residue, FERIND is a soil fertility index, and PSZIND is an index for residue size (Stott et al., 1995).

Equation 3-33 is applied for any type of residue as standing, flat, buried or dead roots.

3.2.3.3. Soil

The soil parameters of WEPP model include random roughness, oriented soil roughness, bulk density, wetting-front suction, hydraulic conductivity, interrill erodibility, rill erodibility, and critical shear stress.

The random soil roughness after a tillage operation is calculated in equation 3-34 (Alberts et al., 1995).

$$RR_i = RR_o T_{ds} + RR_{t-1}[1 - T_{ds}] \qquad \text{(Eq. 3-34)}$$

Where RR_i is the random roughness (m), RR_o is the random roughness promoted by an implement, RR_{t-1} is the random roughness of the previous day, T_{ds} is the fraction of disturbed soil surface.

Ridge height decay is predicted with equation 3-34 (Alberts et al., 1995).

$$RH_t = RH_o e^{-C_{br}\frac{[R_C]^{0.6}}{b}} \qquad \text{(Eq. 3-34)}$$

In the above equation, RH_t is the ridge height (m) at time t; RH_o is the ridge height after tillage (m); C_{br} is an adjustment factor for buried residue; R_c is the cumulative rainfall since tillage in (m); and b is an adjustment coefficient for random roughness.

Another important parameter related to infiltration and soil compaction is bulk density, calculated using the following equation (Alberts et al., 1995).

$$\rho_t = \rho_{t-1} - \left[[\rho_{t-1} - 0.667\rho_c]T_{ds}\right] \qquad \text{(Eq. 3-35)}$$

Where ρ_t is the bulk density after tillage (kg m^{-3}); ρ_{t-1} is the bulk density before tillage (kg m^{-3}); ρ_c is the consolidated soil bulk density (kg m^{-3}) at 0.033 MPa, T_{ds} is the fraction of soil surface disturbed.

A significant value for soil erosion simulation in WEPP is interrill erodibility, which is obtained from field experiments using Eq. 3-36 and Eq. 3-37, both for croplands (Alberts et al., 1995).

$$K_{ib} = 272800 + 19210000vfs \qquad >30\% \text{ of sand} \qquad \text{(Eq. 3-36)}$$

Where K_{ib} is the baseline interrill erodibility, *vfs* is the fraction of very fine sand.

$$K_{ib} = 6054000 - 5513000clay \qquad <30\% \text{ of sand} \quad \text{(Eq. 3-37)}$$

In the above equation, *clay* represents the fraction of clay.

The WEPP model calculates rill erodibility using equations derived from field experiments. Eq. 3-38 and Eq. 3-39 are used for soils containing 30% or more of sand, while Eq. 3-40 and Eq. 3-41 apply to for soil with less than 30% sand (Alberts et al., 1995).

$$K_{rb} = 0.00197 + 0.030vfs + 0.03863e^{-184orgmat} \qquad \text{(Eq. 3-38)}$$

$$\tau_{cb} = 2.67 + 6.5clay - 5.8vfs \qquad \text{(Eq. 3-39)}$$

Where *vfs* is the fraction of very fine sand, *clay* is the fraction of clay, *orgmat* is the fraction of organic matter.

$$K_{rb} = 0.0069 + 0.134e^{-20day} \qquad \text{(Eq.3-40)}$$

$$\tau_{cb} = 3.5 \qquad \text{(Eq. 3-41)}$$

3.2.4. WEPP model application in Mexico

The WEPP model is widely used in Mexico to assess soil erosion under various land use and management practices, providing insights for improving soil conservation and modeling processes.

Larose et al. (2004) tested the hillslope WEPP model for runoff and soil loss under conventional tillage and conservation practices in Veracruz, achieving a Nash-Sutcliffe index of 0.84 and 0.86 for predicted runoff and soil loss, respectively. For conventional tillage, these values were 0.88 and 0.84, indicating strong model accuracy. In Jalisco’s Ayuquila River region, Martínez-Rivera (2004) applied the WEPP model to enhance understanding of local soil erosion dynamics; however, predictions varied across sites, with soil loss underestimated at two locations and overestimated at one, suggesting that WEPP's accuracy may depend on specific site characteristics. Bravo-Espinosa et al. (2006) calibrated erosion parameters in WEPP, identifying interrill and rill erosion values as 774.7 x 10^3 kg s m^{-4} and 0.5 x 10^{-4} s m^{-1}, respectively. Additionally, González-Arqueros et al. (2017) investigated the anthropogenic impact on erosion in the Teotihuacan Valley over three time periods, including the Aztec era and modern times, finding that erosion and runoff were more pronounced during the Aztec period than today.

3.3. Sediment yield modeling

Sediment yield is the mass of sediment that reaches a given point in a watershed. In practice, it is measured considering suspended sediment concentration and bed load (Rai et al., 2017). While soil erosion refers to the process of detachment and movement of soil particles from the land surface, sediment yield represents the portion of that eroded material which actually reaches a downstream point, typically at the outlet of a watershed.

Sediment yield models have evolved to incorporate both empirical and physical approaches for predicting the movement and deposition of eroded material within a watershed. Models like MUSLE, SWAT, EPIC, SEDD, and AnnAGNPS are rooted in the USLE framework, using modifications to incorporate runoff energy, sediment delivery ratios, or spatial variability. These models are effective for estimating sediment yield at various scales, particularly when data availability limits the use of more complex methods. Additionally, GLEAMS applies simplified empirical equations for surface runoff and sediment yield estimation in agricultural systems (Borrelli et al., 2021). On the other hand, physically-based models such as WEPP simulate sediment detachment, transport, and deposition based on hydrological and soil mechanical processes, making them more suited for detailed event-based or continuous sediment yield predictions. Beyond WEPP, models like SHETRAN and DHSVM also take a physically-based approach, accounting for spatial and temporal variations in soil, water, and sediment dynamics. These physically-based models provide more detailed insights into the interactions between land surface processes and sediment movement, making them valuable tools for understanding sediment yield across diverse landscapes (Pandey et al., 2016).

3.3.1. The Runoff Factor in MUSLE

The Modified Universal Soil Loss Equation (MUSLE) is widely recognized for its application in estimating sediment yield. Unlike its predecessor, USLE, which estimates soil loss on an annual basis, MUSLE incorporates runoff data to predict sediment yield on a single event basis. This shift enhances the model's accuracy in areas prone to variable rainfall patterns (Williams, 1975). The basic equation is next:

$$S_y = a\left(Qq_p\right)^b K * LS * C * P \quad \text{(Eq. 3-42)}$$

Where S_y represents sediment yield in t, Q is runoff in m^3, q_p is the peak flow rate in m^3s^{-1}, a and b are constants with default values of 11.8 and 0.56, respectively; 11.8 in the equation is a unit conversion constant, so the resulted sediment yield is in t, and 0.56 is a constaant empirically derived; K is the soil erodibility factor in Mg h^{-1} ha^{-1} MJ^{-1} mm^{-1}; L is the slope length factor (dimensionless), S is the slope steepness factor (dimensionless), C is the land cover and management factor (dimensionless), and P is the soil conservation practices factor (dimensionless).

The idea behind the substitution of runoff-rainfall erosivity (Factor R) by runoff energy factor $a(Qq_P)^b$ was that runoff volume and peak runoff rate have a more direct influence on sediment transport than the amount of rainfall. It reflects the combined effects of water volume flowing over the landscape and the intensity of the flow (represented by the peak runoff rate). The reasoning is that sediment yield is not only dependent on how much water is present but also on how fast it moves, which directly affects its ability to detach, transport, and deposit sediment.

3.3.2. Relevant Applications of MUSLE

Several studies in Mexico have applied MUSLE, demonstrating its effectiveness in storm event predictions and its utility across diverse landscapes for improved land management.

In a study by Prado-Hernández et al. (2017) MUSLE was applied in the El Malacate micro-basin, a 1.5 km^2 area in Michoacán, where forest covers over 60% of the land. The runoff factor in MUSLE was determined using hydrographs measured through a long-throated flume equipped with an ultrasonic sensor. The soil erodibility (K), cover-management (C), and topographic (LS) factors were calculated using default methods. The calibrated K factors of 0.034 and 0.013 led to overestimation, with sediment yields reaching up to 26 tons.

Another study conducted by Velásquez-Valle et al. (2016) applied MUSLE in the La Cruz micro-basin, a 46.8-hectare area in Zacatecas dominated by natural grasslands. Runoff was measured at a monitoring station, while the K factor was determined from ARS (1975) tables based on soil texture and organic matter. The LS factor was derived from a 1:2500-scale topographic map, and the C factor was calculated using the method of Figueroa et al. (1991), accounting for a mean shrub height of 0.5 m, 25% shrub coverage, and 40% basal coverage of pastures. This approach produced sediment yield predictions ranging from 2.5 to 19.5 tons, with strong alignment between observed and simulated values ($r^2 = 0.83$). The calibrated factors used were a K value of 0.24, an LS value of 4.77, and a C value of 0.09.

Galindo et al. (2017) conducted a study in a 7,751 km^2 watershed located in the south of Mexico, Oaxaca, utilizing the Soil and Water Assessment Tool (SWAT) to predict erosion through the MUSLE. SWAT performed a hydrological balance and estimated runoff using the Curve Number (CN2) method, which was assigned based on soil type and vegetation condition. The calibration and validation processes focused on factor P (0.8) and factor C (0.0016 to 0.2), resulting in r^2 of 0.58 and NSE of 0.45.

These studies demonstrate the versatility of MUSLE in varying Mexican landscapes, though they also underscore the need for careful calibration of factors to ensure accurate predictions.

CHAPTER 4. Impacts of soil moisture and tillage on short-term erosion under high-intensity simulated rainfall

Authors: Palmira Bueno Hurtado, Ousmane Seidou, Armando López Santos

Abstract

Soil erosion is a natural process that can be significantly accelerated by anthropogenic activities like agriculture, leading to increased runoff and erosion, causing environmental and economic losses globally. Therefore, incorporating conservation agriculture is crucial. This research aimed to study the effect of tillage practices and antecedent soil moisture conditions (AMC) on both runoff and soil erosion by water in an arid zone of north-central Mexico using simulated rainfall. A randomized complete block design experiment evaluated four tillage treatments: 1) no crop (NC), 2) maize with conventional tillage and crop residues (CTR), 3) maize with conventional tillage (CT), and 4) maize sown by handspike (HS). Two AMC treatments, dry and wet, were also tested. ANOVA showed that dry AMC significantly reduced erosion in HS ($p \leq 0.01$) and CTR ($p \leq 0.05$) compared to wet AMC. Additionally, CT and CTR treatments produced the lowest erosion ($p \leq 0.05$), but only under wet AMC. Similar results were observed for total runoff, where CTR and HS produced the lowest runoff under dry AMC. This underscores the important role of crop residue cover in conventional tillage, and no-tillage cropping in soil erosion prevention, especially when soil is dry.

Keywords: crop residues, no-tillage, runoff, corn, arid lands.

4.1. Introduction

Soil erosion imposes significant economic and environmental burdens, reducing corn yield by up to 65%, soil nitrogen by over 50%, organic matter by 39%, water retention by 7% to 44%, and infiltration by as much as 93%. Economically, replenishing lost water and nutrients in US agricultural lands costs about $27 billion annually, while in India, soil replacement costs $245 million (Pimentel et al., 1995; Nkonya et al., 2016).

While soil erosion is a natural process, human activities like agriculture, construction, and mining accelerate it. Agricultural practices, especially converting native vegetation to farmland and using conventional tillage, worsen erosion. Conventional tillage leads to 56% to 60% more soil loss compared to no-tillage methods. Excessive agrochemical use degrades soil health and pollutes water, while heavy machinery compacts soil, reducing water absorption and increasing runoff. These activities highlight the urgent need for sustainable land management practices (Swaminathan, 2006; Patil, 2018; López-García et al., 2020).

Conventional agriculture in arid and semi-arid regions involves intensive tillage that disrupts soil structure and reduces organic matter, making the soil vulnerable to erosion. This issue is prevalent in regions like the Sahel, the Middle East, South Asia, the southwestern United States, Australia, and southern Europe. (FAO and ITPS, 2015; World Bank, 2019). Poor soil management and lack of vegetation cover exacerbate erosion and runoff, diminishing soil productivity and impacting water quality. Conservation agriculture practices, such as no-tillage and crop residues, can improve soil structure, increase water infiltration, and reduce erosion, promoting sustainable agriculture.

Conservation agriculture mitigates the adverse effects of conventional farming by altering tillage methods and adding crop residues. No-tillage farming enhances water infiltration and reduces runoff, minimizing soil erosion. Crop residues act as protective barriers against raindrop impact, regulate soil temperature and moisture, and create a stable environment for crops. This sustainable approach promotes long-term productivity and environmental conservation (Lal, 1995; Baker and Saxton, 2007).

In Mexico, conservation agriculture covers only 41,000 hectares, but practices like crop rotation, organic matter addition, intercropping, and terracing help mitigate soil erosion, enhance fertility, and improve water retention. Expanding these practices could boost agricultural resilience and productivity (Friedrich et al., 2017; Cotler and Cuevas, 2019). Currently, 52% to 76% of Mexico's land suffers from water erosion, affecting agricultural productivity and food security, especially in states like Chihuahua, Zacatecas, Durango, San Luis Potosí, Tamaulipas, Aguascalientes, Sonora, and Coahuila. Addressing soil erosion through terracing, contour plowing, and cover crops, and promoting no-tillage is crucial for sustainable farming in these regions (Bolaños-González et al., 2016; Cotler et al., 2020).

The objective of this research was to study the effect of agricultural management practices and antecedent soil moisture on soil erosion by water and runoff in an arid zone using simulated rainfall.

4.2. Material and methods

4.2.1. Study site

Seasonal maize was planted on September 11 and 12, 2015, in the Northern Mexican settlement of Santo Domingo, located at 25° 49' 41.94" N and 104° 26' 18.97" W, and at an altitude of 1750 masl (Figure 4-1). The climate of the zone is arid, and the average annual temperature ranges from 14 to 22 °C. The annual rainfall ranges from about 200 to 400 mm. The Reference Soil Group is Leptosol, with a sandy clay loam texture and soil organic carbon content of 0.76%.

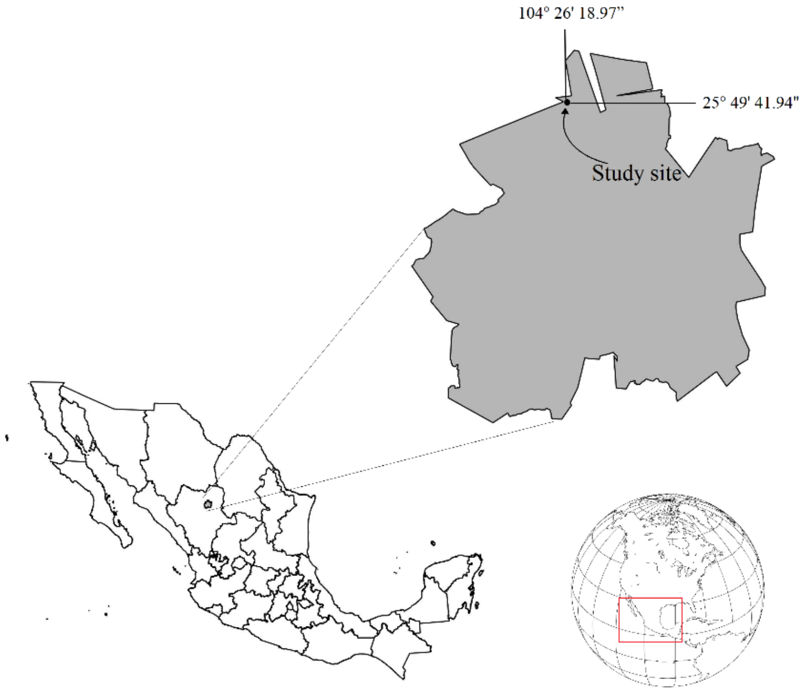

Figure 4-1. Location of the study

4.2.2. Experimental design

The treatments evaluated were dry and wet antecedent soil moisture conditions (AMC) and four tillage systems: 1) No Crop (NC), with no soil and vegetation movement; 2) Conventional Tillage (CT), with moldboard plow followed by harrowing, furrowing, and corn planting; 3) Conventional Tillage + Residues (CTR), which was the same as CT, but with crop residues on the soil surface; and 4) Handspike (HS), which consisted of no soil movement and corn planting using only a wooden stick. The treatments were replicated four times and arranged in a randomized complete block design. The scheme of the experiment is shown in Figure 4-2.

4.2.3. Rainfall simulator

The design of the rainfall simulator was adapted from the Miller (Miller, 1987) experiment (Figure 4-3). It consisted of a water supply tank, a pump with connection to three sprinklers, and three electric solenoid valves. The opening was controlled by a PLC (programmable logic controller) and three 360° spray nozzles. To regulate the flow of water to the valves, pressure was monitored by three manometers. Power was supplied by the spray nozzle of a 5500 watt portable generator producing 110 VAC.

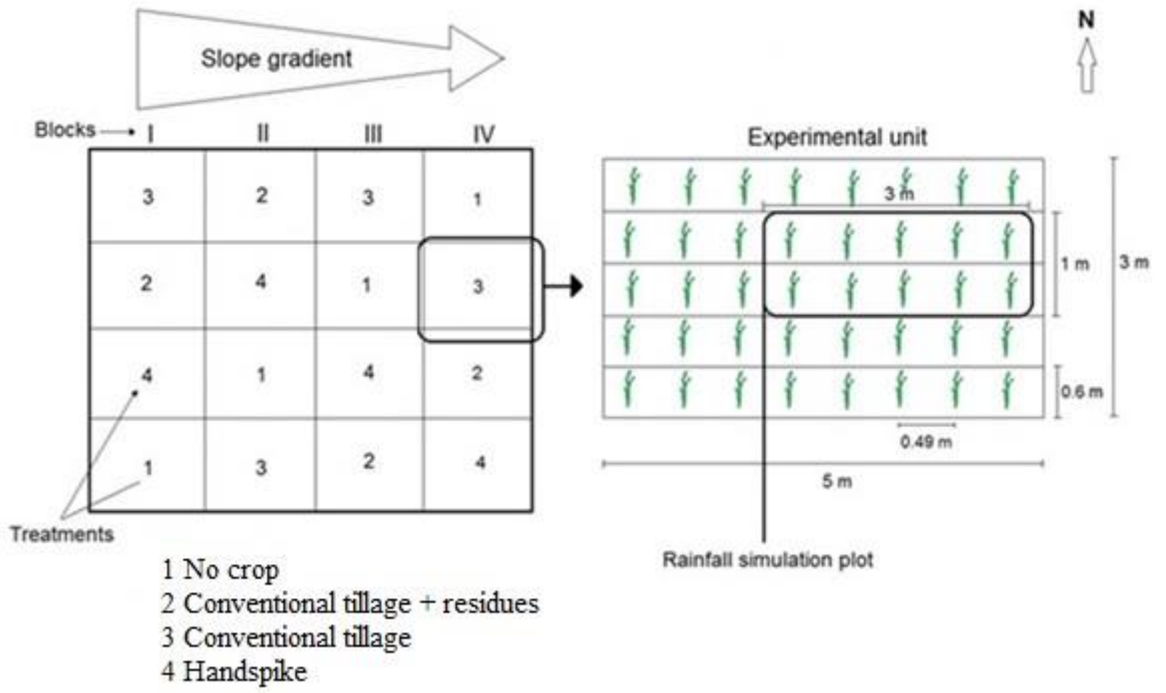

Figure 4-2. Treatment distribution on the experimental plot (left) and dimensions of the experimental unit (right)

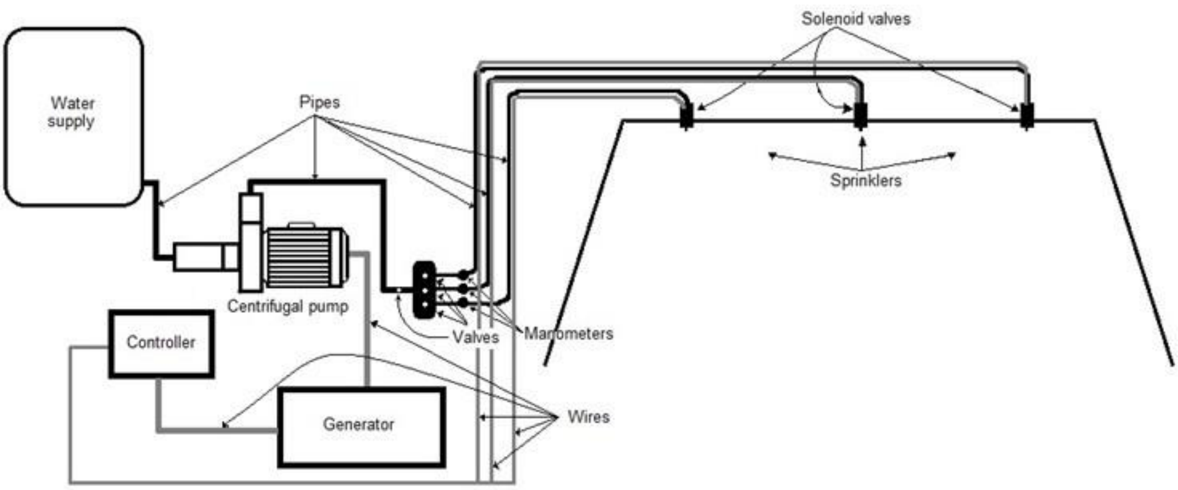

Figure 4-3. Rainfall simulator

At each experimental unit, the simulator operated within a rainfall intensity range of 69 to 172 mm/h and exhibited high spatial variability, as indicated by Christiansen's uniformity coefficient of 38.4% (Figure 4-4).

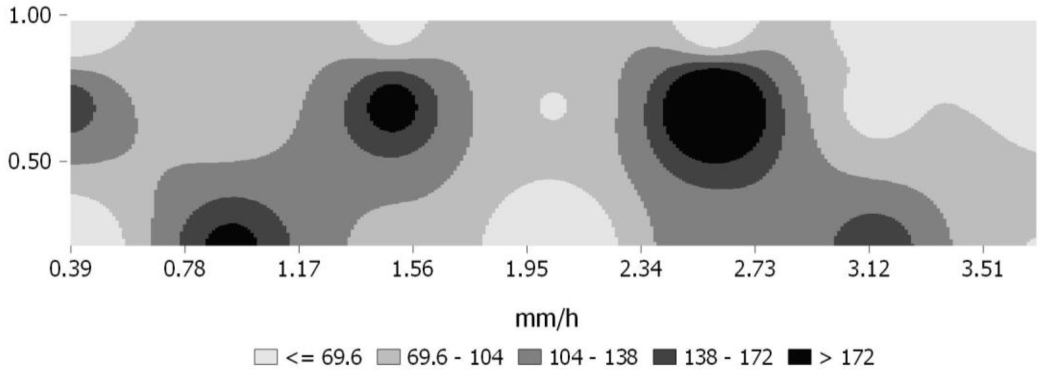

Figure 4-4. Spatial distribution (m) of rainfall intensity induced by rainfall simulator

4.2.4. Rainfall simulation and sampling

Rainfall simulations took place on 1-meter-wide by 3-meter-long plots, surrounded by smooth galvanized sheet barriers and equipped with metal structures to gather surface runoff, from November 11th to 16th, 2015. Each simulation ran for 45 minutes, under varying soil moisture levels, specifically between 16-19% for dry antecedent moisture content (AMC) and 23-25% for wet AMC. The runoff water was captured in 19-liter plastic containers, and its volume was calculated by measuring the water's height and then multiplying this by the container's bottom surface area. To ensure the samples were representative, the collected runoff was stirred every 5 minutes, from which 1-liter samples were then taken. These samples were subsequently filtered and oven-dried at 105°C before their weight was recorded.

4.2.5. Erosion estimation

The experiment should yield 9 samples of soil concentration and several water height measurements (depending on the number of water samples collected). However, some sediment samples were lost, and only water height measurements were collected. The runoff and sediment concentration measured during rainfall simulation are detailed in Table 4-1.

To estimate sediment concentration at points where concentration data could not be collected, we fitted the following equation to data points for each treatment (Table 4-2):

$$C_s = A + Be^{-Ct} \quad \text{(Eq. 4-1)}$$

where *A*, *B* and *C* are parameters to be fitted using the least square method, and *t* is the time step; Once *A*, *B* and *C* are estimated for each treatment, the missing concentrations are estimated using the above equation and used to calculate total erosion inside the time step.

4.2.6. Statistical analysis

We conducted ANOVA tests (at significance levels of $p \leq 0.05$ or $p \leq 0.01$) to detect differences in cumulative soil erosion, erosion rate, total runoff and runoff rate resulting from variations in tillage practices and AMC. Post-hoc analysis using Tukey test was performed when necessary, utilizing R Studio for data analysis. In instances of completely missing data, such as runoff in NC replication 1 under wet AMC, and sediments in CT replication 1 under both dry and wet AMC, the Yates (Yates, 1933) equation was employed to estimate these values. Subsequently, the corresponding ANOVA was adjusted to account for the reduction in necessary degrees of freedom.

Table 4-1. Volume of water and sediment concentration (Cs) measured during rainfall simulation

Treat. & time step		Rep.	Dry AMC Vol. (L)	Dry AMC Cs (g/L)	Wet AMC Vol. (L)	Wet AMC Cs (g/L)
NC	5	1	14.48	16.79	nd*	3.07
NC	10	1	62.44	nd	nd	2.08
NC	15	1	68.59	1.08	nd	1.94
NC	20	1	68.53	0.71	nd	1.76
NC	25	1	70.46	0.70	nd	1.58
NC	30	1	71.77	1.20	nd	3.52
NC	35	1	73.82	0.50	nd	2.93
NC	40	1	68.37	nd	nd	3.27
NC	45	1	81.56	0.46	nd	2.36
NC	5	2	12.48	2.32	46.20	1.80
NC	10	2	54.32	0.78	68.39	1.23
NC	15	2	53.93	0.59	65.37	1.07
NC	20	2	55.19	0.22	73.79	0.58
NC	25	2	56.31	0.46	70.44	0.50
NC	30	2	61.18	0.35	71.09	0.50
NC	35	2	53.29	0.50	57.95	0.42
NC	40	2	61.70	nd	82.93	0.36
NC	45	2	66.23	0.13	64.73	0.36
NC	5	3	17.25	4.00	12.48	2.13
NC	10	3	51.96	1.02	87.72	0.61
NC	15	3	57.64	0.78	64.42	0.23
NC	20	3	60.77	nd	61.22	0.54
NC	25	3	54.91	0.54	68.74	0.55
NC	30	3	53.71	0.45	69.79	0.53
NC	35	3	61.16	0.44	72.16	0.46
NC	40	3	56.83	0.50	62.08	0.13
NC	45	3	70.99	0.49	62.08	0.25
NC	5	4	27.62	nd	50.62	5.83
NC	10	4	50.19	0.41	65.74	5.49
NC	15	4	59.30	nd	68.05	2.23
NC	20	4	62.12	2.34	69.73	1.08
NC	25	4	63.39	0.50	71.07	2.95
NC	30	4	58.61	1.16	70.75	1.39
NC	35	4	66.48	nd	67.05	1.09
NC	40	4	67.37	1.59	69.39	1.13
NC	45	4	80.35	1.60	62.22	1.37
CTR	5	1	3.86	3.84	66.42	0.19

Treat. & time step		Rep.	Dry AMC Vol. (L)	Dry AMC Cs (g/L)	Wet AMC Vol. (L)	Wet AMC Cs (g/L)
CTR	10	1	36.22	1.56	65.04	0.94
CTR	15	1	55.26	0.33	71.10	0.53
CTR	20	1	54.61	0.53	74.97	0.54
CTR	25	1	70.42	0.50	71.37	0.92
CTR	30	1	65.71	nd	59.26	1.05
CTR	35	1	75.25	0.50	74.31	1.01
CTR	40	1	68.42	0.44	76.18	0.90
CTR	45	1	73.13	0.33	81.10	1.06
CTR	5	2	6.50	2.91	36.68	1.26
CTR	10	2	46.33	1.16	68.50	0.72
CTR	15	2	36.45	0.85	61.00	0.85
CTR	20	2	50.64	0.69	70.50	0.74
CTR	25	2	53.81	0.68	75.87	0.37
CTR	30	2	57.90	0.56	63.64	0.16
CTR	35	2	50.97	0.68	78.69	0.15
CTR	40	2	59.84	0.66	64.46	0.12
CTR	45	2	62.72	0.35	96.71	0.12
CTR	5	3	0.00	0.00	11.82	2.43
CTR	10	3	34.96	1.14	62.44	1.34
CTR	15	3	47.46	nd	65.43	1.01
CTR	20	3	40.19	0.46	67.16	0.58
CTR	25	3	42.88	0.63	66.57	0.37
CTR	30	3	48.61	0.32	68.10	0.37
CTR	35	3	54.29	0.01	61.90	0.31
CTR	40	3	55.61	0.27	67.09	0.42
CTR	45	3	57.92	0.25	83.23	0.93
CTR	5	4	1.07	4.76	2.73	1.04
CTR	10	4	35.46	nd	51.28	3.57
CTR	15	4	64.41	0.65	54.56	1.50
CTR	20	4	52.58	nd	59.64	0.41
CTR	25	4	50.62	0.57	58.02	0.69
CTR	30	4	47.30	nd	61.02	nd
CTR	35	4	57.87	0.50	59.98	0.57
CTR	40	4	53.34	0.50	57.00	0.37
CTR	45	4	57.94	nd	63.77	0.32
CT	5	1	28.64	nd	nd	nd
CT	10	1	68.40	nd	nd	nd

Treat. & time step		Rep.	Dry AMC Vol. (L)	Dry AMC Cs (g/L)	Wet AMC Vol. (L)	Wet AMC Cs (g/L)
CT	15	1	39.49	nd	nd	nd
CT	20	1	nd	nd	nd	nd
CT	25	1	nd	nd	nd	nd
CT	30	1	nd	nd	nd	nd
CT	35	1	nd	nd	nd	nd
CT	40	1	nd	nd	nd	nd
CT	45	1	nd	nd	nd	nd
CT	5	2	0.80	nd	2.45	10.80
CT	10	2	27.95	1.05	44.56	0.40
CT	15	2	49.07	0.60	67.06	0.23
CT	20	2	55.30	0.07	57.25	0.08
CT	25	2	55.00	0.15	56.98	0.30
CT	30	2	58.92	0.31	74.84	nd
CT	35	2	59.19	0.14	55.66	0.28
CT	40	2	54.85	0.07	51.00	0.00
CT	45	2	71.42	nd	56.54	0.12
CT	5	3	6.80	0.50	15.85	2.92
CT	10	3	49.26	1.08	58.17	0.81
CT	15	3	54.47	0.70	67.72	1.05
CT	20	3	54.26	0.70	76.88	0.48
CT	25	3	49.30	0.54	61.12	0.27
CT	30	3	54.33	0.58	69.73	0.71
CT	35	3	57.48	0.19	68.05	0.50
CT	40	3	59.18	0.28	67.45	0.36
CT	45	3	59.44	nd	71.07	0.42
CT	5	4	20.13	6.40	31.16	nd
CT	10	4	59.77	1.61	64.38	1.82
CT	15	4	56.36	nd	64.45	0.62
CT	20	4	48.95	nd	65.51	0.58
CT	25	4	117.70	0.72	68.38	0.49
CT	30	4	23.87	0.52	66.71	0.89
CT	35	4	46.18	nd	68.37	0.44
CT	40	4	68.68	0.47	64.76	nd
CT	45	4	81.22	nd	75.05	0.37
HS	5	1	9.89	6.80	34.78	6.82
HS	10	1	47.94	nd	44.35	1.63
HS	15	1	60.69	nd	53.93	3.03

Treat. & time step		Rep.	Dry AMC Vol. (L)	Dry AMC Cs (g/L)	Wet AMC Vol. (L)	Wet AMC Cs (g/L)
HS	20	1	58.35	nd	44.61	2.11
HS	25	1	58.62	nd	23.32	9.68
HS	30	1	60.41	0.50	nd	0.09
HS	35	1	65.57	0.38	nd	nd
HS	40	1	61.23	nd		nd
HS	45	1	74.94	nd		nd
HS	5	2	0.53	6.80	14.65	2.44
HS	10	2	38.76	nd	81.25	0.55
HS	15	2	42.87	nd	77.28	2.97
HS	20	2	52.02	nd	67.23	3.25
HS	25	2	52.39	nd	77.59	0.24
HS	30	2	43.18	0.50	87.97	0.27
HS	35	2	56.95	0.38	83.16	0.12
HS	40	2	54.90	0.33	84.88	0.37
HS	45	2	40.94	nd	101.64	0.35
HS	5	3	0.00	0.00	7.71	nd
HS	10	3	19.41	0.74	62.40	4.46
HS	15	3	34.89	1.89	68.00	0.27
HS	20	3	51.55	0.50	70.00	0.75
HS	25	3	51.28	0.36	67.25	0.24
HS	30	3	51.67	0.34	66.07	nd
HS	35	3	50.28	0.16	71.52	0.07
HS	40	3	60.68	nd	69.08	nd
HS	45	3	60.43	1.70	79.63	nd
HS	5	4	39.90	5.67	47.24	2.77
HS	10	4	40.53	nd	63.35	1.87
HS	15	4	71.01	1.98	63.21	1.84
HS	20	4	125.35	1.96	63.25	1.69
HS	25	4	75.74	nd	61.30	1.42
HS	30	4	0.00	1.15	74.97	3.41
HS	35	4	0.00	1.00	67.05	2.73
HS	40	4	49.53	nd	59.88	3.17
HS	45	4	55.25	nd	52.14	2.32

*nd = no data

Table 4-2. Exponential models for estimating missing sediment concentration, where “y” is the sediment concentration and “x” is the time

Treat.	Rep.	Dry AMC	RMSE	Wet AMC	RMSE
NC	1	y=0.4+50exp(-0.22x)	0.54	No missing data	
NC	2	y= 0.3+6exp(-0.22x)	0.14	No missing data	
NC	3	y= 0.46+14exp(-0.27x)	0.14	No missing data	
NC	4	y= 1.15+8exp(-0.19x)	0.97	No missing data	
CTR	1	y=0.32+10.5exp(-0.22x)	0.16	No missing data	
CTR	2	No missing data		No missing data	
CTR	3	y= 0.2+1.5exp(-0.11x)	0.43	No missing data	
CTR	4	y=0.5+16.5exp(-0.27x)	0.06	y= 0.4+8exp(-0.17x)	1.17
CT	1	No records		No records	
CT	2	y= 0.14+5.5exp(-0.18x)	0.11	y= 0.1+65exp(-0.36x)	0.53
CT	3	y= 0.4+1.7exp(-0.18x)	0.30	No missing data	
CT	4	y= 0.5+20exp(-0.24x)	0.33	y=0.3+15exp(-0.36x)	0.50
HS	1	Y= 0.37+14.5exp(-0.16x)	0.05	y= 0.7+15exp(-0.15x)	3.71
HS	2	y=0.3+13exp(-0.14x)	0.02	No missing data	
HS	3	y= 0.2+5exp(-0.20x)	1.03	y= 0.09+15exp(-0.15x)	1.03
HS	4	y=1+11exp(-0.17x)	0.27	No missing data	

4.3. Results and discussion

4.3.1. Runoff

Tillage treatments had a statistically significant impact on total runoff, but these differences were observed only under DAMC and not under WAMC. Under DAMC, the NC treatment produced the maximum mean runoff per plot at 518.83 L, indicating poor infiltration. The CTR and HS treatments induced the lowest mean runoff, with 432.64 L and 429.42 L, respectively, suggesting that the presence of crop residues in addition to a conventional tillage and cropping on a soil with no-tillage improved soil structure and increased infiltration. The treatment CT did not show statistically significant difference from these three treatments (Figure 4-5), highlighting the complex interactions between soil management practices and runoff dynamics.

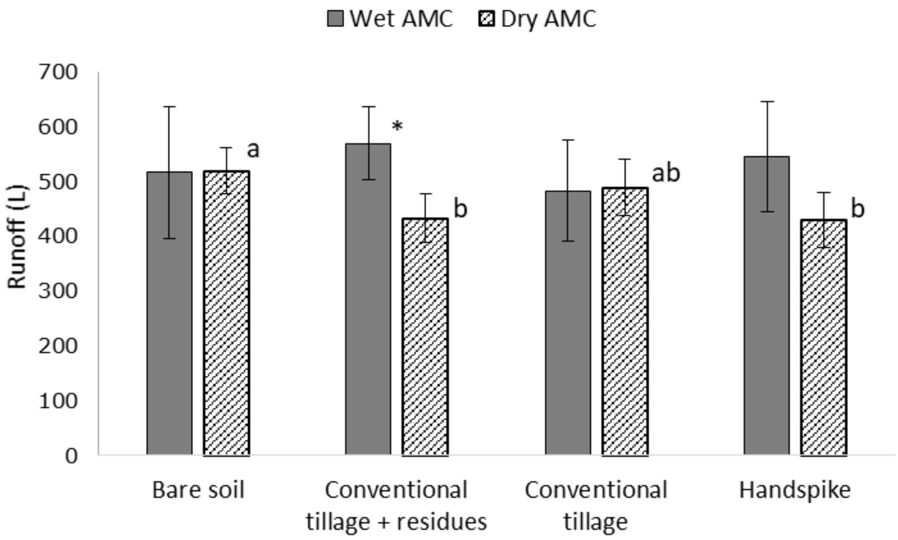

Figure 4-5. Mean total runoff for each treatment under wet and dry antecedent soil moisture conditions (AMC). Different letters in dry AMC different effects promoted by tillage treatments. An asterisk denotes statistically higher runoff under wet AMC for the Conventional tillage + residues treatment.

The finding that the CTR treatment resulted in less runoff compared to the NC treatment is consistent with other research, which has shown that surface litter significantly reduces runoff by enhancing water infiltration and minimizing soil crusting. For example, similar studies have demonstrated that surface litter can reduce runoff by 29.5% and 31.3% compared to bare soil plots (Li et al., 2014). Additionally, our data revealing no statistical differences between CT with or without residues and the HS treatment contrasts with results from Wang et al. (Wang et al., 2017) and Nyamadzawo et al. (Nyamadzawo et al., 2012). These studies found that wheat stubble cover plots produced less runoff than traditional plowing, and that conventional tillage increased runoff compared to conservation agriculture.

Under wet antecedent moisture conditions (WAMC), the highest runoff was recorded in the CTR treatment (569.38 L) and the lowest in the CT treatment (482.12 L). However, these differences were not statistically significant, likely due to the soil being near saturation, which reduces the capacity of crop residues to enhance infiltration. When the soil is saturated, additional rainfall is more likely to produce surface runoff regardless of tillage treatment. This suggests that crop residues are more effective in reducing runoff under dry conditions, where they can improve infiltration substantially, than under wet conditions.

Regarding the effects of AMC on runoff, we observed that only the CTR treatment exhibited the highest runoff under wet AMC induced the highest runoff under wet AMC (Figure 4-5). This behaviour is consistent with findings from Zhao et al. (Zhao et al., 2015), in agricultural lands with rainfall simulation and Meyles et al. (Meyles et al., 2003), in a small catchment, they observed similar patterns as the current research. Although soil moisture variability is widely reported as a critical factor in runoff production (Bronstert and Bardossy, 1999), our research found that only one of the four tillage treatments (CTR) was significantly influenced by AMC. This suggests that the presence of crop residues in agricultural lands plays a crucial role in modulating runoff, particularly under varying moisture conditions. In other studies conducted in semiarid shrub-steppe landscapes, bare soil surfaces exhibited higher runoff compared to other landscape types, but these differences were only relevant under dry soil conditions (Mayor et al., 2009), that suggests the crop residues can mitigate runoff more effectively in dry conditions by enhancing soil infiltration and reducing surface sealing.

The analysis of variance indicated that tillage treatments had a statistically significant effect on runoff rate ($p \leq 0.05$) under dry AMC, but not under wet AMC. These differences were observed only at the time step 45. Under dry AMC, the CTR treatment had the lowest runoff rate at 11.43 mm/h at the time step 5, suggesting that the presence of residues helped to enhance infiltration early in the simulation. In contrast, the CT treatment exhibited the highest runoff rate with 306.80 mm/h at the time step 25, indicating a rapid increase in runoff due to reduced infiltration capacity. Under wet AMC, the lowest runoff rate was 91.19 mm/h at minute 5 in the CT treatment, while the highest was 324.81 mm/h at the minute 45 in the CTR treatment. The most dramatic changes in runoff rate occurred within the first five to ten minutes of the simulation, highlighting the initial response of the soil to rainfall. After this period, the runoff rates stabilized, reflecting a balance between rainfall input and the soil's infiltration capacity (Figure 4-6).

The impacts of AMC on runoff rate showed statistically significant differences at various time points during the simulation. Specifically, significant differences were observed at minute 5 in HS treatment and at the minutes 10, 20 and 40 in CTR treatment ($p \leq 0.05$ and $p \leq 0.01$) (Figure 4-6).

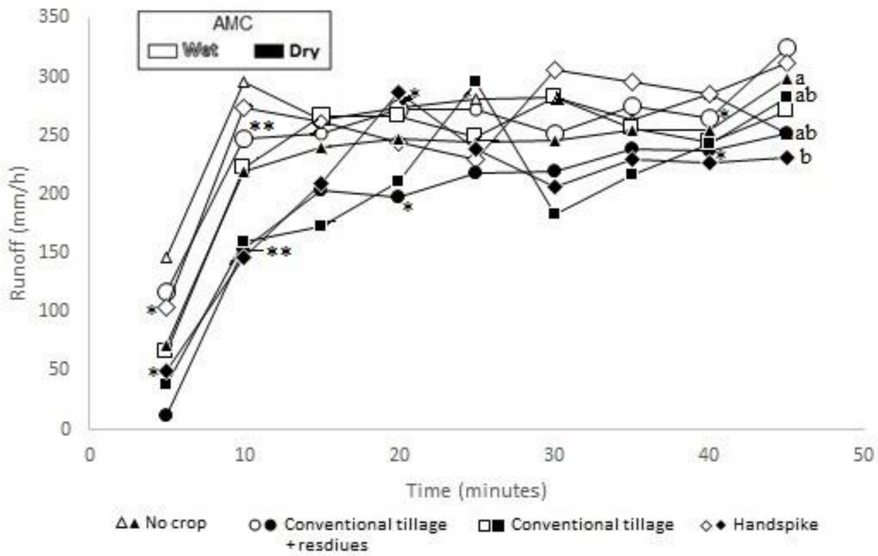

Figure 4-6. Mean runoff rates for each treatment. Asterisks indicate statistically significant differences ($p \leq 0.05$ and $p \leq 0.01$) of antecedent soil moisture conditions, while letters denote statistically significant differences ($p \leq 0.05$) due to tillage treatments.

Generally, runoff increased with the time of simulation, a trend that is consistent with other studies using simulated rainfall on bare ground, wheat, ryegrass, and purple medic (Huang et al., 2013). This pattern suggests that as the soil surface becomes increasingly saturated, its ability to absorb additional water decreases, leading to higher runoff rates. Similarly, other researchers have reported comparable maximum runoff rates between conventional tillage and no-tillage treatments, with significant differences observed under very wet soil moisture conditions, where no-tillage plots showed the highest runoff rate (Wilson et al., 2004). These findings underscore the importance of considering both tillage practices and antecedent soil moisture conditions in soil and water conservation strategies. Implementing residue cover and conservation tillage can effectively reduce runoff, particularly in dry conditions, while understanding the dynamics of runoff under varying moisture levels can help in designing more resilient agricultural systems.

4.3.2. Erosion

The analysis of variance detected statistical differences in cumulative soil erosion promoted by tillage treatments during minutes 30 – 40 under wet AMC. However, the Tukey test did not find significant differences between the means of these treatments. Numerically, the HS treatment under wet AMC resulted in the highest total erosion with 802.11 g. In contrast, under dry AMC, the NC treatment experienced the highest erosion at 581.34 g. The least total erosion was observed in the CTR treatment under dry AMC with 249.30 g, and in CT treatment under wet AMC with 311.90 g (Figure 4-7). The high erosion observed in HS under wet conditions could be due to reduced soil cohesion when saturated, whereas the minimal erosion in CTR under dry AMC, and CT under wet AMC might be attributed to improved soil structure and reduced surface sealing.

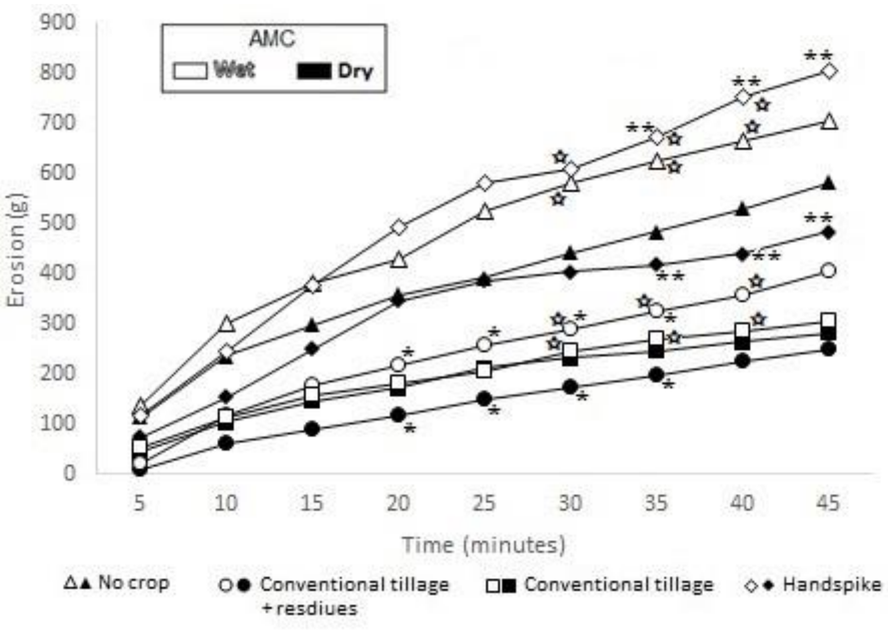

Figure 4-7. Cumulative soil erosion of the studied tillage and AMC's treatments. The asterisks denote statistical differences caused by the AMC's, one asterisk specifies p ≤ 0.05, and two

asterisks indicate $p \le 0.01$. Stars indicate statistical differences ($p \le 0.05$) caused by tillage treatments

Literature generally reports that no-tillage and crop residue coverage prevent soil erosion better than conventional tillage (Nolan et al., 1997; Diallo et al., 2008; Lanzanova et al., 2013; Biddoccu et al., 2020), which is only consistent in our experiment in the case of CTR under dry AMC, but not in the case of no tillage in HS, which produced the highest erosion. Gura et al. (Gura et al., 2022) conducted a three-year-study on maize and soybean rotation, finding that no-till practices significantly increased soil organic carbon and microbial biomass carbon, reducing erosion susceptibility (Xiaojun et al., 2013). However, they found no significant effects from crop rotation and residue management. In a simulated rainfall experiment, Stašek et al. (Stašek et al., 2023) showed that reduced tillage and direct seeding reduced soil loss. Mhazo et al. (Mhazo et al., 2016) reviewed literature and found inconsistent effects of no-tillage on erosion prevention, influenced by environmental differences. No-tillage was more effective in temperate zones than in tropical regions with more consolidated soils. This highlights the importance of environmental context in understanding tillage impacts, as observed in our arid zone study.

Most cited studies focus on long-term impacts because information on short-term conservation practices is limited. Short-term studies, typically spanning one to three years under natural rainfall, contrast with our 45-minute rainfall simulation. Short-term studies are crucial for understanding immediate effects of tillage practices and soil moisture on erosion, informing immediate management decisions. The lack of distinct effects from tillage treatments on soil erosion in our study might be due to the experiment's brief duration, unlike the observed effects of soil moisture conditions.

Regarding the effects of AMC, the ANOVA detected a distinct effect ($p \le 0.05$) in the CTR treatment during minutes 20 – 35, with wet AMC promoting the highest cumulative erosion. Also, the HS treatment showed statistically significant differences ($p \le 0.01$) during minutes 35 – 45, with higher erosion under wet AMC (Figure 4-7). These results suggest that dry AMC under no-till cropping conditions and crop residue coverage led to less erosion compared to the same tillage treatments under wet AMC. Wet AMC likely decreases soil cohesion, making it more susceptible to detachment and transport by water. In contrast, dry AMC may enhance the soil's ability to resist erosion due to higher shear strength and reduced pore water pressure. The presence of crop residues further mitigates erosion by protecting the soil surface from the direct impact of raindrops and reducing the velocity of surface runoff. This interplay between soil moisture and surface cover underscores the complexity of erosion processes.

Soil moisture significantly influences soil's resistance to erosion. Typically, dry soil exhibits lower resistance to erosion, which gradually increases with the antecedent soil moisture content. However, once soil resistance reaches its maximum level, it starts to decrease because the soil becomes saturated (Moragoda et al., 2022), reducing its shear strength and making it more prone to detachment and transport (Wei et al., 2019). In our current investigation, we consistently observed higher erosion rates under wet AMC across all tillage treatments and time steps of the simulation (Figure 4-8). This pattern indicates that excessive soil moisture reduces the soil's ability to resist erosive forces, leading to greater soil loss. The observed trends align with the theoretical understanding of soil moisture dynamics (Pierzynsky et al., 2005; Moragoda et al., 2022) and highlight the critical role of managing soil moisture to minimize erosion risks, particularly in arid and semi-arid regions where rainfall events can lead to rapid saturation and subsequent erosion.

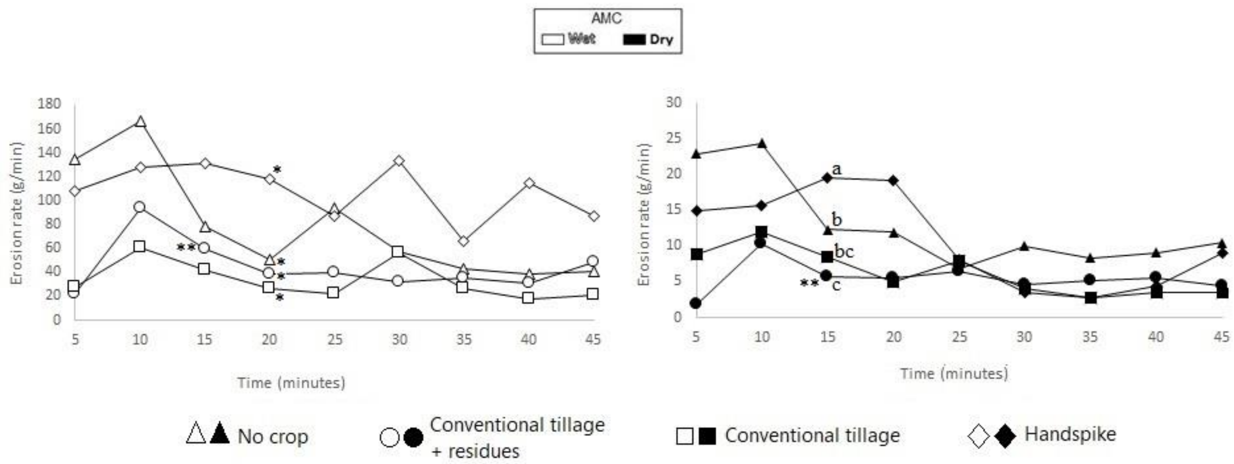

Figure 4-8. Erosion rate of tillage and AMC's treatments during rainfall simulation

In another investigation, Wei et al. (Wei et al., 2007) also found that the largest amounts of soil erosion occurred under wet AMC in peanut and tree crops. This pattern was consistent with the findings of Ziadat and Taimeh (Ziadat and Taimeh, 2013), who reported significantly higher soil loss in wet AMC and very wet AMC in rangeland and barley crops. These studies, like ours, highlight the pronounced impact of soil moisture on erosion rates. The consistent observation of higher erosion under wet AMC across different crop types and environments underscores the importance of soil moisture management in preventing soil erosion. Our results align with these findings, as we also observed increased erosion under wet conditions across all tillage treatments. The similarities between these studies and our findings suggest that the relationship between soil moisture and erosion is robust across various agricultural contexts, reinforcing the need for practices that mitigate the impact of excessive soil moisture on erosion.

The present results revealed that dry soils managed with conventional tillage plus soil covered by crop residues promoted the least erosion. Numerous studies have demonstrated the potential of surface cover to reduce soil erodibility. For example, surface residues slow down surface runoff, promoting infiltration and reducing the volume and velocity of water capable of causing erosion

(Jin et al., 2008; Mailapalli et al., 2013; Li et al., 2014). These mechanisms are essential for maintaining soil integrity, particularly in regions prone to high-intensity rainfall events.

Given the consistent rainfall and soil texture throughout our experiments, general effects can be assumed. High rainfall intensities, as in current research (Figure 4-4), have a great impact on soil erosion, which was demonstrated in an investigation by Zhao et al. (Zhao et al., 2021), who evaluated rainfall intensity and duration ranges. They concluded that an intensity of 120 mm/h promoted greater erosion than a rainfall intensity of 60 mm/h under the same soil management. On the other hand, soil texture is one of the major factors impacting erosion (Kilinc and Richardson, 1973), due to its close relation to moisture retention (Magdić et al., 2022), being the clayey and sandy soils the least erosive (Middleton, 1930) and silty soils or fine sands are the most erosive (O'geen et al., 2006). Furthermore, the interplay of high rainfall intensity with soil of high sand levels has been associated with more erosion compared to scenarios with lower rainfall intensities and higher proportions of fine particles (Mrubata et al., 2024).

With regard to the observed erosion rate, the tillage treatments showed statistical differences ($p \leq 0.05$) at minute 15 under dry AMC, where the HS treatment presented the highest erosion rate, while the CTR treatment showed the lowest. Under wet AMC, the ANOVA detected differences in erosion rates in minute 20, but Tukey test did not detect differences between the tillage treatments. Regarding the effects of AMC on runoff rate, the ANOVA detected differences ($p \leq 0.01$) in treatment CTR at minute 15, the dry AMC that promoted lower erosion rate. The interaction between soil moisture and tillage practices creates a complex dynamic where the protective effects of crop residues in the CTR treatment are more beneficial under dry conditions. The erosion rate was characterized by initially higher rates followed by a subsequent decrease, then it appeared to stabilize after an augmentation in soil water content (Figure 4-8). This stabilization phase alluded to by studies such as Lo and Lee (Lo and Lee, 2015) and Mrubata et al.

(Mrubata et al., 2024) is linked with phenomena like soil crusting, which although not directly measured in our study, it is considered to reduce infiltration and consequently to increase overland flow that occurred at the minute 10 of our experiment (see Figure 4-6).

4.4. Conclusions

Our study aimed to investigate the impact of agricultural management practices and antecedent soil moisture on short-term soil erosion in an arid zone of North Central Mexico using simulated rainfall. The comparative analysis between the studied treatments revealed several key findings.

This research demonstrated that, in the short term, conventional tillage with or without crop residue cover is more effective at preventing soil erosion than no-tillage cropping, particularly under dry antecedent moisture conditions (AMC). In a sandy clay loam agricultural land in an arid zone of Mexico, dry AMC significantly reduced cumulative erosion in no-tillage cropping (HS) and in conventional tillage with crop residue cover, compared to their corresponding treatments under wet AMC.

When considering the effects of tillage treatments on cumulative erosion, the lowest erosion was observed in the CT and CTR treatments, while the highest was in HS and NC treatments, but only under wet AMC. This finding contradicts the common notion that no-till cropping and crop residue cover are universally effective in preventing erosion in agricultural lands (Zhao et al., 2020; Pedroza-Parga et al., 2022). This discrepancy might be because these practices have a more significant impact on less consolidated soils than the soil studied here (Mhazo et al., 2016). Additionally, the short-term nature of the current investigation may have influenced the performance of soil management practices compared to other long-term studies.

The erosion rate was also affected differently by AMC in the CTR treatment. Under dry AMC, the CTR treatment presented a lower erosion rate compared to other tillage treatments at the 15-20-minute time steps.

The erosion results are consistent with runoff data. The CTR and HS treatments under dry AMC produced the lowest runoff, supporting the conclusion that these treatments are effective at reducing both erosion and runoff under dry conditions.

Overall, the study highlights the importance of considering both tillage practices and soil moisture conditions when developing soil erosion prevention strategies. The effectiveness of no-till and crop residue cover may vary based on soil type and environmental conditions, underscoring the need for site-specific management practices to achieve optimal soil conservation. Future research should focus on long-term impacts and explore the interaction between soil consolidation and erosion control measures to provide more comprehensive guidelines for sustainable agriculture in arid regions.

References

Baker, C.J., Saxton, K.E., 2007.The “what” and “why” of no-tillage farming. In: Baker, C.J., Saxton, K.E. (Eds.): No Tillage Seeding in Conservation Agriculture. FAO and CAB International 2007, pp. 1–10.

Biddoccu, M., Guzmán, G., Capello, G., Thielke, T., Strauss, P., Winter, S., Zaller, J.G., Nicolai, A., Cluzeau, D., Popescu, D., Bunea, C., Hoble, A., Cavallo, E., Gómez, J.A., 2020.Evaluation of soil erosion risk and identification of soil cover and management factor (C) for RUSLE in European vineyards with different soil management.International Soil and Water Conservation Research., 8, 337–353.

Bolaños-González, M.A., Paz-Pellat, F., Cruz-Gaistardo, C.O., Argumedo-Espinoza, J.A.., Romero-Benítez, V.M., DelaCruz-Cabrera, J.C., 2016.Mapa de erosión de los suelos de México y posibles implicaciones en el almacenamiento de carbono orgánico del suelo.Terra Latinoamericana., 34, 271–288.

Bronstert, A., Bardossy, A., 1999.The role of spatial variability of soil moisture for modelling surface runoff generation at the small catchment scale.Hydrology and Earth System Sciences., 3, 505–516.

Cotler, H., Corona, J.A., Galeana-Pizaña, J.M., 2020.Erosión de suelos y carencia alimentaria en México: una primera aproximación.Investigaciones Geográficas.

Cotler, H., Cuevas, M.L., 2019.Adoption of soil conservation practices through knowledge governance: the Mexican experience.Journal of Soil Science and Environmental Management., 10, 1–11.

Diallo, D., Soli, Z., Roose, E., 2008.Influence of No-Tillage on Soil Conservation , Carbon Sequestration and Yield of Intensive Rotation Maize-Cotton : Research on Sandy Alfisols of Cameroon and Mali. In: Goddart, T., Zoebisch, M., Gan, Y., Ellis, W., Watson, A., Sombatpani, S. (Eds.): No-Tillage Farming Systems. WASWC, pp. 383–392.

FAO, ITPS, 2015.Status of the World's Soil Resources (SWSR) - Main Report. Rome, Italy.

Friedrich, T., Derpsch, R., Kassam, A., 2017.Overview of the global spread of conservation agriculture.Field Actions Science Reports [Online]., 8, 53–68.

Gura, I., Mnkeni, P.N.S., Du Preez, C.C., Barnard, J.H., 2022.Short-term effects of conservation agriculture strategies on the soil quality of a Haplic Plinthosol in Eastern Cape, South Africa.Soil and Tillage Research., 220, 105378.

Huang, J., Zhao, X., Wu, P., 2013.Surface runoff volumes from vegetated slopes during simulated rainfall events.Journal of Soil and Water Conservation., 68, 283–295.

Jin, K., Cornelis, W.M., Gabriels, D., Schiettecatte, W., De Neve, S., Lu, J., Buysse, T., Wu, H., Cai, D., Jin, J., Harmann, R., 2008.Soil management effects on runoff and soil loss from field rainfall simulation.Catena., 75, 191–199.

Kilinc, M., Richardson, E. V., 1973.Mechanics of Soil Erosion From Overland Flow Generated By Simulated Rainfall.Colo State Univ (Fort Collins), Hydrol Papers.

Lal, R., 1995.Tillage systems in the tropics : management options and sustainability implications, FAO Soils Bulletin (FAO). Food and Agriculture Organization of the United Nations, Rome, Italy.

Lanzanova, M.E., Eltz, F.L.F., Nicoloso, R. da S., Cassol, E.A., Bertol, I., Amado, T.J.C., Girardello, V.C., 2013.Residual effect of soil tillage on water erosion from a Typic Paleudalf under long-term no-tillage and cropping systems.Revista Brasileira de Ciência do Solo., 37, 1689–1698.

Li, X., Niu, J., Xie, B., 2014.The effect of leaf litter cover on surface runoff and Soil Erosion in Northern China.PLoS ONE., 9.

Lo, W.C., Lee, J.W., 2015.Effect of water content and soil texture on consolidation in unsaturated soils.Advances in Water Resources., 82, 51–69.

López-García, E.M., Torres-Trejo, E., López-Reyes, L., Flores-Domínguez, Á.D., Peña-Moreno, R.D., López-Olguín, J.F., 2020.Estimation of soil erosion using USLE and GIS in the locality of Tzicatlacoyan , Puebla , México.Soil and Water Research., 15, 9–17.

Magdić, I., Safner, T., Rubinić, V., Rutić, F., Husnjak, S., Filipović, V., 2022.Effect of slope position on soil properties and soil moisture regime of Stagnosol in the vineyard.Journal of Hydrology and Hydromechanics., 70, 62–73.

Mailapalli, D.R., Burger, M., Horwath, W.R., Wallender, W.W., 2013.Crop residue biomass effects on agricultural runoff.Applied and Environmental Soil Science., 2013.

Mayor, G.Á., Susana, B., Juan, B., 2009.Factors and interactions controlling infiltration, runoff, and soil loss at the microscale in a patchy Mediterranean semiarid landscape.Earth Surface Processes and Landforms., 34, 1702–1711.

Meyles, E., Williams, A., Ternan, L., Dowd, J., 2003.Runoff generation in relation to soil moisture patterns in a small Dartmoor catchment, Southwest England.Hydrological Processes., 17, 251–264.

Mhazo, N., Chivenge, P., Chaplot, V., 2016.Tillage impact on soil erosion by water: Discrepancies due to climate and soil characteristics.Agriculture, Ecosystems and Environment., 230, 231–241.

Middleton, H.E., 1930.Properties of soils which influence soil erosion, Technical Bulletin No. 178. Wahington, DC.

Miller, W.P., 1987.A Solenoid-Operated, Variable Intensity Rainfall Simulator1.Soil Science Society of America Journal., 51, 832–834.

Moragoda, N., Kumar, M., Cohen, S., 2022.Representing the role of soil moisture on erosion resistance in sediment models: Challenges and opportunities.Earth-Science Reviews., 229, 1–56.

Mrubata, K., Nciizah, A.D., Wakindiki, I.I.C., Mudau, N., 2024.Effects of rainfall intensity and slope gradient on soil sealing and crusting , erosion , and phosphorus solubilizing bacteria.Scientific African., 23, 11.

Nkonya, E., Mirzabaev, A., von Braun, J., 2016.Economics of land degradation and improvement - A global assessment for sustainable development. In: Economics of Land Degradation and Improvement - A Global Assessment for Sustainable Development. pp. 117–165.

Nolan, S.C., Van Vliet, L.J.P., Goddard, T.W., Flesch, T.K., 1997.Estimating storm erosion with a rainfall simultor.Canadian Journal of Soil Science., 77, 669–676.

Nyamadzawo, G., Nyamugafata, P., Wuta, M., Nyamangara, J., Chikowo, R., 2012.Infiltration and runoff losses under fallowing and conservation agriculture practices on contrasting soils, Zimbabwe.Water SA., 38, 233–240.

O’geen, A.T., Elkins, R., Lewis, D., 2006.Erodibility of Agricultural Soils, with Examples in Lake and Mendocino Counties.Reducing Runoff from Irrigated Lands. Publication 8194.

Patil, R.J., 2018.Spatial techniques for soil erosion estimation: remote sensing and GIS approach. Springer, Cham.

Pedroza-Parga, E., Velásquez-Valle, M.A., Pedroza-Sandoval, A., Sánchez-Cohen, I., Yáñez-Chávez, L.G., 2022.The impact of vegetation cover on soil erosion and soil deposition due to runoff.Ingeniería Agrícola y Biosistemas., 144, 17–31.

Pierzynsky, G.M., Vance, F.G., Sims, T.J., 2005.Soils and Environmental Quality.3rd ed. CRC Press.

Pimentel, D., Harvey, C., Resosudarmo, P., Sinclair, K., Kurz, D., Mcnair, M., Shpritz, L., Fitton, L., Saffouri, R., Blair, R., Pimentel, D., Harvey, C., Resosudarmo, P., Sinclair, K., Kurz, D., Mcnair, M., Crist, S., Shpritz, L., Fitton, L., Saffouri, R., Blair, R., 1995.Environmental and Economic Costs of Soil Erosion and Conservation Benefits.Science., 267, 1117–1123.

Stašek, J., Krása, J., Mistr, M., Dostál, T., Devátý, J., Středa, T., Mikulka, J., 2023.Using a Rainfall Simulator to Define the Effect of Soil Conservation Techniques on Soil Loss and Water Retention.Land., 12.

Swaminathan, M.S., 2006.An evergreen revolution.Crop Science., 46, 2293–2303.

Wang, L., Ma, B., Wu, F., 2017.Effects of wheat stubble on runoff, infiltration, and erosion of farmland on the Loess Plateau, China, subjected to simulated rainfall.Solid Earth., 8, 281–290.

Wei, L., Zhang, B., Wang, M., 2007.Effects of antecedent soil moisture on runoff and soil erosion in alley cropping systems.Agricultural Water Management., 94, 54–62.

Wei, Y., Wu, X., Xia, J., Miller, G.A., Cai, C., Guo, Z., Arash, H., 2019.The effect of water content on the shear strength characteristics of granitic soils in South China.Soil and Tillage Research., 187, 50–59.

Wilson, G. V, Dabney, S.M., McGregor, K.C., Barkoll, B.D., 2004.Tillage and residue effects on runoff and erosion dynamics.Transactions of the American Society of Agricultural Engineers., 47, 119–128.

World Bank, 2019.Sustainable land management and restoration in the middle east and North Africa Region - Issues, chanllenges and recommendations.

Xiaojun, N., Jianhui, Z., Zhengan, S., 2013.Dynamics of Soil Organic Carbon and Microbial Biomass Carbon in Relation to Water Erosion and Tillage Erosion.PLoS ONE., 8.

Yates, F., 1933.The analysis of replicated experiments when the field results are incomplete.Empire Journal of Experimental Agriculture., 1, 129–142.

Zhao, J., Feng, X., Deng, L., Yang, Y., Zhao, Z., Zhao, P., Peng, C., Fu, B., 2020.Quantifying the Effects of Vegetation Restorations on the Soil Erosion Export and Nutrient Loss on the Loess Plateau.Frontiers in Plant Science., 11, 1–13.

Zhao, L., Fang, Q., Hou, R., Wu, F., 2021.Effect of rainfall intensity and duration on soil erosion on slopes with different microrelief patterns.Geoderma., 396.

Zhao, N., Yu, F., Li, C., Zhang, L., Liu, J., Mu, W., Wang, H., 2015.Soil Moisture Dynamics and Effects on Runoff Generation at Small Hillslope Scale.Journal of Hydrologic Engineering., 20.

Ziadat, F.M., Taimeh, A.Y., 2013.Effect of rainfall intensity, slope, land use and antecedent soil moisture on soil erosion in an arid environment.Land Degradation and Development., 24, 582–590.

CHAPTER 5. Empirical and physical modeling of soil erosion in agricultural hillslopes

Authors: Palmira Bueno Hurtado, Ousmane Seidou

Abstract

Soil erosion is a complex and highly heterogeneous process with a wide range of environmental and economic impacts. Its estimation is particularly challenging and modeling is typically used for erosion estimation over large areas. The aim of this study was to compare the two leading empirical and physical erosion estimation models, i.e. the Revised Universal Soil Loss Equation (RUSLE) and the Water Erosion Prediction Project (WEPP). The models were calibrated and validated using data collected from field experiments conducted in agricultural lands of Mexico. The simulated rainfall experiments involved measuring erosion from field plots subjected to four tillage systems (No crop, Conventional tillage, Conventional tillage + residues, and Handspike) under two antecedent soil moisture conditions (dry and wet). Different calibration approaches based on the factors K and C for RUSLE, and interrill erodibility and hydraulic conductivity in WEPP were tested. The best-performing methods in RUSLE involved measuring the K factor and adopting the recommended C factor by the National Forestry Commission of Mexico. In WEPP, the best results were obtained when interrill erodibility was estimated from experimental measurements. Overall, RUSLE outperformed WEPP in most of the treatments except for CT under WAMC.

Keywords: RUSLE, WEPP, tillage systems, rainfall simulation.

5.1. Introduction

Soil erosion by water occurs when raindrops cause detachment of soil particles, which are then transported by runoff and eventually deposited elsewhere in the landscape. While soil erosion is a natural process, it can be exacerbated by human activities such as agriculture, construction, and mining. The impacts of soil erosion can be both negative and positive. Areas with long-term soil accumulation are typically the most fertile lands while the eroded zones have lower fertility and capacity for supporting life. Globally, water erosion leads to an estimated annual soil loss of 20-30 Gt. Erosion rates vary depending on factors such as land use and climate, ranging from 10-20 t ha^{-1} yr^{-1} in hilly croplands under conventional agriculture and temperate climate to 50-100 t ha^{-1} yr^{-1} in tropical and subtropical regions (FAO and ITPS, 2015). Soil erosion also has significant economic consequences, with an estimated cost of $44 billion per year in the United States (Pimentel et al., 1995), and a 0.43% annual loss of crop productivity in severely eroded agricultural lands in the European Union, amounting to EUR 1.25 billion (Panagos et al., 2018). Erosion is significant in agricultural lands located in semi-arid regions, where intense rainstorms and low soil organic matter exacerbate the erosive effects.

Given the economic importance of soil erosion, accurate prediction over large areas based on precipitation data is essential. Selecting the right model for a given soil erosion process is critical as uncertainties are typically large in erosion modeling. For instance, the Universal Soil Loss Equation (USLE) and its variants are the most used erosion models but have limitations (Roose, 1996). USLE is based on experimental relations that can hide the effects of key variables which limit their replicability, also has temporal limitations because it is designed for long-term erosion and may not be effective in predicting short-term erosion. USLE-type models provide broad estimations that are often sufficient for determining the best practices in land use management. Many models have been developed since 1940 and can be classified as empirical, physical and conceptual. The Revised Universal Soil Loss Equation (RUSLE) is the most applied soil erosion model worldwide due to its flexibility and accessibility. It calculates long-term average annual soil erosion by considering factors such as rainfall-runoff erosivity, soil erodibility, slope length, slope steepness, land cover and management, and soil conservation practices (Wischmeier and Smith, 1978; Renard et al., 1991; Alewell et al., 2019). Empirical USLE-type models rely on statistical relationships derived from field observations.

Alternative to empirical models are the conceptual and physical models. Physical models aim to describe the underlying processes and interactions, while conceptual models take an intermediate approach, combining empirical and physical elements (Zingg, 1940; Patil, 2018). Since 1940, numerous physical and conceptual models have been developed, based on the continuity equation for both runoff and erosion prediction. Although sharing the same root, they present variations in approaches and methods showing similarities and differences.

Examples of physical models include the Areal Nonpoint Source Watershed Environment Response Simulation (ANSWERS) (Beasley et al., 1980), the Cellular Automaton Evolutionary Slope and River Model (CAESAR) (Coulthard et al., 2002), and CASC2D. Conceptual models encompass SWAT (Arnold et al., 1998) and WATEM/SEDEM (Notebaert et al., 2006), the latter being a combination of the Water and Tillage Erosion Model (WATEM), which estimates erosion using the Revised Universal Soil Loss Equation (RUSLE), and the Sediment Delivery model (SEDEM). Additionally, empirical models like EGEM (Woodward, 1999) and EPIC, which employs the Universal Soil Loss Equation (USLE) and Modified Universal Soil Loss Equation (MUSLE) to predict soil erosion (Williams, 1990), offer alternative approaches to erosion modeling.

Worldwide, the most employed soil erosion and sediment yield models in descending order of importance are RUSLE, USLE, WEPP, SWAT, and WATEM/SEDEM, they are all based on USLE-type equations with the exception of WEPP (Borrelli et al., 2021). WEPP was developed as a replacement of empirical models. It takes a physical-based approach and offers a more detailed understanding of erosion processes (Flanagan et al., 2007). WEPP considers various processes at both hillslope and watershed scale, offering a comprehensive perspective on erosion dynamics (Flanagan et al., 1995).

For calibrating USLE-types models, experiments are often conducted, mainly focused on changes of Factor C (soil surface condition) and Factor K (soil erodibility). For instance, Prado-Hernández et al. (2017) calibrated MUSLE based on Factor K, replacing the default method and suggestions from FAO (Food and Agriculture Organization) with their own estimations obtained from regressions with the least squares method. In the case of calibrating WEPP in single storm mode, it is recommended for soil losses prediction, doing adjustments in erodibility parameters, including interrill erodibility, rill erodibility and critical shear stress (Flanagan and Frankenberger, 2012). In a study by Wang et al. (2022), the WEPP was calibrated modifying the range of values for hydraulic conductivity according to Risse et al., (1994) and subsequently adjusting shear stress, rill erodibility and interrill erodibility, like the ranges of Nearing et al. (1990). Searching for the perfect method for calibrating environmental models is impractical due to uncertainties in inputs, outputs and the model structure itself. Nevertheless, to obtain reliable results, a robust calibration setup proves valuable, especially in cases where certain parameters are challenging to measure. Therefore, a carefully design in calibration process is essential (Mai, 2023).

The objective of this paper is to compare the performance of RUSLE and WEPP, two widely used empirical and physical models, studying different calibration approaches in simulating erosion at a small scale. The experiment was conducted in Mexico, a country where 76% of the total area is affected by soil erosion by water.

5.2. Material and methods

5.2.1. Experimental setup

The experiment was conducted in the locality of Santo Domingo, Durango, México, at the coordinates 25° 49' 41.94" N and 104° 26' 18.97" W, with an altitude of 1750 m. a. s. l. The climate is arid with an average annual temperature ranging from 14 to 22 °C. The annual rainfall typically falls between 200 and 400 mm. The soil in this area is classified as Leptosol, with sandy clay loam texture and soil organic matter of 2.31%.

5.2.2. Rainfall simulation and sediment sampling

To perform the simulated rainfall, we developed a rainfall simulator based on the apparatus of Miller (1987). The setup consisted of a water supply tank, a pump, a Programmable Logic Controller, three 360° nozzles, solenoid valves, manometers and hoses. To power the simulator, we used a portable generator of 5500 Watts (Figure 5-1).

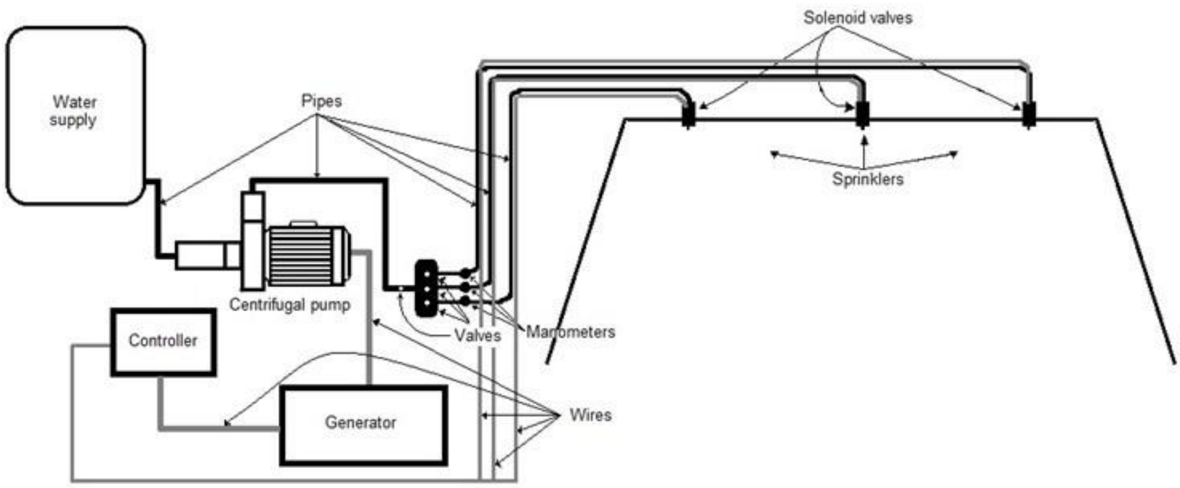

Figure 5-1. Rainfall simulator.

The rainfall simulations were conducted from November 11 and 16, 2015. The soil moisture levels during these simulations ranged from 16 to 19% for DAMC and 23 to 25% for WAMC (Table 5). Each simulation lasted 45 minutes. We measured the rainfall intensity every minute using a standard pluviometer placed randomly at each plot. Every 5 minutes, we collected a 1-liter sample from 19-liter containers after mixing the runoff collected. These samples were later filtered, oven-dried at 105 °C, and weighed for further analysis.

5.2.3. Treatments

We set experiments under different treatments: 1. No crop (NC), without movement of soil and vegetation; 2. Conventional tillage (CT), with moldboard plow following by harrowing, furrowing and corn sowing; 3. Conventional tillage + residues (CTR) that was the same as CT but with crop residues on soil surface; and 4. Handspike (HS), without movement of soil and the corn sowing was using a wooden stick (Figure 5-2). The density of plants in CT and CTR was 68000 per hectare. Each treatment was replicated four times, and the experiments were conducted under both dry and wet antecedent soil moisture conditions (DAMC and WAMC). The erosion plots were delimitated with smooth galvanized sheets measuring 1 x 3 m. To facilitate the collection of surface runoff, a structure was installed at the lower part of each plot. The slope of the plots was 2.8%. In total, there were 16 plots under DAMC and 14 plots under WAMC because of missing data.

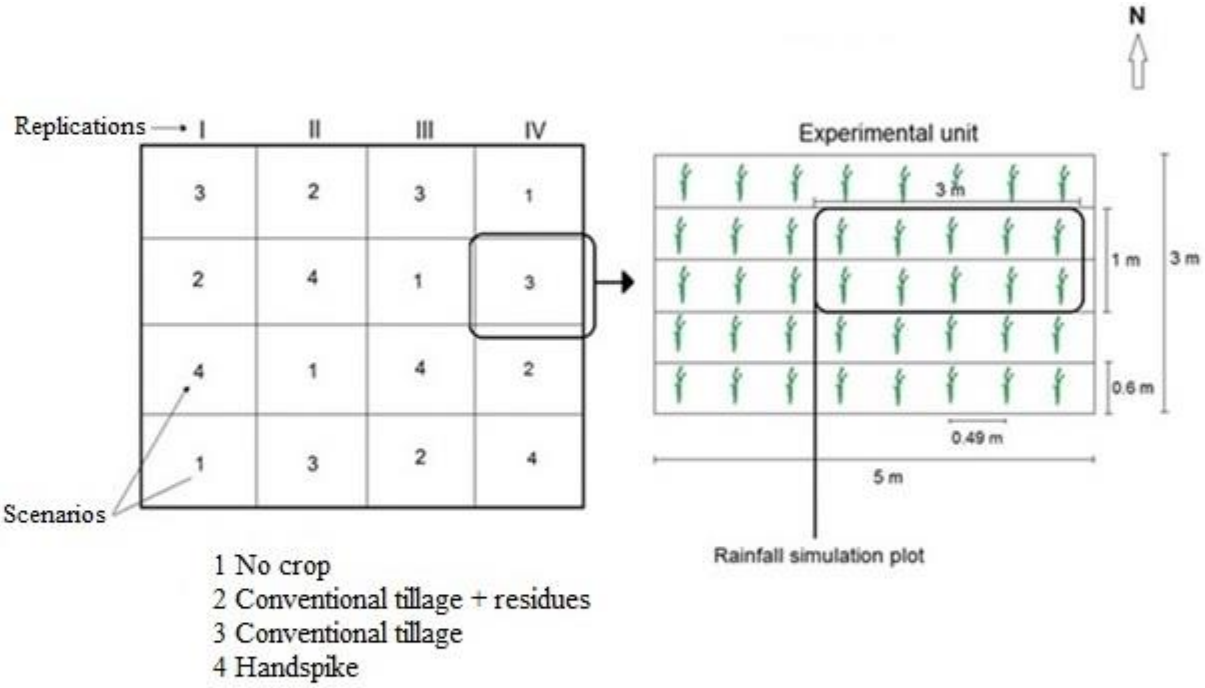

Figure 5-2. Distribution of scenarios on the experiment and dimensions of the rainfall simulation plot.

5.2.4. RUSLE parameterization

The main equation of RUSLE is the next:

$$A = R * K * LS * C * P \qquad \text{(Eq. 5-1)}$$

Where A is the annual average soil erosion (Mg ha^{-1} $year^{-1}$); R is the rainfall-runoff erosivity factor (mm h^{-1} ha^{-1} $year^{-1}$); K is the soil erodibility factor (Mg h^{-1} MJ^{-1} mm^{-1}); L is the slope length factor (dimensionless); S is the slope steepness factor (dimensionless); C is the land cover and management factor (dimensionless), and P is the soil conservation or prevention practices factor (dimensionless). All the factors were considered in this study, with exception of P factor, which value was equal to 1.

5.2.4.1. Calculation of R-factor

Renard et al. (1997) recommended calculating the R factor with equation 5-2.

$$R = \frac{\Sigma_{i=I}^{j}\,(EI_{30})_i}{N} \quad \text{(Eq. 5-2)}$$

Where R is the rainfall erosivity (M.J. mm^{-1} ha^{-1} h^{-1} $year^{-1}$); N is the number of years of observations; E is the kinetic energy (M.J. ha^{-1}), and I_{30} is the maximum intensity in 30 minutes for storm i; j is the number of storms in N years. The suggested value of kinetic energy by Renard et al., (1997) is 0.283 MJ ha^{-1} mm^{-1} for rainfall intensities greater than 76 mm h^{-1}, the mean measured rainfall intensity was 152 mm h^{-1}. The maximum measured rainfall intensity was assumed as the I_{30}, which was 352 mm h^{-1}. In this research, the resulted R factor was 99.61 MJ mm^{-1} ha^{-1} h^{-1}.

5.2.4.2. Calculation of K-factor

We calculated K factor based on a nonlinear relationship (Eq. 5-3) developed by Wang et al. (2016).

$$K = 0.0667 - 0.0013\left[\ln\left(\frac{SOM}{Dg}\right) - 5.6706\right]^2 - 0.015\ \exp\left[-28.9589\left((\log D\,g) + 1.827\right)^2\right] \quad \text{(Eq. 5-3)}$$

$$Dg = \exp(0.01 \cdot \Sigma_{i=1}^{n} f_i \ln m_i) \qquad \text{(Eq. 5-4)}$$

Where *Dg* is the geometric mean diameter (mm); *fi* is the weight of the particle size fraction, *mi* is the arithmetic mean of the particle size (mm), and *n* is the number of particle size fractions; *SOM* is the soil organic matter in %. The calculated K factor in the current study was 0.059 t ha^{-1} h^{-1}/ha MJ^{-1} mm^{-1} for all the scenarios because the equation considered SOM and Dg that were the same throughout the experiment.

5.2.4.3. Calculation of LS-factor

We used the equations 5-5 to 5-9 for calculating the LS factor.

$$L = \left(\frac{\lambda}{22.1}\right)^m \qquad \text{(Eq. 5-5)}$$

Where 22.1 is the RUSLE unit plot length (m); *m* is a variable slope-length exponent, λ is the horizontal projection of the plot length, which was 3 meters in this case.

The values of "m" exponent were 0.172 for conventional tillage and 0.454 for no till scenarios. These were obtained from the Table 2 of a research of McCool et al. (1989).

To calculate the slope steepness factor (S) we used the equations 5-6 and 5-7, for conventional tillage and no tillage scenarios, respectively (McCool et al., 1997).

$$S = 10.8\ \sin\theta + 0.03 \qquad s<9\% \quad \text{(Eq. 5-6)}$$

$$S = 16.8\ \sin\theta - 0.50 \qquad s\geq 9\% \quad \text{(Eq. 5-7)}$$

5.2.4.4. Calculation of C-factor

The C factor was obtained using the Eq. 5-8, we considered the conditions did not change rapidly, so EI was not in the calculation. The most subfactors of C are listed in Table 5-1.

$$SLR = PLU \cdot CC \cdot SC \cdot SR \cdot SM \quad \text{(Eq. 5-8)}$$

PLU is the prior land use, *CC* is the canopy cover, *SC* is the surface cover, *SR* is the surface roughness, and *SM* is the soil moisture.

The *PLU* includes the subsurface residual and tillage practices effects from the previous crop.

$$PLU = C_f \cdot C_b \cdot \exp\left[(-c_{ur} \cdot B_{ur}) + \left(\frac{c_{us} \cdot B_{us}}{C_f^{c_{uf}}}\right)\right] \quad \text{(Eq. 5-9)}$$

Where *PLU* ranges from 0 to 1, C_f is a soil consolidation factor (dimensionless), C_b is the effectiveness of subsurface residue in consolidation, B_{ur} is the mass density of roots (kg ha^{-1} cm^{-1}), B_{us} is the mass density of incorporated residues (kg ha^{-1}), c_{uf} is the impact of soil consolidation, C_{ur} and C_{us} are calibration coefficients. The prior land use (PLU) and the *b* value of surface cover subfactor (SC) were the same for all treatments, 0.45 and 0.030, respectively. The C_f was 0.45 because is the default value for undisturbed soil, the B_u, B_{ur}, B_{us}, C_b, c_{ur}, c_{us}, c_{uf} were not considered in the equation.

The canopy cover effect is represented by equation 5-10.

$$CC = 1 - F_c \cdot \exp(-0.1 \cdot H) \quad \text{(Eq. 5-10)}$$

F_c is the fraction of area covered by the canopy, and *H* is the distance that drops have to travel on the plant to reach the soil.

The % of canopy cover was estimated based on Equation 5-10 but with modifications proposed by Roloff and Bertol (1998). The relationship is presented in equation 5-11.

$$F_{C_d} = (1 - e^{-\varepsilon Bm} d)\delta \qquad \text{(Eq. 5-11)}$$

Where F_{Cd} is the soil fraction covered by canopy, Bm_d is the above-ground biomass in kg ha^{-1}, δ and ε are parameters according to a specific crop, in corn, δ is 0.67 and ε is 1.5 x 10^{-3}.

The surface cover subfactor *SC* accounts for everything on soil, such as crop residue, rocks, etc. The effect of *SC* is given by Eq. 5-12 (Yoder et al., 1997).

$$SC = \exp\left[-b \cdot S_p \cdot \left(\frac{0.24}{R_u}\right)^{0.08}\right] \quad \text{(Eq. 5-12)}$$

Where *b* is a coefficient of the effectiveness of surface cover. This varies from 0.030 to 0.070 in row crops; S_p is the percentage of covered area, R_u is the surface roughness.

The higher the *b*, the more significant the rill erosion. Large *b* corresponds to steep and/or long slopes. In contrast, the *b* value decreases if interrill erosion is more significant than rill erosion, common in flat and/or short slopes. *b* is also influenced by soil texture and soil cover.

The area covered by residue was obtained with Eq.5-13.

$$S_p = [1 - \exp(-\alpha \cdot B_s)] \cdot 100 \qquad \text{(Eq. 5-13)}$$

Where α is the ratio of covered area and the mass of the residue, B_s is the dry weight of residue.

The surface roughness was calculated using the Eq. 5-14 (Yoder et al., 1997).

$$SR = \exp[-0.66(R_u - 0.24)] \quad \text{(Eq. 5-14)}$$

Where R_u is the roughness before the tillage operation.

The soil moisture subfactor (SM) was obtained applying equation 5-15, considering the soil moisture, field capacity, and wilting point calculated with Eq. 5-16 and Eq. 5-17.

The soil moisture is near to 1.0 if the water content is close to field capacity. In contrast, a value of 0 indicates that soil moisture is near to the wilting point. Lianes Revilla (2008) proposed the following equation for SM:

$$SM = \frac{M - WP}{FC - WP} \qquad \text{(Eq. 5-15)}$$

Where *M* is the soil moisture (dimensionless); *W.P.* is the wilting point (%), and *F.C.* is the field capacity (%).

There are several approximations to obtain field capacity and wilting point considering the particle sizes of soil, as the equations proposed by Smith (1917) for field capacity (Eq. 5-16) and Silva et al. (1988) for wilting point (Eq. 5-17). Both were used in the present research.

$$FC = 0.1(\%\ sands) + 0.15(\%\ silt) + 0.61(\%\ clay) \quad \text{(Eq. 5-16)}$$

$$WP = FC * 0.74 - 5 \quad \text{(Eq. 5-17)}$$

Table 5-1. Subfactors used to calculate C factor in RUSLE for all the scenarios.

Scenario	R[a]	Rb[b]	Cc[c] (%)	AFH[d] (m)	Ru[e] (cm)	RC[f] (%)	VRC[g] (%)	SM dry[h]	SM wet[i]
No crop	1				1.68	1.66	0.00	0.20	0.92
	2				nd[j]			0.25	0.81
	3				nd			0.30	0.90
	4				1.93			0.45	0.90
Cinventional tillage + residues	1	48.88	3.32	0.26	1.27		23.33	0.31	0.98
	2	44.61	3.04	0.20	1.50		29.17	0.20	0.89
	3	111.14	7.31	0.48	1.45	1.66	35.00	0.40	0.89
	4	15.35	1.06	0.18	1.50		29.17	0.39	0.90
Conventional tillage	1	97.09	6.43	0.34	1.12	3.33		0.20	0.92
	2	55.93	3.79	0.32	1.70			0.28	0.90
	3	19.75	1.36	0.18	1.91			0.44	0.90
	4	33.68	2.31	0.29	1.09			0.44	0.90
Handspike	1	64.42	4.34	0.23	1.78			0.20	0.86
	2	38.67	2.64	0.25	1.85			0.28	0.94
	3	9.23	0.64	0.20	2.36			0.20	0.90
	4	28.54	1.96	0.26	1.42			0.47	0.90

[a] Replication. [b] Root biomass. [c] Canopy cover. [d] Average fall height. [e] Roughness; [f] Rock cover; [g] Vegetative residue cover. [h] Soil moisture subfactor under DAMC. [i] Soil moisture subfactor under WAMC. [j] No data.

5.2.5. WEPP parameterization

There are three modules of parameters in WEPP: weather, management and soil. The next paragraphs describe how we parameterized them.

In the single storm mode, the data for the weather module were 114.28 mm of storm amount, 0.75 of duration, 182.14 mm h^{-1} of maximum intensity, which was the maximum value registered of the mean, and 51 of duration to peak intensity.

Regarding the management parameterization, some parameters were measured, and others calculated from equations found in literature, some were not applicable, and they were left blank or with zero. WEPP has two groups of parameters in the management section, these are initial conditions and plant databases. The initial conditions are listed in Table 5-2, the canopy cover was estimated with the equation 11. The rill and interrill cover, ridge height and roughness were measured with a pin meter. The plant database is organized in plant growth and harvest, temperature and radiation, canopy, LAI (Leaf Are Index) and root, senescence, residue, and other. The biomass energy ratio and the parameter value for canopy height equation was obtained from the WEPP manual, as well as the base daily air temperature, optimal temperature for plant growth, radiation extinction coefficient which were 10, 25 and 0.65°C, respectively (Arnold et al., 1995; Flanagan and Livingston, 1995). The maximum canopy height was measured at field. The parameter of flat residue cover was based on investigations of Gregory (1982), he studied different types of residues, for corn he obtained 0.0004 ha kg^{-1}. This applied just for the treatment CTR. To obtain the growing degree days to emergence on October 1, 2015, we used the recorded temperature from a weather station located in the site of study applying the equation 5-18 (Abendroth et al., 2011)**.**

$$GDU = \left(\frac{T_{max}+T_{min}}{2}\right) - 10 \qquad \text{(Eq.5-18)}$$

Where GDU is the growing degree units, T_{max} is the maximum temperature, in this case was 29.2 ^{o}C, T_{min} is the minimum temperature, it was 8.6 ^{o}C. The number 10 is the base temperature of corn**.** To estimate the growing degree days for the growing season, the same equation was applied but adding all the days of the crop cycle.

Table 5-2. Parameters of initial conditions and plant database in management module of WEPP

Scenario	**NC[a]**				**CTR[b]**				**CT[c]**				**HS[d]**			
Replication	**I**	**II**	**III**	**IV**	**I**	**II**	**III**	**IV**	**I**	**II**	**III**	**IV**	**I**	**II**	**III**	**IV**
Bulk density (g cm^{-3})	1.5															
Canopy cover (%)					3	3.3	7.3	1.1	6.4	3.8	2.3	1.4	4.3	2.6	0.6	2
Rill cover (%)					48	15	11	21								
Interrill cover (%)					36	15	33	38								
Ridge height (cm)					4	4.3	4.3	5.7	3.7	4.7	6	4				
Roughness (cm)	1.7	1.2	1.7	2	1.3	1.5	1.5	1.5	1.1	1.7	1.9	1.1	1.8	1.9	2.4	1.5
Rill spacing (cm)					49											
Rill width (cm)					60											
Depth of primary tillage (cm)					15											
Depth of secondary tillage (cm)					10											
Biomass energy ratio (kg MJ^{-1})					28											
Growing degree days to emergence (°C)					8.9											
Growing degree days for growing season (°C)					266											
In-row plant spacing (cm)					49											
Stem diameter at maturity (cm)					2.7											
Parameter value for canopy height equation	3															
Maximum canopy height (cm)					20	27	49	19	34	33	29	19	24	25	21	26
Maximum root depth (cm)					15											
Root to shoot ratio					0.2											
Percent of growing season when leaf area index starts to decline					50											
Period over which senescence occurs					10											
Percent canopy remaining after senescence					30											
Percent of biomass remaining after senescence					20											
Parameter for flat residue cover equation (m^2 kg^{-1})					4											
Ridge height value after tillage (cm)					4	4.3	4.3	5.7	3.7	4.7	6	4				
Ridge interval (cm)					49											
Random roughness value after tillage (cm)	1.7	1.2	1.7	2	1.3	1.5	1.5	1.5	1.1	1.7	1.9	1.1	1.8	1.9	2.4	1.5
Mean tillage depth (cm)					10											
Optimum yield under no stress conditions (kg m^{-2})					0.8											

[a] No crop. [b] Conventional tillage + residues. [c] Conventional tillage. [d] Handspike.

The percent of growing season when LAI starts to decline was 50%, the period over which senescence occurs was fixed to 105 days, just through observing LAI and phenology of a four-month corn crop (Boedhram et al., 2001; Sacks and Kucharik, 2011).

In the soil module, the values for Cation Exchange Capacity (CEC), albedo, effective hydraulic conductivity, organic matter, sand and clay were 18, 0.23, 0.84 mm h^{-1}, 2.31%, 47%, 27%, respectively. The equation to determine the soil albedo (Eq. 5-19) was proposed by Baumer (1990).

$$SALB = \frac{0.6}{e^{0.4 \cdot OM}} \quad \text{(Eq. 5-19)}$$

Where *OM* is the percentage of soil organic matter.

To estimate the effective hydraulic conductivity, the default method was applied (Eq. 5-20) for all the scenarios (Alberts et al., 1995). It was 9.84 mm h^{-1}.

$$K_{hc} = -0.265 + 0.0086(sand)^{1.8} + 11.46CEC^{-0.75} \qquad \text{(Eq. 5-20)}$$

Other parameters like rock cover, and initial saturation level varied for each scenario. The coverage of soil by rocks was measured with a pin meter, and the initial saturation level with the oven drying method (Reynolds, 1970).

The flow and erosion parameters are enclosed in the soil module also, we assumed as negligible the rill erodibility and critical shear due to the dimensions of the plots, thus we set the rill erodibility to 0.002 s m^{-1} and the critical shear stress to $1x10^{-7}$ Pa. The interrill erodibility was set automatically to 5300000 kg s^{-1} m^4, which was then adjusted by WEPP according to canopy effects, ground cover and slope.

5.2.6. Evaluation of model performance

To evaluate the performance of RUSLE and WEPP, we selected the Nash-Sutcliffe efficiency index (NSE), the coefficient of determination (r^2) and percent bias (PBIAS). The equations are next:

$$r^2 = \left(\frac{\sum_{i=1}^{n}(O_i - \overline{O})(P_i - \overline{P})}{\sqrt{\sum_{i=1}^{n}(O_i - \overline{O})^2}\sqrt{\sum_{i=1}^{n}(P_i - \overline{P})^2}} \right)^2 \qquad \text{(Eq. 5-21)}$$

Where r^2 is the coefficient of determination, *Oi* is each of *i* observations, *Pi* is each of *i* predicted data, $\bar{O}$ is the mean of observed data, is the mean of predicted data and *n* is the number of total observations.

$$NSE = 1 - \frac{\sum_{i=1}^{n}(O_i - P_i)^2}{\sum_{i=1}^{n}(O_i - \overline{O})^2} \qquad \text{(Eq. 5-22)}$$

Where *NSE* is the Nash-Sutcliffe efficiency index, *Oi* is each of *i* observations, *Pi* is each of *i* predicted data, $\bar{O}$ is the mean of observed data, and *n* is the number of observations.

$$PBIAS = \left(\frac{\sum_{i=1}^{n}(Y_i obs - Y_i sim) \cdot (100)}{\sum_{i=1}^{n}(Y_i obs)} \right) \qquad \text{(Eq. 5-23)}$$

Where *PBIAS* is the deviation of evaluated data (%), $Y_i obs$ is the observed data, $Y_i sim$ is the simulated data, and *n* is the total of observations.

According to Moriasi et al. (2007) the performance of hydrological models is satisfactory when NSE is 0.50 or greater and PBIAS is 55% or lower for sediments.

5.2.7. Calibration and validation

We implemented new methods dividing the observed erosion in two groups, one for calibration and another for validation. The calibrated parameters were then considered in the validation phase.

5.2.7.1. RUSLE calibration

We focused just on changing the methods for calculating factors K and C during the calibration of RUSLE, keeping the methods of the other factors in the model unchanged. The new methods applied included the “measurement method” for estimating factor K and “expert suggestions” for factor C. These additional methods were combined with the ones originally used, resulting in four sets to calibrate RUSLE. Table 5-3 presents such sets, being the first, the methods also used in uncalibrated RUSLE. The estimated K and C factors are listed in Table 5-4.

The measurement method was based on the equations 5-24 and 5-25.

$$a_u = \frac{a_f}{L_f S_f C_f P_f} \quad \text{(Eq. 5-24)}$$

$$K = \frac{\Sigma_{j=1}^{n}(a_u)}{\Sigma_{j=1}^{n}(EI)_j} \quad \text{(Eq. 5-25)}$$

Where a_u is the estimated soil loss for a specific EI; a_f is the measured soil loss; L_f, S_f, C_f, and P_f are the other factors of USLE for a given plot (Foster et al., 1981).

In estimation of C factor, we considered expert suggestions from CONAFOR (2010), who proposed the following empirical values: 0.80 in CT, 0.15 in HS and 0.20 in CTR; they did not include no cropping, thus we used the mean of DAMC and WAMC obtained with the Eq. 5-8.

5.2.7.2. WEPP calibration

For calibrating WEPP, we changed the methods only for estimating the parameters interrill erodibility and effective hydraulic conductivity. We combined these new methods resulting in three sets for calibrating WEPP (Table 5-3)

We calculated the interrill erodibility (Table 5-5) with the Eq. 5-26 of Liebenow et al. (1990) and the effective hydraulic conductivity with the Eq. 5-27 (Ferrer Julià et al., 2004) for all the scenarios and Eq. 5-28 just for the CTR and CT (Alberts et al., 1995).

$$K_i = \frac{D_i}{I^2\left(1.05 - 0.85\exp^{-4\sin\emptyset}\right)} \qquad \text{(Eq. 5-26)}$$

Where K_i is the interrill erodibility in kg s^{-1} m^4, *Di* is the interrill erosion rate in kg m^{-2} m^{-1}, *I* is the rainfall intensity in m s^{-1}, and *ø* is the slope angle in radians.

Table 5-3 Methods used to estimate the parameters in calibration and validation of RUSLE and WEPP.

Set	RUSLE		WEPP	
	K Factor	**C Factor**	**Interrill erodibility**	**Effective hydraulic conductivity**
1	Eq. 3 of Wang et al. (2016). $K = 0.0667 - 0.0013\left[\ln\left(\frac{SOM}{Dg}\right) - 5.6706\right]^2 - 0.015\ \exp\left[-28.9589\left((\log D\ g) + 1.827\right)^2\right]$	Default. Eq. 8 $SLR = PLU \cdot CC \cdot SC \cdot SR \cdot SM$	Eq. 26 of Liebenow et al. (1990) $K_i = \frac{D_i}{I^2(1.05 - 0.85\exp^{-4\sin\emptyset})}$	Default. Eq. 28 of Alberts et al. (1995) for fallow conditions $K_{ef} = 1.17 + 7.2(sand)$
2	Measurement method. Eq. 25 $K = \frac{\Sigma_{j=1}^{n}(a_u)}{\Sigma_{j=1}^{n}(EI)_j}$	Same as Set 1	Same as Set 1	Eq. 27 of Ferrer Julià et al. (2004) $K_s = -4.994 + 0.56728 \cdot sand - 0.131 \cdot clay - 0.0127 \cdot org.mat$
3	Same as Set 1	Expert suggestions	Same as Set 1	Default. Eq. 20 of Alberts et al. (1995) just for all conditions $K_{hc} = -0.265 + 0.0086(sand)^{1.8} + 11.46CEC^{-0.75}$
4	Same as Set 2	Expert suggestions	Same as Set 1	

Table 5-4. Factors used in calibration and validation of the RUSLE. R and P factors are equal in all treatments and replications. R = 99.6; P = 1.2

<table>
<tr><th rowspan="2">Set</th><th rowspan="2">Treat.</th><th rowspan="2">Rep.</th><th rowspan="2">LS</th><th colspan="2">C</th><th colspan="2">K</th></tr>
<tr><th>Dry AMC</th><th>Wet AMC</th><th>Dry AMC</th><th>Wet AMC</th></tr>
<tr><td rowspan="4">1</td><td>NC[a]</td><td>1 - 4</td><td>0.31</td><td>0.10</td><td>0.42</td><td rowspan="4" colspan="2">0.06</td></tr>
<tr><td>CTR[b]</td><td>1 - 4</td><td>0.24</td><td>0.04</td><td>0.16</td></tr>
<tr><td>CT[c]</td><td>1 - 4</td><td>0.24</td><td>0.10</td><td>0.28</td></tr>
<tr><td>HS[d]</td><td>1 - 4</td><td>0.31</td><td>0.07</td><td>0.29</td></tr>
<tr><td rowspan="16">2</td><td rowspan="4">NC</td><td>1[e]</td><td rowspan="4">0.31</td><td>0.06</td><td>nd[h]</td><td>2.17</td><td>nd</td></tr>
<tr><td>2[e]</td><td>0.13</td><td>0.42</td><td>0.24</td><td>0.15</td></tr>
<tr><td>3[f]</td><td>0.10</td><td>0.42</td><td>1.20</td><td>0.15</td></tr>
<tr><td>4[f]</td><td>0.10</td><td>0.42</td><td>1.20</td><td>0.15</td></tr>
<tr><td rowspan="4">CTR</td><td>1[e]</td><td rowspan="4">0.24</td><td>0.03</td><td>0.14</td><td>1.55</td><td>0.65</td></tr>
<tr><td>2[e]</td><td>0.06</td><td>0.18</td><td>0.99</td><td>0.28</td></tr>
<tr><td>3[f]</td><td>0.04</td><td>0.16</td><td>1.27</td><td>0.47</td></tr>
<tr><td>4[f]</td><td>0.04</td><td>0.16</td><td>1.27</td><td>0.47</td></tr>
<tr><td rowspan="4">CT</td><td>1</td><td rowspan="4">0.24</td><td rowspan="4">0.09</td><td rowspan="4">0.28</td><td>nd</td><td>nd</td></tr>
<tr><td>2[e]</td><td>0.23</td><td>0.07</td></tr>
<tr><td>3[f]</td><td>0.23</td><td>0.07</td></tr>
<tr><td>4[f]</td><td>0.23</td><td>0.07</td></tr>
<tr><td rowspan="4">HS</td><td>1[e]</td><td rowspan="4">0.31</td><td>0.06</td><td>nd</td><td>1.15</td><td>nd</td></tr>
<tr><td>2[e]</td><td>0.09</td><td>0.29</td><td>0.41</td><td>0.32</td></tr>
<tr><td>3[f]</td><td>0.07</td><td>0.29</td><td>0.78</td><td>0.32</td></tr>
<tr><td>4[f]</td><td>0.07</td><td>0.29</td><td>0.78</td><td>0.32</td></tr>
<tr><td rowspan="7">3</td><td rowspan="4">NC</td><td>1</td><td rowspan="4">0.31</td><td>0.18[g]</td><td>nd</td><td rowspan="7" colspan="2">0.06</td></tr>
<tr><td>2</td><td colspan="2">0.27[g]</td></tr>
<tr><td>3</td><td colspan="2">0.23[g]</td></tr>
<tr><td>4</td><td colspan="2">0.23[g]</td></tr>
<tr><td>CTR</td><td>1 - 4</td><td>0.24</td><td colspan="2">0.20</td></tr>
<tr><td>CT</td><td>1 - 4</td><td>0.24</td><td colspan="2">0.80</td></tr>
<tr><td>HS</td><td>1 - 4</td><td>0.31</td><td colspan="2">0.15</td></tr>
<tr><td rowspan="16">4</td><td rowspan="4">NC</td><td>1</td><td rowspan="4">0.31</td><td>0.18[g]</td><td>nd</td><td>0.76</td><td>nd</td></tr>
<tr><td>2</td><td colspan="2">0.27[g]</td><td>0.11</td><td>0.22</td></tr>
<tr><td>3</td><td colspan="2">0.23[g]</td><td>0.44</td><td>0.22</td></tr>
<tr><td>4</td><td colspan="2">0.23[g]</td><td>0.44</td><td>0.22</td></tr>
<tr><td rowspan="4">CTR</td><td>1</td><td rowspan="4">0.24</td><td rowspan="4" colspan="2">0.20</td><td>0.25</td><td>0.47</td></tr>
<tr><td>2</td><td>0.28</td><td>0.25</td></tr>
<tr><td>3</td><td>0.26</td><td>0.36</td></tr>
<tr><td>4</td><td>0.26</td><td>0.36</td></tr>
<tr><td rowspan="4">CT</td><td>1</td><td rowspan="4">0.24</td><td rowspan="4" colspan="2">0.80</td><td>nd</td><td>Nd</td></tr>
<tr><td>2</td><td>0.03</td><td>0.03</td></tr>
<tr><td>3</td><td>0.03</td><td>0.03</td></tr>
<tr><td>4</td><td>0.03</td><td>0.03</td></tr>
<tr><td rowspan="4">HS</td><td>1</td><td rowspan="4">0.31</td><td rowspan="4" colspan="2">0.15</td><td>0.47</td><td>Nd</td></tr>
<tr><td>2</td><td>0.24</td><td>0.62</td></tr>
<tr><td>3</td><td>0.35</td><td>0.62</td></tr>
<tr><td>4</td><td>0.35</td><td>0.62</td></tr>
</table>

[a]No crop. [b]Conventional tillage + residues. [c]Conventional tillage. [d]Handspike. [e]Replications used in calibration. [f]Replications used in validation. [g]No experts suggestions available, the default method was applied. [h]No data.

$$K_s = -4.994 + 0.56728 \cdot sand - 0.131 \cdot clay - 0.0127 \cdot org.mat \quad \text{(Eq. 5-27)}$$

Where K_s is the hydraulic conductivity in mm h^{-1}, *sand*, *clay* and *org.mat* are in percentage.

$$K_{ef} = 1.17 + 7.2(sand) \qquad \text{(Eq. 5-28)}$$

Where K_{ef} is the hydraulic conductivity for fallow conditions in mm h^{-1}.

The resulted hydraulic conductivity was 18. 10 mm h^{-1} applying the equation 5-27, and 7.19 mm h^{-1} with the equation 5-28.

Table 5-5. Interrill erodibility and initial saturation level used in calibration and validation of WEPP for both Dry and Wet Antecedent Soil Moisture conditions (DAMC and WAMC).

Treatment & Replication			**Interrill erodibility ($kg\ m^{-4}\ s^{-1}$)**	**Int. sat. (%)**
DAMC	NC[a]	1[e]	232597.91	16.19
		2[e]	51803.65	16.85
		3[f]	142200.78	17.4
		4[f]	142200.78	19.08
	CTR[b]	1[e]	63875.37	16.19
		2[e]	72618.16	17.56
		3[f]	68246.76	18.52
		4[f]	68246.76	18.48
	CT[c]	2[e]	27088.93	17.21
		3[e]	57633.29	18.99
		4[f]	42361.11	18.98
	HS[d]	1[e]	117446.29	16.19
		2[e]	60327.99	17.21
		3[f]	88887.1083	16.28
		4[f]	88887.1083	19.38
WAMC	NC	2	102210.90	23.32
		3	102210.90	24.39
		4	102210.90	24.36
	CTR	1	121300.76	24.28
		2	64445.72	25.33
		3	92873.24	24.24
		4	92873.24	24.32
	CT	2	26609.36	24.32
		3	84752.14	24.37
		4	55680.75	24.36
	HS	2	154591.55	24.80
		3	154591.55	24.33
		4	154591.55	24.35

[a] No crop. [b] Conventional tillage + residues. [c] Conventional tillage. [d] Handspike.
[e]Replications used in Calibration. [f]Replications used in validation.

5.3. Results and discussion

5.3.1. Performance of RUSLE

The uncalibrated RUSLE exhibited good performance in treatments of CT and HS under DAMC and NC, CT, and HS under WAMC, where the r^2 was high (more than 0.70). During calibration, RUSLE performance improved in CT under WAMC using method 1, and in all treatments using methods 2 and 4, as these methods incorporated observed erosion data into their calculations. Later, during validation, RUSLE exhibited good performance (with PBIAS from -43.98% to 49.19%) in all treatments using different methods. Methods 2 and 4 generally yielded the best performances, except for CT under the two AMC's, where method 3 outperformed the others (see Table 5-6).

Table 5-6. Statistics of performance for uncalibrated, calibrated and validated RUSLE for both Dry and Wet Antecedent Soil Moisture conditions (DAMC and WAMC).

	Uncalibrated	Calibration				Validation			
		1	**2**	**3**	**4**	**1**	**2**	**3**	**4**
Dry AMC									
No crop									
NSE	-2.97	-2.23	1	-1.86	1	-5.51	-1.26	-4.44	-0.35
PBIAS	91.33	93.25	0	84.19	0	92.91	-44.39	83.40	-23.26
r^2	0.49	na[a]	na	na	na	na	na	na	na
Conventional tillage + residues									
NSE	-16.86	-219.86	1	-146.8	1	-11.69	-2.59	-6.53	-1.65
PBIAS	93.62	95.06	0	77.61	0	93.32	-43.98	69.75	-35.08
r^2	0.03	na	na	na	1	na	na	na	na
Conventional tillage									
NSE	-2.26	na	na	na	na	-7.46	-4.17	-0.78	-4.17
PBIAS	85.17	74.55	0	-125.66	0	92.08	68.85	29.70	68.85
r^2	0.93	na	na	na	na	na	na	na	na
Handspike									
NSE	-2.56	-8.24	1	-6.73	1	-2.92	-0.33	-2.60	-0.46
PBIAS	92.11	91.73	0	83.32	0	94.87	31.74	89.59	37.59
r^2	0.74	na	na	na	1	na	na	na	na
Wet AMC									
No crop									
NSE	-1.25	na	na	na	na	-1.32	-0.50	-1.65	-0.69
PBIAS	77.35	59.82	0	73.62	0	79.58	49.19	88.84	57.71
r^2	0.99	na	na	na	na	na	na	na	na
Conventional tillage + residues									

NSE	-16.73	-8.13	1	-7.45	1	-161.76	-0.30	-150.81	-1.23
PBIAS	88.76	86.82	0	83.54	0	87.83	3.78	84.80	7.65
r^2	0.23	na	na	na	1	na	na	na	na
Conventional tillage									
NSE	-2.07	na	na	na	na	-41.77	-36.46	-9.28	-36.46
PBIAS	68.57	18.41	0	-129.73	0	77.45	72.37	36.52	72.37
r^2	0.79	na	na	na	na	na	na	na	na
Handspike									
NSE	-3.52	na	na	na	na	-3.24	-0.31	-3.75	-0.31
PBIAS	85.44	81.49	0	90.41	0	86.45	26.78	92.98	26.78
r^2	0.79	na	na	na	na	na	na	na	na

[a] Not applicable.

The good performance of uncalibrated RUSLE may be questionable due to the calculation of r^2 using 4 replications, a small number of data points. In this context, it is prudent to consider the other two statistics available, NSE and PBIAS. Both NSE and PBIAS indicated poor model performance, with negative values for NSE and PBIAS exceeding 55% in all treatments.

The calibration of RUSLE aimed to enhance model performance by changing parameter values for further validation. Table 5-4 lists the calibrated and validated parameters, which varied depending on the method used and treatments.

For the validated K factor, it was evident that methods 2 and 4 consistently produced K values with the best performance across all treatments, except for method 3. Method 3 exhibited good performance specifically in CT under both AMC's. Notably, method 4 generally produced lower K values compared to method 2, except in the case of NC under DAMC.

Regarding the influence of AMC on K values, we observed they were generally lower under WAMC compared to DAMC. This suggests a higher resistance to erosion when the soil is moist, leading to lower soil erodibility. In terms of tillage treatments, there was no clear trend observed in K values. The influence of tillage treatment on K factor varied across different scenarios, indicating that the impact of tillage practices on soil erodibility may be complex and context-dependent.

For the validated C factor, Method 4 generally yielded larger values of the C factor across all treatments, except for in CT under both AMC's, where Method 3 produced the highest C value recorded in the study, reaching 0.80. Additionally, in the case of HS under wet AMC, Method 2 also resulted in a higher C value compared to Method 4.

Additionally, the C values were generally higher under WAMC compared to DAMC in most treatments that may indicate a higher susceptibility to erosion when the soil is moist. Notably, Method 2 exhibited sensitivity to AMC, with C values being higher under WAMC compared to DAMC, which was not observed with other methods. Also, the highest value of C factor emerged in CT (with method 3 under both AMC's), while the lowest value occurred in CTR.

In other studies applying the RUSLE, researchers have obtained wide ranges of model performances. Spaeth et al. (2003), similar to the current study, reported negative and low values of NSE for experiments conducted in U.S. with natural vegetation and rainfall simulation. The best performance happened under DAMC. The methods used to calculate K factor included the nomograph and the NRCS, while the estimation of C involved field measurements and values derived from the best fitting of a relation of vegetation with root mass, production potential and soil roughness. These results contrasted with ours as the best performance statistics were observed under WAMC, also the methods involved in calculation of factors were different.

Other study conducted by Biddoccu et al. (2020) in vineyards of Europe showed negative values of NSE as low as -33.69, similar to the present research, but the authors obtained positive values as high as 0.84. These investigators also achieved an r^2 from 0.14 to 0.83, a statistic that we could not calculate in validation here due to few replications. Their best results were obtained under CT, where the K factor (0.025 to 0.064 t ha^{-1} h^{-1}/ha MJ^{-1} mm^{-1}) was calculated using a nomograph constant based on a model proposed by Borselli et al. (2012), and C factor (0.13 to 0.54) applying default equation.

In a watershed study in India, Das et al., 2021 simulated erosion using RUSLE, achieving an NSE of 0.73. The watershed comprised 26.4% agriculture lands and scrubland, with slopes ranging from 0 to 8% and sandy clay loam soil texture in those areas. The mean K factor was 0.18 t ha^{-1} h^{-1}/ha MJ^{-1} mm^{-1}, derived from a modification of the nomograph method. The C factor ranged between 0.50 and 1, calculating it with the NDVI as suggested by van der Knijff et al. (2000). Comparing our results, the closest K factor value to theirs was 0.15, occurring in NC under WAMC, calculated with the measurement method (PBIAS= 49.19%). Similarly, our closest C factor values to theirs were 0.42 and 0.80, observed in NC under WAMC (PBIAS= 49.19%, obtained with the default method), and in CT under both DAMC and WAMC, respectively. The latter was determined using methods 3 (PBIAS=29.70% under DAMC and PBIAS= 36.52% under WAMC) and 4 (PBIAS=68.85% under DAMC and PBIAS= 72.37% under WAMC).

In a one-year study conducted by Vieira et al. (2018) with natural rainfall on post-fire soils in Portugal, researchers calculated K factor (0.017 t ha^{-1} h^{-1}/ha MJ^{-1} mm^{-1}) using the nomograph method and the C factor (0.13) using an equation proposed by Borrelli et al. (2016), which provided specific values for disturbed lands. The RUSLE predicted soil loss with a NSE of 0.70, r^2 of 0.89 and PBIAS of -20.1, indicating good model performance. We also evaluated model performance using these three statistics in the current research, but our experiment achieved good performance based solely on PBIAS.

5.3.2. Performance of WEPP

Without calibration, WEPP exhibited poor performance, which improved after calibration in most treatments. Particularly, the best performance was observed in CT treatment under both DAMC and WAMC when all three calibration methods were applied. Among these methods, Method 1 stood out, incorporating interrill erodibility based on observed erosion and effective hydraulic conductivity calculated with Equation 5-28 tailored for fallow conditions, yielding the most favorable performance statistics.

During validation, Method 1demonstrated superior performance in CT under WAMC, with a PBIAS of 25.97%. Conversely, Method 3 exhibited the lowest level of acceptable performance in CT under DAMC, with a PBIAS of 50.37%, as shown in Table 5-7.

Table 5-7 Statistics of performance for uncalibrated, calibrated and validated WEPP for both Dry and Wet Antecedent Soil Moisture conditions (DAMC and WAMC).

	Uncalibrated	Calibration			Validation		
		1	2	3	1	2	3
Dry AMC							
No crop							
NSE	-1192.19		-0.24	0.02		-1.35	-0.80
PBIAS	-1827.68		57.49	35.92		51.31	42.81
r^2	0.09		na[a]	na		na	na
Conventional tillage + residues							
NSE	-18953.49	-52.38	-68.53	-49.77	-0.94	-2.26	-1.34
PBIAS	-3097.38	45.02	51.89	49.68	28.00	42.02	32.91
r^2	0.13	na	na	na	na	na	na
Conventional tillage							
NSE	-9179.04	0.99	0.70	0.98	na	na	na
PBIAS	-4964.64	-1.75	18.10	3.89	47.78	57.83	50.37
r^2	0.83	na	na	na	na	na	na
Handspike							
NSE	-1555.20		-2.48	-1.70		-1.80	-1.58
PBIAS	-2024.44		49.42	40.46		80.30	76.70
r^2	0.00		na	na		na	na
Wet AMC							
No crop							
NSE	-463.33		na	na		-1.09	-0.98
PBIAS	-1564.35		45.10	35.92		72.13	72.35
r^2	0.29		na	na		na	

Conventional tillage + residues							
NSE	-7566.72	-2.58	-3.64	-2.84	-82.54	-150.30	-60.08
PBIAS	-1863.23	47.68	57.50	50.26	61.89	84.69	53.62
r^2	0.96	na	na	na	na	na	na
Conventional tillage							
NSE	-10758.72	0.99	0.84	0.99	na	na	na
PBIAS	-4545.98	-1.41	17.82	3.52	25.97	40.74	29.74
r^2	0.44	na	na	na	na	na	na
Handspike							
NSE	-929.09		na	na		-2.18	-1.87
PBIAS	-1230.56		23.40	9.55		76.82	72.71
r^2	0.05		na	na		na	na

[a] Not applicable.

These results are in line with those of Onsamrarn et al. (2020), who conducted a study under natural rainfall conditions with corn, soil texture of sandy loam to clay loam, and slope gradients from 6 to 12%. Their validation results showed an NSE of -1.89 and an r^2 of 0.26 with no PBIAS calculated. They proposed calibrated interrill erodibility (250000 kg s^{-1} m^{-4}) and hydraulic conductivity (80 mm h^{-1}) parameters for both maize monocropping with conventional tillage and intercropping high-value chili with *Leucaena* hedgerow with minimum tillage. Our closest calibrated and validated interrill erodibility value to theirs was 154591.55 kg m^{-4} s^{-1}, with hydraulic conductivity values of 18.10 and 9.8 mm h^{-1} in HS treatment under WAMC, where WEPP performed poorly.

In our treatment with the best WEPP performance, CT under WAMC, the interrill erodibility was 55680.75 kg s^{-1} m^{-4} and hydraulic conductivity 18.10, 9.8 and 7.19 mm h^{-1}. Interestingly, the interrill erodibility in Onsamrarn et al.’s investigation was almost three times higher than ours, despite similar soil conditions in their monocrop practice and our CT treatment. Onsamrarn et al. (2020) did not vary this parameter between treatments, consistent with the recommendation in WEPP manual to define a baseline interrill erodibility modified by the model based on vegetation and soil crusting characteristics.

However, we used an equation for calculating interrill erodibility that already included effects from rainfall intensity, sediments rate and slope, potentially resulting in an inaccurate baseline interrill erodibility as required by the WEPP software. Despite this potential discrepancy, our validated interrill erodibility contributed to good WEPP performance (PBIAS of 25.97 and 29.74%). It is worth noting that the uncalibrated WEPP in CT under WAMC showed poor performance, possibly due to WEPP-calculated interrill erodibility.

The baseline interrill erodibility value (for croplands) used by WEPP, assuming 20% of the sand fraction as very fine sand (Panagos et al., 2014), would be 4533740 kg s^{-1} m^{-4}. The WEPP manual recommends a range of interrill erodibility baseline of 500000 to 12000000 kg s^{-1} m^{-4}, indicating that both Onsamrarn et al. (2020) and our study had relatively low interrill erodibility inputs. Hypothetically, a better value of interrill erodibility would fall between the range of 140000 and 250000 kg s^{-1} m^{-4}, disregarding the lowest value suggested in the WEPP manual.

In another study, Mirzaee and Ghorbani-Dashtaki (2021) conducted experiments with artificial rainfall on bare fallow conditions and calcareous soils with slopes mostly greater of 25%. Initially, they observed poor performance from the WEPP model (r^2= 0.09) when using baseline erodibility parameters calculated following WEPP manual recommendations. However, they achieved significant improvement in results (r^2= 0.68) by adopting a new method for calculating erodibility parameters, as proposed by Mirzaee et al. (2017), which involved stepwise multiple-linear regression and artificial neural networks.

Mirzaee and Ghorbani-Dashtaki (2021) reported a mean of interrill erodibility of 2000000 kg s^{-1} m^{-4}, contrasting with the calculated mean of 3300000 kg s^{-1} m^{-4} using the WEPP manual suggestions. Once again, the study demonstrated that lower values of interrill erodibility than the recommended led to better prediction outcomes.

In another study with rainfall simulation in forest environments, Xia et al. (2019) reported NSE values of -0.901 and 0.81 for uncalibrated and calibrated WEPP, respectively. Initially, the researchers followed WEPP recommendations for calculating the erodibility parameter, resulting in a value of 1041200 kg s^{-1} m^{-4}. However, after artificially calibrating it to fit the observed data, they improved model performance, with the interrill erodibility adjusted to 4974960 kg s^{-1} m^{-4}. The authors concluded that lower values of soil erodibility and hydraulic conductivity led to enhanced WEPP performance.

5.3.3. Comparison of RUSLE and WEPP

Before calibration, WEPP exhibited poor performance, unlike RUSLE, which showed good performance in all treatments except in CTR, based on r^2 values. WEPP underpredicted soil erosion by over 1000%, while RUSLE overpredicted it by more than 68%.

Following calibration, RUSLE's performance improved to perfection in all treatments, whereas WEPP showed good performance, particularly in the CT treatment (refer to Tables 5-6 and 5-7). In validation, RUSLE performed well in all the treatments except in CT under both DAMC and WAMC, while WEPP performed well only in CT under WAMC.

Both RUSLE and WEPP performances were influenced not only by their respective parameters but also by the methods employed in their calculation. Notably, default methods impacted better in RUSLE performance than in WEPP. It is worth mentioning that, in RUSLE, the equation referred to as the default method for calculating the K factor the equation was not the one recommended by RUSLE developers, but rather an enhanced version of it. The methods that worked better in calibration of both models included observed data.

PBIAS ranged from 53.62 % to 28% in WEPP and from 49.19% to 3.78% in RUSLE. In NC under DAMC, RUSLE demonstrated superior performance, whereas WEPP excelled in simulating soil erosion in CTR under the same conditions. Furthermore, RUSLE outperformed WEPP in CT under DAMC and HS under DAMC scenarios. Similarly, RUSLE exhibited better simulation results in NC and CTR under DAMC conditions. Conversely, WEPP showed better performance in CT under WAMC conditions, while RUSLE was more effective in predicting erosion in HS under WAMC conditions.

5.4. Conclusions

The empirical approach of RUSLE simulated better the soil erosion than the physical approach of WEPP in the specific conditions of the current study: short term erosion in corn cropping under conventional tillage plus residues or zero tillage, high rainfall intensities, sandy clay loam soil and slopes near to 2.8%.

The input data to parameterize the two models played a crucial role on their performance. The wider use of RUSLE made easier to find a C factor suggested by other researchers for crop management, as well as alternative equations of K factor. The developers of WEPP suggested to calibrate based on soil parameters (Flanagan and Frankenberger, 2012), but in the current research conditions, like the absence of measured hydraulic conductivity and flow velocity, it may be useful to calibrate based on crop management too.

The RUSLE simulated successfully the erosion in all the studied treatments except in CT under both DAMC and WAMC, while WEPP performed well just in CT under WAMC.

These findings underscore the importance of considering specific agricultural management practices and environmental conditions when selecting erosion prediction models for accurate soil erosion.

References

Abendroth, L.J., Elmore, R.W., Boyer, M.J., Marlay, S.., 2011.Corn growth and development. Iowa State University, University Extension.

Alberts, E.E., Nearing, M.A., Weltz, M.A., Risse, L.M., Pierson, F.B., Zhang, X.C., Laflen, J.M., Simanton, J.R., 1995.SOIL COMPONENT. In: USDA-Water Erosion Prediction Project (WEPP). National Soil Erosion Research Laboratory. NSERL Report No. 10, West Lafayette, IN, pp. 1–47.

Alewell, C., Borrelli, P., Meusburger, K., Panagos, P., 2019.Using the USLE: Chances, challenges and limitations of soil erosion modelling.International Soil and Water Conservation Research., 7, 203–225.

Arnold, J.G., Srinivasan, R., Muttiah, R.S., Williams, J.R., 1998.LARGE AREA HYDROLOGIC MODELING AND ASSESSMENT PART I: MODEL DEVELOPMENT.Journal of American Water Resources Association., 34, 73–89.

Arnold, J.G., Weltz, M.A., Alberts, E.E., Flanagan, D.C., 1995.PLANT GROWTH COMPONENT. In: USDA-Water Erosion Prediction Project (WEPP). National Soil Erosion Research Laboratory. NSERL Report No. 10, West Lafayette, IN, pp. 1–41.

Baumer, O., 1990.Predictions of Soil Hydraulic Parameters. In: WEPP Data Files for Indiana SCS National Soil Survey Lab. Lincoln, Nebraska, United States.

Beasley, D.B., Huggins, L.F., Monke, E.J., 1980.ANSWERS: a model for watershed planning.Transactions, American Society of Agricultural Engineers., 23, 938–944.

Biddoccu, M., Guzmán, G., Capello, G., Thielke, T., Strauss, P., Winter, S., Zaller, J.G., Nicolai, A., Cluzeau, D., Popescu, D., Bunea, C., Hoble, A., Cavallo, E., Gómez, J.A., 2020.Evaluation of soil erosion risk and identification of soil cover and management factor (C) for RUSLE in European vineyards with different soil management.International Soil and Water Conservation Research., 8, 337–353.

Boedhram, N., Arkebauer, T.J., Batchelor, W.D., 2001.Season-long characterization of vertical distribution of leaf area in corn.Agronomy Journal., 93, 1235–1242.

Borrelli, P., Alewell, C., Alvarez, P., Anache, J.A.A., Baartman, J., Ballabio, C., Bezak, N., Biddoccu, M., Cerdà, A., Chalise, D., Chen, S., Chen, W., De Girolamo, A.M., Gessesse, G.D., Deumlich, D., Diodato, N., Efthimiou, N., Erpul, G., Fiener, P., Freppaz, M., Gentile, F., Gericke, A., Haregeweyn, N., Hu, B., Jeanneau, A., Kaffas, K., Kiani-Harchegani, M., Villuendas, I.L., Li, C., Lombardo, L., López-Vicente, M., Lucas-Borja, M.E., Märker, M., Matthews, F., Miao, C., Mikoš, M., Modugno, S., Möller, M., Naipal, V., Nearing, M., Owusu, S., Panday, D., Patault, E., Patriche, C.V., Poggio, L., Portes, R., Quijano, L., Rahdari, M.R., Renima, M., Ricci, G.F., Rodrigo-Comino, J., Saia, S., Samani, A.N., Schillaci, C., Syrris, V., Kim, H.S., Spinola, D.N., Oliveira, P.T., Teng, H., Thapa, R., Vantas, K., Vieira, D., Yang, J.E., Yin, S., Zema, D.A., Zhao, G., Panagos, P., 2021.Soil erosion modelling: A global review and statistical analysis.Science of the Total Environment., 780.

Borrelli, P., Panagos, P., Langhammer, J., Apostol, B., Schütt, B., 2016.Assessment of the cover changes and the soil loss potential in European forestland: First approach to derive indicators to capture the ecological impacts on soil-related forest ecosystems.Ecological Indicators., 60, 1208–1220.

Borselli, L., Torri, D., Poesen, J., Iaquinta, P., 2012.A robust algorithm for estimating soil erodibility in different climates.Catena., 97, 85–94.

CONAFOR, 2010.Coordinación general de producción y productividad.Estudios técnicos especializados para la recuperación de áreas degradadas por disturbios y/o perturbaciones antropogénicas.

Coulthard, T.J., Macklin, M.G., Kirkby, M.J., 2002.A cellular model of Holocene upland river basin and alluvial fan evolution.Earth Surface Processes and Landforms., 27, 269–288.

Das, S., Deb, P., Bora, P.K., Katre, P., 2021.Comparison of rusle and mmf soil loss models and evaluation of catchment scale best management practices for a mountainous watershed in india.Sustainability (Switzerland)., 13, 1–22.

FAO, ITPS, 2015.Status of the World's Soil Resources (SWSR) - Main Report. Rome, Italy.

Ferrer Julià, M., Estrela Monreal, T., Sánchez Del Corral Jiménez, A., García Meléndez, E., 2004.Constructing a saturated hydraulic conductivity map of Spain using pedotransfer functions and spatial prediction.Geoderma., 123, 257–277.

Flanagan, D.C., Frankenberger, J.R., 2012.Wepp: model use, calibration, and vaidation.Transactions of the American Society of Agricultural and Biological Engineers., 55, 1463–1477.

Flanagan, D.C., Gilley, J.E., Franti, T.G., 2007.Water Erosion Prediction Project (WEPP).Transactions of the ASABE., 50, 1603–1612.

Flanagan, D.C., Ii, J.C.A., Nicks, A.D., Nearing, M.A., Laflen, J.M., 1995.OVERVIEW OF THE WEPP EROSION PREDICTION MODEL. In: USDA-Water Erosion Prediction Project. U.S. Department of Agriculture, West Lafayette, IN, pp. 1–12.

Flanagan, D.C., Livingston, S.J., 1995.WEPP user summary., 141.

Foster, G.R., McCool, D.K., Renard, K.G., Moldenhauer, W.C., 1981.Conversion of the universal soil loss equation to SI metric units.Journal of Soil and Water Conservation., 36, 355–359.

Gregory, J.M., 1982.Soil Cover Prediction with Various Amounts and Types of Crop Residue.Transactions of the ASAE., 25, 1333–1337.

Lianes Revilla, E., 2008.Estudio del factor vegetación "C" de la ecuación universal de pérdidas de suelo revisada "RUSLE" en la cuenca del río Birrís (Costa Rica). Universidad Politécnica de Madrid.

Liebenow, A.M., Elliot, W.J., Laflen, J.M., Kohl, K.D., 1990.of Data From Cropland Soils.American Society of Agricultural Engineers., 33, 1882–1888.

M. Risse, L., A. Nearing, M., R. Savabi, M., 1994.Determining the Green-Ampt Effective Hydraulic Conductivity from Rainfall-runoff Data for the WEPP Model.Transactions of the ASAE., 37, 411–418.

Mai, J., 2023.Ten strategies towards successful calibration of environmental models.Journal of Hydrology., 620, 129414.

McCool, D.K., Foster, G.R., Mutchler, C.K., Meyer, L.D., 1989.Revised Slope Length Factor for the Universal Soil Loss Equation.Transactions of the American Society of Agricultural Engineers., 32, 1571–1576.

McCool, D.K., Foster, G.R., Weesies, G.A., 1997.Slope length and steepness factors (LS). In: Renard, K.G., Foster, G.R., Weesies, G.A., McCool, D.K., Yoder, D.C. (Eds.): Predicting Soil Erosion by Water: A Guide to Conservation Planning With the Revised Universal Soil Loss Equation (RUSLE). Agriculture Handbook No. 703. US Department of Agriculture, Wahington, DC, pp. 101–118.

Miller, W.P., 1987.A Solenoid-Operated, Variable Intensity Rainfall Simulator1.Soil Science Society of America Journal., 51, 832–834.

Mirzaee, S., Ghorbani-Dashtaki, S., 2021.Calibrating the WEPP model to predict soil loss for some calcareous soils.Arabian Journal of Geosciences., 14, 1–10.

Mirzaee, S., Ghorbani-Dashtaki, S., Mohammadi, J., Asadzadeh, F., Kerry, R., 2017.Modeling WEPP erodibility parameters in calcareous soils in northwest Iran.Ecological Indicators., 74, 302–310.

Moriasi, D.N., Arnold, J.G., Van Liew, M.W., Bingner, R.L., Harmel, R.D., Veith, T.L., 2007.Model evaluation guidelines for systematic quantification of accuracy in watershed simulations.American Society of Agricultural and Biological Engineers., 50, 885–900.

Nearing, A.M., Deer-Ascough, L., Laflen, M.J., 1990.SENSITIVITY ANALYSIS OF THE WEPP HILLSLOPE PROFILE EROSION MODEL.Transactions of the ASAE., 33, 839–849.

Notebaert, B., Vaes, B., Govers, G., 2006.WaTEM / SEDEM version 2006 Manual.Physical and Regional Geography Research Group.

Onsamrarn, W., Chittamart, N., Tawornpruek, S., 2020.Performances of the WEPP and WaNuLCAS models on soil erosion simulation in a tropical hillslope, Thailand.PLoS ONE., 15, 1–20.

Panagos, P., Meusburger, K., Ballabio, C., Borrelli, P., Alewell, C., 2014.Soil erodibility in Europe: A high-resolution dataset based on LUCAS.Science of the Total Environment., 479–480, 189–200.

Panagos, P., Standardi, G., Borrelli, P., Emanuele, L., Montanarella, L., Bosello, F., 2018.Cost of agricultural productivity loss due to soil erosion in the European Union : From direct cost evaluation approaches to the use of macroeconomic models.Land Degradation & Development., 29, 471–484.

Patil, R.J., 2018.Spatial techniques for soil erosion estimation: remote sensing and GIS approach. Springer, Cham.

Pimentel, D., Harvey, C., Resosudarmo, P., Sinclair, K., Kurz, D., Mcnair, M., Shpritz, L., Fitton, L., Saffouri, R., Blair, R., Pimentel, D., Harvey, C., Resosudarmo, P., Sinclair, K., Kurz, D., Mcnair, M., Crist, S., Shpritz, L., Fitton, L., Saffouri, R., Blair, R., 1995.Environmental and Economic Costs of Soil Erosion and Conservation Benefits.Science., 267, 1117–1123.

Prado-Hernández, J.V., Rivera-Ruiz, P., DeLeón-Mojarro, B., Carrillo-García, M., Martínez-Ruiz, A., 2017.Calibration of the USLE and MUSLE soil loss models in a mexican forest watershed: El Malacate case study.Agrociencia., 51, 265–284.

Renard, K.G., Foster, G.R., Weesies, G.A., Porter, J.P., 1991.RUSLE: revised universal soil loss equation.Journal of Soil & Water Conservation., 46, 30–33.

Renard, K.G., McCool, D.K., Cooley, K.R., Foster, G.R., Istok, J.D., Mutchler, C.K., 1997.Rainfall-Runoff Erosivity Factor (R). In: Renard, K.G., Foster, G.R., Weesies, G.A., McCool, D.K., Yoder, D.C. (Eds.): Predicting Soil Erosion by Water: A Guide to Conservation Planning With the Revised Universal Soil Loss Equation (RUSLE). Agriculture Handbook No. 703. US Department of Agriculture., Washington, D.C., pp. 19–38.

Reynolds, S.G., 1970.The gravimetric method of soil moisture determination Part I: A study of equipment, and methodological problems.Journal of Hydrology., 11, 258–273.

Roloff, G., Bertol, O.J., 1998.Method to estimate canopy cover and height of several summer crops.R. Bras. Ci. Solo., 22, 319–327.

Roose, E., 1996.Land husbandry: components and strategy, Soil Resources Management and Conservation Service Land and Water Development Division, FAO. Rome.

Sacks, W.J., Kucharik, C.J., 2011.Crop management and phenology trends in the U.S. Corn Belt: Impacts on yields, evapotranspiration and energy balance.Agricultural and Forest Meteorology., 151, 882–894.

Silva, A., Ponce de León, J., García, F., Durán, A., 1988.Aspectos metodológicos en la determinación de la capacidad de retener agua de los suelos de Uruguay.Boletín de investigación 10.

Smith, A., 1917.Relation of the mechanical analysis to the moisture equivalent of soils.Soil Science., 471–476.

Spaeth, K.E., Pierson, F.B., Weltz, M.A., Blackburn, W.H., 2003.Evaluation of USLE and RUSLE estimated soil loss on rangeland.Journal of Range Management., 56, 234–246.

van der Knijff, J.M., Jones, R.J.A., Montanarella, L., 2000.Soil erosion risk assessment in Europe, Luxembourg: Office for Official Publications of the European Communities.

Vieira, D.C.S., Serpa, D., Nunes, J.P.C., Prats, S.A., Neves, R., Keizer, J.J., 2018.Predicting the effectiveness of different mulching techniques in reducing post-fire runoff and erosion at plot scale with the RUSLE, MMF and PESERA models.Environmental Research., 165, 365–378.

Wang, B., Zheng, F., Guan, Y., 2016.Improved USLE- K factor prediction : A case study on water erosion areas in China.International Soil and Water Conservation Research., 4, 168–176.

Wang, S., McGehee, R.P., Guo, T., Flanagan, D.C., Engel, B.A., 2022.Calibration, validation, and evaluation of the Water Erosion Prediction Project (WEPP) model for hillslopes with natural runoff plot data.International Soil and Water Conservation Research.

Williams, J.R., 1990.The erosion-productivity impact calculator (EPIC) model: a case history.Philosophical Transactions of the Royal Society of London. Series B: Biological Sciences., 329, 421–428.

Wischmeier, W.H., Smith, D.D., 1978.Predicting rainfall erosion losses - a guide to conservation planning.

Woodward, D.E., 1999.Method to predict cropland ephemeral gully erosion.Catena., 37, 393–399.

Xia, L., Song, X., Fu, N., Cui, S., Li, L., Li, H., Li, Y., 2019.Effects of forest litter cover on hydrological response of hillslopes in the Loess Plateau of China.Catena., 181.

Yoder, D.C., Porter, J.P., Laflen, J.M., Simanton, J.R., Renard, K.G., McCool, D.K., Foster, G.R., 1997.Cover-Management Factor (C). In: Renard, K.G., Foster, G.R., Weesies, G.A., McCool, D.K., Yoder, D.C. (Eds.): Predicting Soil Erosion by Water: A Guide YODER DC, PORTER JP, LAFLEN JM, SIMANTON JR, RENARD KG, MCCOOL DK and FOSTER GR (1997) Cover-Management Factor (C). In: RENARD KG, FOSTER GR, WEESIES GA, MCCOOL DK and YODER DC (Eds.) Predicting Soil Erosion by Wa. U.S. Department of Agriculture, Wahington, DC, pp. 143–167.

Zingg, A.W., 1940.Degree and length of land slope as it affects soil loss in run-off.Agric. Engng., 21, 59–64.

CHAPTER 6.Sediment yield modeling: linking hillslope and watershed-scale analysis

Authors: Palmira Bueno Hurtado, Ousmane Seidou

Abstract

The modeling of sediment yield is crucial for evaluating soil erosion and informing conservation strategies. This research employed the Modified Universal Soil Loss Equation (MUSLE) to forecast sediment yield in an ungauged watershed located in North-Central Mexico. USLE factors LS, K, C, and Runoff were obtained from a prior hillslope-scale study, with the runoff factor being determined from the Curve Number (CN) and peak runoff estimated utilizing the Rational Method. The daily sediment yield was modeled using a water balance approach, which involved adjusting Actual Evapotranspiration (AET) according to variations in soil moisture. The findings demonstrated a nonlinear correlation between precipitation and sediment yield, where yield peaked at specific thresholds before stabilizing. Although numerous yield estimates corresponded to anticipated ranges, peak values were often higher than those recorded in comparable watersheds, suggesting that MUSLE proficiently captured sediment trends but might overestimate yields during high-intensity rainfall events. These results underscore the necessity for refining sediment yield models to achieve greater precision during extreme weather conditions.

Keywords: soil moisture, arid lands, MUSLE.

6.1. Introduction

Soil erosion remains a significant environmental challenge, particularly in regions susceptible to heavy rainfall and land use changes. It affects agricultural productivity, water quality, and ecosystem integrity (Pimentel and Kounang, 1998). The transport of eroded soil from hillslopes to water bodies is a critical component of this process, contributing to downstream sediment deposition that exacerbates flood risks, damages infrastructure, and degrades water quality (Lal, 2001). Accurate sediment yield estimation is therefore essential for conservation planning, especially in semi-arid regions where land degradation threatens environmental and agricultural sustainability (Boardman and Poesen, 2006).

The Modified Universal Soil Loss Equation (MUSLE), a widely used empirical model, has gained prominence for its adaptability in diverse environments and practical integration of runoff as a dynamic agent of sediment transport (Williams, 1975; Sadeghi et al., 2014). By replacing rainfall energy with runoff volume and peak flow, MUSLE allows robust sediment yield estimation in areas where direct measurements of soil and water properties are limited. Its flexibility has made it a valuable tool for addressing erosion in regions with highly variable hydrological conditions, such as arid and semi-arid landscapes (Renard et al., 1997a; Sadeghi et al., 2014).

Studies in Mexico have demonstrated MUSLE's utility in predicting sediment yield across diverse landscapes and hydrological conditions. Prado-Hernández et al. (2017) applied MUSLE in the El Malacate micro-basin, a 1.5 km² forested area in Michoacán, where over 60% of the land is covered by forests, the study concluded that MUSLE overestimated sediment yield, underscoring the importance of site-specific calibration for reliable predictions. Velásquez-Valle et al. (2016) utilized MUSLE in the La Cruz micro-basin, a 46.8-hectare grassland area in Zacatecas. The study produced sediment yield predictions ranging from 2.5 to 19.5 tons, with a strong correlation to observed values ($r^2 = 0.83$), demonstrating the importance of accurate parameterization.

In a larger-scale application, Galindo et al. (2017) employed the Soil and Water Assessment Tool (SWAT) to predict erosion in a 7,751 km^2 watershed in Oaxaca. SWAT incorporated MUSLE for sediment yield estimation, with runoff calculated using the Curve Number (CN2). Researchers validated the model based on the support practice factor (P) and the cover-management factor (C), achieving an r^2 of 0.58 and a Nash-Sutcliffe Efficiency (NSE) of 0.45. These studies highlight MUSLE's versatility across varied Mexican landscapes while emphasizing the need for careful calibration to local conditions.

Despite its widespread use, the precision of MUSLE in estimating sediment yield depends on effectively capturing factors such as topography, soil properties, and land cover, all of which influence erosion and sediment transport (Merritt et al., 2003). This is particularly critical in semi-arid regions, where variable rainfall and sparse vegetation can lead to sharp fluctuations in sediment yield. The nonlinear response of sediment transport to precipitation events, influenced by soil moisture, vegetation cover, and seasonal patterns, further complicates modeling efforts (Nearing et al., 2005; Beven, 2012). Addressing these challenges requires adapting models like MUSLE to better reflect the dynamic interactions between hydrological and sediment transport processes.

This study aimed to predict daily sediment yield in an ungauged watershed in North-Central Mexico using MUSLE, parameterized with data from hillslope-scale measurements and adapted to account for daily hydrological changes. By enhancing sediment yield estimation methods, this research supports sustainable watershed management and erosion control strategies tailored to semi-arid regions.

6.2. Materials and methods

This research focuses on watershed-scale analysis, using the SCS-Curve Number method from USDA Soil Conservation Service (1986), derived from a separate hillslope study. These values were applied in the MUSLE to estimate sediment yield across a watershed in North-Central Mexico. The study area is characterized by an arid climate, with average annual temperatures between 14 and 22 °C and annual rainfall ranging from 200 to 400 mm (Figure 6-1).

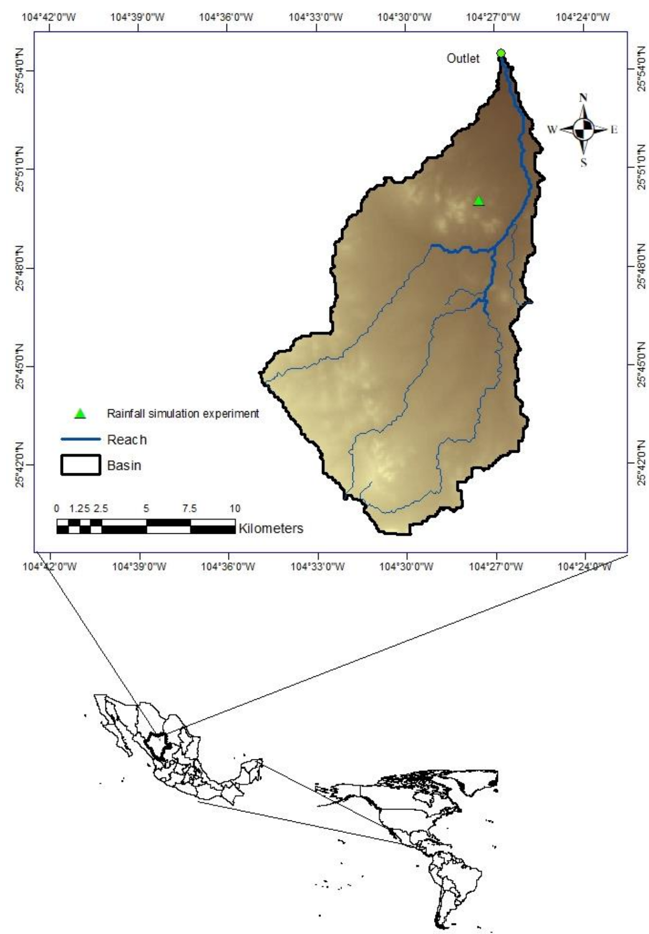

Figure 6-1. Location of the studies

For estimating sediment yield at the outlet of the studied basin, we recurred to the Equation 6-1.

$$S_y = a(Qq_p)^b K * LS * C * P \qquad \text{(Eq. 6-1)}$$

Where S_y represents sediment yield in t, Q is runoff in m^3, q_p is the peak flow rate in m^3s^{-1}, a and b are constants with default values of 11.8 and 0.56, respectively; K is the soil erodibility factor in Mg h^{-1} ha^{-1} MJ^{-1} mm^{-1}; L is the slope length factor (dimensionless), S is the slope steepness factor (dimensionless), C is the land cover and management factor (dimensionless), and P is the soil conservation practices factor (dimensionless). For our study, P was set to 1, indicating the absence of soil conservation practices.

Factors K and C were obtained from the hillslope scale study where the RUSLE was calibrated and validated under high-intensity simulated rainfall in a small portion of the current basin (Bueno-Hurtado and Seidou, 2024). Given the dominant land use of natural pastures and shrubs, we selected parameters from similar soil uses with the best performances. Specifically, we used the non-tillage treatment with maize for C with a value of 0.15 and the no crop treatment for K with a value of 0.11 (see Figure 6-2).

The LS factor was computed using equation 6-2 for L and equation 6-3 for Slope steepness.

$$L = \left(\frac{\lambda}{22.1}\right)^m \qquad \text{(Eq. 6-2)}$$

Where 22.1 is the standard unit plot length in m, λ is the slope length in m, and m is a variable slope-length calculated with equation 6-2 that is based in Table 2, for slight rill erosion, from a research of McCool et al. (1989).

$$m = \frac{x}{a + bx^{\gamma}} \qquad \text{(Eq. 6-3)}$$

Where x is the slope steepness in %, a is 10.60, b is 2.04, and γ is 0.94

The slope length λ was estimated using a digital elevation model (DEM) with a resolution of 15 meters (INEGI, 2019), processed with ArcMap, involving the Fill, Flow direction, and Flow accumulation tools to generate a map with slope lengths ranging from 0 to 132 m. The slope steepness factor was estimated using equation 6-4 (Wischmeier and Smith, 1978).

$$Slope\ steepness = 65.41\ sin^2\theta + 4.56 \sin\theta + 0.065 \quad \text{(Eq. 6-4)}$$

Where θ is the slope angle in radians. The LS factor values ranged from 0 to 114.945.

Runoff was estimated using the SCS-Curve Number method (Eq. 6-5).

$$Q = \frac{(P-I_a)^2}{(P-I_a)+S} \quad \text{(Eq. 6-5)}$$

Where Q is the runoff in mm, P is the precipitation in mm, I_a is the initial abstraction in mm (equal to λS, with λ set to 0.2), and S is the potential maximum retention in mm (Eq. 6-6).

$$S = \frac{25400}{CN} - 254 \quad \text{(Eq. 6-6)}$$

Rearranging equation 6-6 and solving for CN yields:

$$CN = \frac{25400}{S} + 254 \quad \text{(Eq.6-7)}$$

Only the CN values for the HS treatments were employed, as they were the most representative of the watershed conditions (Table 6-2).

To account for variations in soil moisture, the Curve Number (CN) was updated daily based on soil moisture conditions. Soil moisture was calculated using the Hargreaves method for potential evapotranspiration (PET) and a water balance approach to update soil moisture and actual evapotranspiration (AET). Specifically, daily soil moisture measurements informed adjustments to CN values, reflecting the effects of moisture on runoff potential.

Potential evapotranspiration was estimated with equation 6-8, which incorporates temperature data and extraterrestrial radiation.

$$ET_0 = \alpha(T + 17.8)\sqrt{(T_{max} - T_{min})}\, R_a \qquad \text{(Eq. 6-8)}$$

Where $T_{\max}$ and $T_{\min}$ are the daily maximum and minimum temperatures, and T is the mean temperature, R_a is calculated using equations 6-9 to 6-12.

$$R_a = \frac{(24)(60)}{\pi} 0.0820\, dr\left((\omega_s \sin\phi \sin\delta) + (\cos\phi \cos\delta \sin\omega_s)\right) \qquad \text{(Eq. 6-9)}$$

$$\delta = 0.409\ \sin\left(\frac{2\pi J}{365} - 1.39\right) \qquad \text{(Eq. 6-10)}$$

$$dr = 1 + 0.033\cos\left(\frac{2\pi J}{365}\right) \qquad \text{(Eq. 6-11)}$$

$$\omega_s = \arccos(-\tan\phi \tan\delta) \qquad \text{(Eq. 6-12)}$$

Where ϕ is the latitude in radians, J is the day of the year, δ is the solar declination, dr is the relative distance earth-sun, and ω_s is the sunset hour angle.

Actual evapotranspiration (AET) was derived based on the availability of water in the soil and the demand indicated by PET. The calculation of AET was constrained by soil moisture content, with AET being equal to PET when moisture was sufficient, less than PET when moisture was below field capacity (25%), and zero when soil moisture was at or below the wilting point (13%). The daily soil moisture was updated using a water balance approach that considered the previous day's soil moisture, daily precipitation, and AET. This method adjusted soil moisture based on rainfall and AET, ensuring that the values remained within the field capacity and wilting point limits.

The peak discharge q_p , that was obtained using the Rational Method with equation 6-13.

$$Q = CiA \qquad \text{(Eq. 6-13)}$$

Where Q is the peak discharge in m^3/s, C is the runoff coefficient, i is the rainfall intensity in m^3/s, and A is basin area in km^2.

Rainfall intensity was estimated from daily precipitation recorded at the nearest weather station, "Cinco de mayo", located at 25.774 N and 104.288 W (CONAGUA, 2020) for the period 1964 – 2003. We fit Gumbel distribution to extreme value analysis. We first converted daily precipitation data into maximum monthly precipitation values for a 2-year return period, then we adjusted to a 24-hour duration using a factor of 1.13 (Hershfield, 1961), we further multiplied the result by a factor corresponding to the portion of 1 hour.

The runoff coefficient was calculated by dividing the runoff obtained from equations 6-5 and 6-6 by historical precipitation.

Sediment yield was estimated by multiplying daily runoff values with pre-calculated KLSC raster. Each day's result was stored as a separate raster, we then aggregated these values to generate a comprehensive dataset, summarizing daily sediment yields, and further processed it to obtain per-hectare sediment yields (see Figure 6-2).

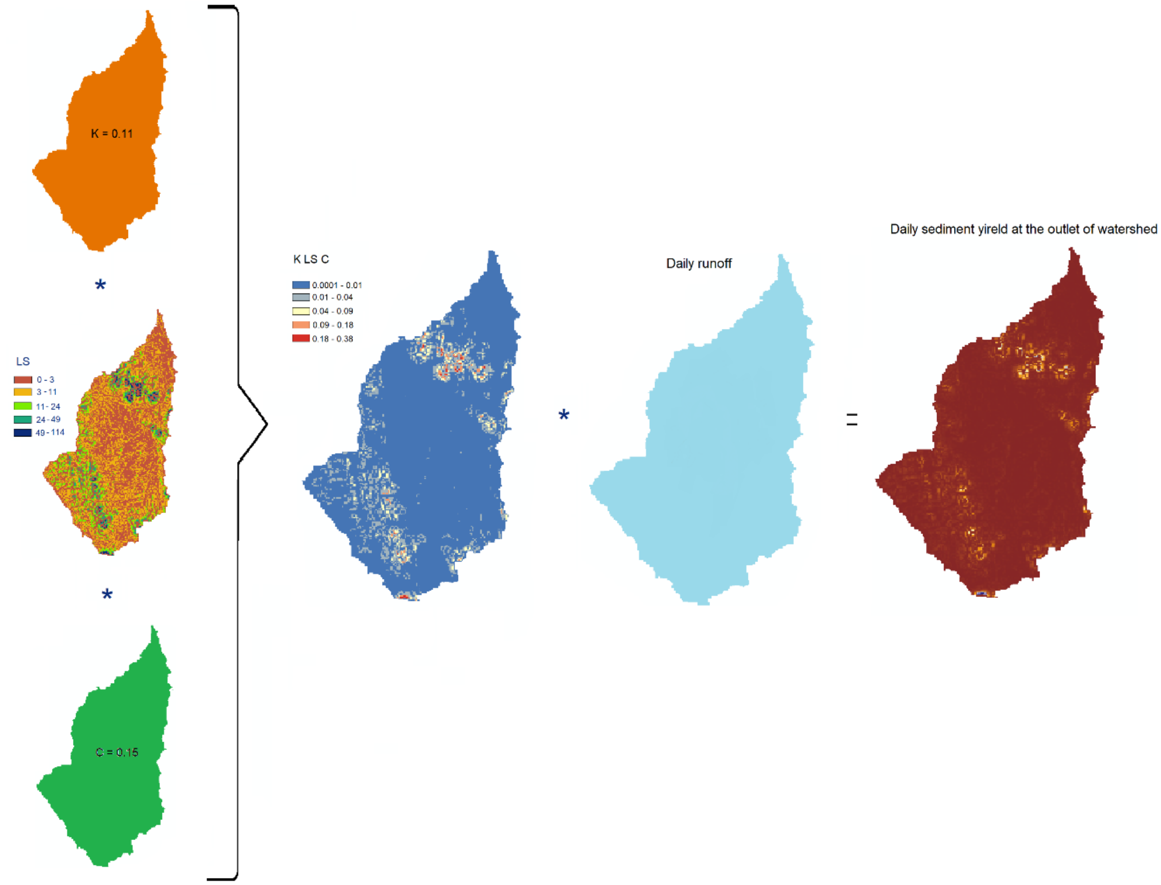

Figure 6-2. Procedure for obtaining daily sediment yield: A combined raster (K×LS×C) was multiplied by daily runoff, and cell values were summed to calculate total sediment yield.

6.3. Results and discussion

6.3.1. Water Balance

The Potential Evapotranspiration (PET) and Actual Evapotranspiration (AET), used for determining soil moisture variations and being able to assign CN accordingly, are summarized in Table 6-2, along with the estimated soil moisture and peak discharge. The average PET was 12.12 mm, with a range from 0 to 21.43 mm. Ruíz Álvarez et al. (2018) estimated PET through Penman-Monteith (Monteith, 1965), PET monthly values were around 110 mm for the coldest months, and 220 mm for the warmest months. These findings are equivalent to approximately 3.33 and 7.33 mm daily, respectively, which may reflect higher accuracy in their estimations due to inclusion of more parameters in PET estimation, like wind speed and vapour pressure. Lower values of PET can lead to higher soil moisture levels because more water remains in the soil, then if rainfall occurs and depending on the amount, can conclude in runoff. The mean AET was 3.97 mm, varying from 0 to 19.82 mm. AET represents the moisture actually used by plants and evaporated from the soil. The variability in AET indicates fluctuations in moisture availability and plant water use efficiency.

Under the current study conditions, where PET and AET influence soil moisture dynamics, the mean soil moisture was 82.45 mm, ranging between the wilting point (78 mm) and field capacity (150 mm). In general, lower PET values result in reduced atmospheric demand for water, leading to slower soil moisture depletion and better retention of water within the soil profile. If we adopt the PET values suggested by Ruíz Álvarez et al. (2018), with daily PET ranging from 3.33 mm on the coldest days to 7.33 mm on the warmest days, the slower rate of moisture loss would allow soil moisture to accumulate more effectively, potentially keeping the soil moisture closer to field capacity for longer periods after rainfall. However, runoff would only occur when rainfall exceeds the soil's saturation point, meaning lower PET values do not directly cause faster runoff but rather allow for more efficient moisture retention until the soil becomes saturated.

Table 6-1. Summary of estimated input data for sediment yield calculation. Only days with precipitation were included.

	Mean	**Median**	**SD**	**Min**	**Max**
Soil Moisture (mm)	82.45	78	9.95	78.00	150.00
Actual Evapotranspiration (AET) (mm)	3.97	0	5.65	0.00	19.82
Precipitation (PCP) (mm)	9.49	7	8.92	0.10	80.00
Potential Evapotranspiration (PET) (mm)	12.12	12.45	3.54	0	21.43
Runoff Coefficient	0.02	0.01	0.03	0.00004	0.21

Peak Discharge (m^3)	0.0003	0.0001	0.0004	0.0000006	0.003

The runoff coefficient in our study appears relatively low compared to McCuen's (2017) recommendations for cultivated lands, which suggest values between 0.11 and 0.21 for similar soil conditions. However, a regional study conducted by CONAGUA (2024) reported a runoff coefficient of 0.07, calculated using an indirect method (CONAGUA, 2000). In a research from a nearby region, Loyer et al. (2000) noted that runoff coefficient of 10% is considered high for this area. Our data shows low values (mean of 0.02), though some fall within the expected range.

6.3.2. Runoff estimation based on SCS-CN

As described in the methodology section, the potential maximum retention (S) is crucial in determination of runoff, the estimated S was around 129 mm, being the lowest 123 mm in dry AMC and the highest 130.91 mm in wet AMC during the time series of the study. And CN of 65.98 for dry AMC and 67.33 for wet AMC (Table 6-2). These values originated a mean runoff of 1.18 mm, with minimum and maximum values of 0.001 and 17.16 mm, respectively.

There are several studies on the implementation of CN in regions similar to ours. For example, Sánchez Cohen et al. (2003) conducted direct measurements of runoff and rainfall in a 47-hectare basin and estimated a standard CN of 82.21, with an S value of 41.88 mm for a 2-year return period, increasing to 137.32 mm for a 30-year return period. Our CN values were lower (Table 6-2), regarding HS treatment, suggesting lower runoff potential and higher retention. This difference is likely due to slope variations, as soil properties and vegetation are comparable. Although our rainfall intensity was higher (see Figure 4-4), it did not significantly increase the CN because in controlled experiments with smaller plots and gentler slopes (2.8%), infiltration often occurs more rapidly, limiting runoff despite the intense rainfall. Additionally, the smaller scale and uniformity of the plots allow for more consistent infiltration, while larger watersheds, with steeper slopes and natural heterogeneity, often generate more runoff, resulting in higher CN values even under lower rainfall intensities (Morgan and Kirkby, 1980).

In a study conducted near our research area, Velásquez-Valle et al. (2013) performed rainfall simulation experiments under conditions similar to ours in terms of soil type and rainfall intensity. They estimated CN values ranging from 79 for pastures to 89 for abandoned lands. Compared to our findings, their CN values were higher for treatments without tillage, such as our No Crop and Handspike treatments, but were more closely aligned with the other treatments. Their estimates were based solely on wet AMC conditions, which typically produce higher CN values compared to dry AMC conditions. This pattern is also evident in our results, where the mean CN for dry AMC was 75, while for wet AMC it was 81.6 (Table 6-2).

Table 6-2. S and CN estimated at hillslope scale

Treat	Rep	Dry AMC			Wet AMC		
		Runoff (mm)	**S**	**CN**	**Runoff (mm)**	**S**	**CN**
NC	1	193.35	37.60	87.11	102.67	180.80	58.42
NC	2	158.21	80.59	75.91	200.29	30.31	89.34
NC	3	161.74	75.73	77.03	186.89	44.69	85.04
NC	4	178.48	54.44	82.35	198.20	32.46	88.67
CT	1	185.13	46.69	84.47	112.44	159.03	61.50
CT	2	144.17	101.34	71.48	155.45	84.48	75.04
CT	3	148.17	95.17	72.74	185.35	46.43	84.54
CT	4	174.29	59.52	81.02	189.59	41.69	85.90
CTR	1	167.63	67.93	78.90	213.25	17.58	93.53
CTR	2	141.72	105.23	70.71	205.35	25.21	90.97
CTR	3	127.31	129.85	66.17	184.58	47.31	84.30
CTR	4	140.20	107.67	70.23	156.00	83.70	75.21
HS	1	165.88	70.21	78.34	131.00	123.22	67.33

HS	2	127.52	129.47	66.24	225.22	6.72	97.42
HS	3	126.73	130.91	65.99	187.22	44.32	85.14
HS	4	152.44	88.83	74.09	184.13	47.82	84.15

6.3.3. Sediment Yield

Sediment yield was consistent with the extreme rainfall events recorded (Figure 6-3), reflecting the effectiveness of the model in capturing the impact of precipitation on soil moisture dynamics and sediment yield estimation. The estimated sediment yield in our study ranged from 0.00000119 to 0.028 t/ha, with a mean of 0.0000097 t/ha. The maximum sediment yield in our study (0.028 t/ha) was higher than that observed by Mauricio-Pérez et al. (2023) in a nearby 1.5 km² basin located 50 km from our study area, where the maximum yield was 0.0005 t/ha. However, the average yield in our study was lower overall. In their study, runoff began with 6 mm of rainfall, and 10 mm of precipitation produced 0.1 mm of runoff; in the previous year, the same rainfall produced 0.99 mm, highlighting the significant effects of changes in soil management practices. While sediment load was not directly measured in the previous year, rainfall simulation showed higher soil losses under changed soil practices, suggesting this trend could extend to the watershed scale. However, the initial increase in erosion following tillage is often followed by stabilization, indicating that short-term effects could mask longer-term outcomes. It is likely that sediment load values in the previous year were much higher, but our estimates would still exceed those.

In another study of the Tijuana River watershed along the US-Mexico border, Biggs et al. (2022) reported a mean suspended sediment yield of 1.19 t/ha/year, which they noted as low compared to southern California watersheds with yields of 50 t/ha/year. Although the Tijuana River basin is largely urban, the study provides a reference for evaluating the accuracy of our model. In comparison, our results were considerably lower than those observed in their study.

Furthermore, Casabella-González et al. (2023), estimated sediment yield using the improved MPSIAC empirical model in three watershed in the north-central Mexican state of San Luis Potosí. In their most conservative scenario, sediment yield varied from 0.56 to 9.77 t/ha, while in the most adverse scenario, estimates ranged from 0.58 to 73.36 t/ha.

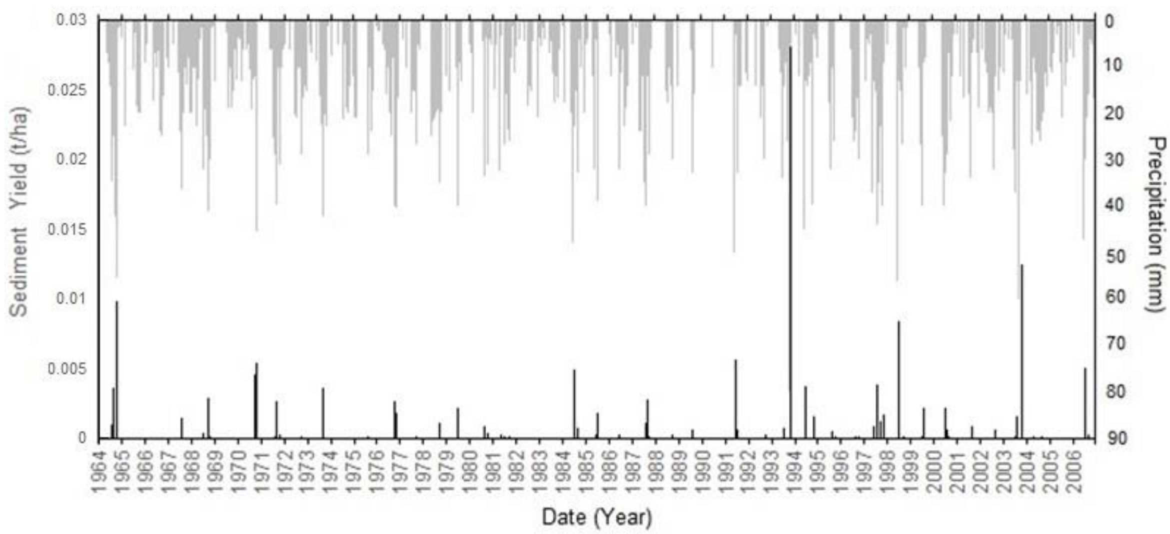

Figure 6-3. Sediment yield and rainfall over the study period in the watershed

To better describe the relationship between sediment yield and precipitation, we fit a third-order polynomial regression (Figure 6-4). Sediment yield begins after approximately 30 mm of precipitation, below which no significant yield occurs. As precipitation increases, sediment yield rises slowly at first but then accelerates due to the cubic term in the model indicating a nonlinear relationship, where sediment yield peaks at a certain precipitation level before tapering off at very high levels. The negative quadratic coefficient suggests that at very high precipitation levels, the rate of sediment yield growth slows slightly.

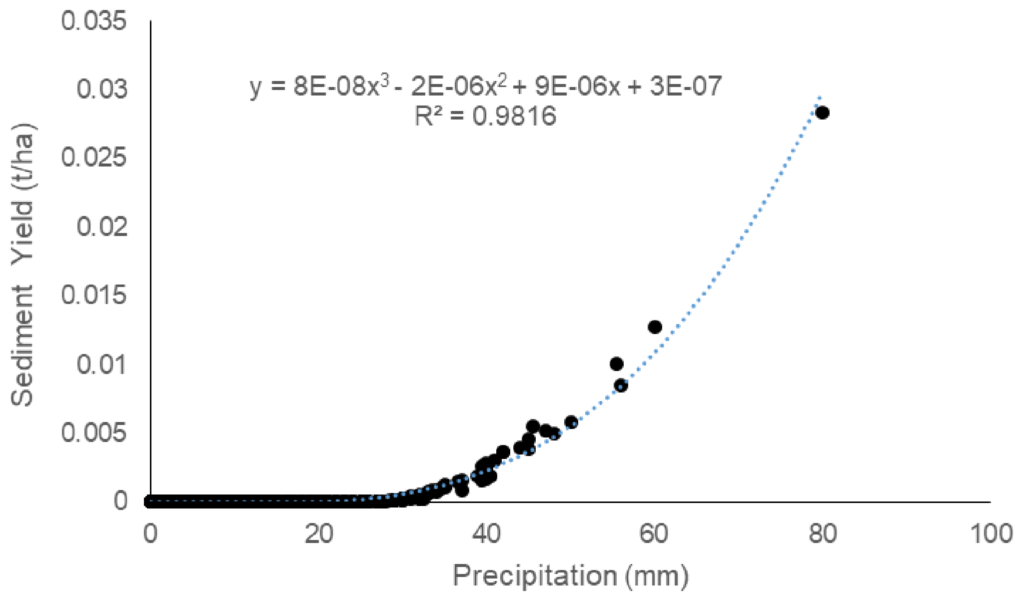

Figure 6-4. Sediment yield response to rainfall in the studied watershed.

6.4. Conclusions

The study successfully linked hillslope measurements to broader watershed-scale predictions, providing valuable insights for erosion management in data-scarce regions, providing Curve Number (CN) values for obtaining runoff to further parameterized the MUSLE for sediment yield prediction. Curve Numbers (CN) were adjusted daily based on soil moisture dynamics and precipitation variability adjusted based on a water balance.

The MUSLE model effectively captured non-linear relationships between precipitation and sediment yield, showing a significant impact of extreme rainfall events; however, it tended to overestimate yield during these extremes. This highlights the need for careful selection and refinement of erosion models to reflect specific agricultural practices and environmental conditions and to enhance accuracy under extreme scenarios.

These conclusions support more effective conservation planning and soil management strategies, which are essential for sustainable watershed management. Future research should prioritize understanding long-term erosion impacts and improving soil consolidation strategies to strengthen erosion control efforts in arid regions.

References

Beven, K., 2012.Data for Rainfall–Runoff Modelling. In: Rainfall-Runoff Modelling. pp. 51–82.

Biggs, T., Zeigler, A., Taniguchi-Quan, K.T., 2022.Runoff and sediment loads in the Tijuana River: Dam effects, extreme events, and change during urbanization.Journal of Hydrology: Regional Studies., 42, 101162.

Boardman, J., Poesen, J., 2006.Soil Erosion in Europe: Major Processes, Causes and Consequences. In: Soil Erosion in Europe. pp. 477–487.

Bueno-Hurtado, P., Seidou, O., 2024.Empirical and physical modelling of soil erosion in agricultural hillslopes.Journal of Hydrology and Hydromechanics., 72, 279–291.

Casabella-González, M.J., Borselli, L., García-Meza, J. V., 2023.Improved MPSIAC model for soil erosion rate assessment in semiarid zones.Journal of Arid Environments., 212.

CONAGUA, 2000.Norma Oficial Mexicana NOM-011-CNA-200: Conservación del recurso agua.

CONAGUA, 2020.Weather database [WWW Document]. URL https://smn.conagua.gob.mx/tools/RESOURCES/Diarios/10008.txt

CONAGUA, 2024.Actualización de la disponibilidad media anual de agua en el acuifero de la victoria (1012), estado de Durango.

Galindo, M.S., Reynoso, D.S.F., Menes, M.M., Granados, E.R., Berber, J.D.R., 2017.Modelo hidrológico de la cuenca del río Sordo, Oaxaca, México, con SWA.Tecnologia y Ciencias del Agua., 8, 141–156.

Hershfield, D.M., 1961.Rainfall Frequency Atlas of the United States, for Durations from 30 Minutes to 24 Hours and Return Periods from 1 to 100 Years, Technical Paper No. 40.

INEGI, 2019.Continuo de Elevaciones Mexicano (CEM) [WWW Document].National Institute of Geography, Statistics and Informatics. URL https://www.inegi.org.mx/app/geo2/elevacionesmex/

Lal, R., 2001.Soil degradation by erosion.Land Degradation & Development., 12, 519–539.

Loyer, J.Y., Estrada, J.. A., Descroix, L., González Barrios, J.L., 2000.Uso y Manejo del Agua en las Cuencas Hidrograficas del norte de Mexico.Folleto Científico No. 12 del Proyecto Franco-Mexicano IRD, INIFAP-CENID RASPA., 57.

Mauricio-Pérez, A.M., Sánchez-Cohen, I., Pedroza-Sandoval, A., Velásquez-Valle, M.A., 2023.Land imprinter hydrological impacts for grasslands in a watershed with natural rainfall and rainfall simulation, Tecnologia y Ciencias del Agua.

McCool, D.K., Foster, G.R., Mutchler, C.K., Meyer, L.D., 1989.Revised Slope Length Factor for the Universal Soil Loss Equation.Transactions of the American Society of Agricultural Engineers., 32, 1571–1576.

McCuen, R.H., 2017.Hydrologic Analysis and Design.4th Editio. ed. University of Maryland.

Merritt, W.S., Letcher, R.A., Jakeman, A.J., 2003.A review of erosion and sediment transport models.Environmental Modelling & Software., 18, 761–799.

Monteith, J.L., 1965.Evaporation and environment. In: The State Anf Movement of Water in Living Organisms (Symposia of the Society for Expetimental Biology. Cambridge University Press, pp. 205–234.

Morgan, R.P.C., Kirkby, M.J., 1980.Soil erosion. Wiley.

Nearing, M.A., Jetten, V., Baffaut, C., Cerdan, O., Couturier, A., Hernandez, M., Le Bissonnais, Y., Nichols, M.H., Nunes, J.P., Renschler, C.S., Souchère, V., van Oost, K., 2005.Modeling response of soil erosion and runoff to changes in precipitation and cover.CATENA., 61, 131–154.

Pimentel, D., Kounang, N., 1998.Ecology of Soil Erosion in Ecosystems.Ecosystems., 1, 416–426.

Prado-Hernández, J.V., Rivera-Ruiz, P., DeLeón-Mojarro, B., Carrillo-García, M., Martínez-Ruiz, A., 2017.Calibration of the USLE and MUSLE soil loss models in a mexican forest watershed: El Malacate case study.Agrociencia., 51, 265–284.

Renard, K.G., Foster, G.R., Weesies, G.A., McCool, D.K., Yoder, D.C., 1997.Predicting soil erosion by water: A guide to conservation planning with the Revised Universal Soil Loss Equation (RUSLE).

Ruíz Álvarez, O., Corrales Suastegui, A., González Jasso, L.A., Díaz García, L.A., Narváez Mendoza, M.P., Ontiveros Capurata, R.E., Ruíz Corral, J.A., 2018.Comportamiento espacio temporal de la evapotranspiración de referencia en la República Mexicana.Revista Mexicana de Ciencias Agrícolas., 1963–1976.

Sadeghi, S.H.R., Gholami, L., Khaledi Darvishan, A., Saeidi, P., 2014.A review of the application of the MUSLE model worldwide.Hydrological Sciences Journal., 59, 365–375.

Sánchez Cohen, I., Velázquez Valle, M., Jasso Ibarra, R., Gonzalez Barrios, J.L., 2003.Caracterización de la retención potencial máxima de humedad en el suelo del método SCS-CN. Aplicación a una cuenca de México.Ingenieria Hidraulica en Mexico., 18, 111–117.

USDA Soil Conservation Service, 1986.Urban Hydrology for Small Watersheds.

Velásquez-Valle, M.A., Esquivel-Arriaga, G., Sánchez-Cohen, I., Gutiérrez-Luna, R., Muñoz-Villalobos, J.A., Macías-Rodriguez, H., Bueno-Hurtado, P., 2013.Respuesta Hidrológica de Diferentes Usos del Suelo en las Zonas Áridas del Estado de Durango , México . Gómez Palacio, Durango.

Velásquez-Valle, M.A., Sánchez-Cohen, I., Esquivel-Arriaga, G., Bueno-Hurtado, P., Martínez-Burciaga, O.U., 2016.Aplicación de la MUSLE para predecir las pérdidas de suelo en una cuenca de pastizal al sur de Zacatecas, México. In: II Congreso Nacional de Riego y Drenaje COMEII. COMEII, Chapingo, Edo. de México, pp. 1–8.

Williams, J.R., 1975.Sediment-yield prediction with universal equation using runoff energy factor. In: Present and Prospective Technology for Predicting Sediment Yields and Sources. ARS, pp. 244–252.

Wischmeier, W.H., Smith, D.D., 1978.Predicting rainfall erosion losses - a guide to conservation planning.

CHAPTER 7. Conclusions

This thesis presents a comprehensive investigation into soil erosion processes and sediment yield modeling across hillslope and watershed scales, emphasizing the importance of conservation practices in arid regions. The chapters provide knowledge about erosion dynamics, model effectiveness, and the role of tillage and soil moisture in sediment transport, ultimately supporting soil and water conservation strategies.

The findings from Chapter 4 demonstrate that soil moisture and tillage practices significantly impact short-term erosion rates under high-intensity rainfall. The study revealed that under dry antecedent moisture conditions, both the Handspike and Conventional Tillage plus Residues treatments showed substantial reductions in erosion and runoff, underscoring the importance of maintaining crop residue cover and no-till practices. These results suggest that conservation-oriented tillage systems can mitigate soil loss, particularly when soil moisture is limited, offering practical guidance for erosion control in semi-arid agricultural areas. This is particularly relevant for rainfed systems, which dominate agricultural production in much of north-central Mexico and are highly susceptible to soil erosion due to the reliance on seasonal rainfall.

In Chapter 5, the comparative analysis of empirical and physical erosion models highlighted the strengths and limitations of the RUSLE and the WEPP for estimating erosion on agricultural hillslopes. RUSLE generally performed better across treatments, particularly when measured K factors and nationally recommended C factors were applied, while WEPP demonstrated reliable results only for certain tillage and moisture conditions, such as Conventional Tillage under wet AMC. These findings underscore RUSLE’s adaptability and accuracy for erosion estimation in similar semi-arid agricultural settings. Meanwhile, WEPP's detailed process-based approach highlights its potential for application in rainfed systems where erosion dynamics are influenced by soil, topography, and rainfall variability, though it may require precise calibration for specific conditions.

Chapter 6 extended sediment yield modeling to the watershed scale, applying the MUSLE with parameters derived from hillslope measurements to estimate daily sediment yield in an ungauged watershed. The integration of a water balance approach, incorporating Actual Evapotranspiration (AET) and Curve Numbers (CN), allowed for improved daily predictions that account for soil moisture variability. The study observed a nonlinear relationship between precipitation and sediment yield, with peak sediment yield occurring at specific rainfall thresholds before tapering off, indicating that MUSLE effectively captured general sediment trends. However, the model tended to overestimate yields during extreme rainfall events, emphasizing the need for refined sediment yield models that more accurately represent high-intensity precipitation scenarios. These findings are particularly relevant to rainfed systems, where soil erosion is strongly influenced by rainfall variability, but can also inform conservation practices in irrigated systems, where runoff from irrigation events might similarly contribute to sediment transport.

Bibliography

Aguirre-Salado, C.A., Miranda-Aragón, L., Pompa-García, M., Reyes-Hernández, H., Soubervielle-Montalvo, C., Flores-Cano, J.A., Méndez-Cortés, H., 2017.Improving Identification of Areas for Ecological Restoration for Conservation by Integrating USLE and MCDA in a GIS-Environment : A Pilot Study in a Priority Region Northern Mexico.International Journal of Geo-Information., 6, 17.

Alberto Ramos Castillo, L., Orozco Medina, I., 2020.Sediment production modelling in a basin with little information including the potential effects of climate change and land use change.Acta Universitaria., 30, 1–19.

Alberts, E.E., Nearing, M.A., Weltz, M.A., Risse, L.M., Pierson, F.B., Zhang, X.C., Laflen, J.M., Simanton, J.R., 1995.SOIL COMPONENT. In: USDA-Water Erosion Prediction Project (WEPP). National Soil Erosion Research Laboratory. NSERL Report No. 10, West Lafayette, IN, pp. 1–47.

Alewell, C., Borrelli, P., Meusburger, K., Panagos, P., 2019.Using the USLE: Chances, challenges and limitations of soil erosion modelling.International Soil and Water Conservation Research., 7, 203–225.

Bennett, H.H., 1931.The problem of Soil Erosion in the United States.Annals of the Association of American Geographers., XXI, 147–170.

Bolaños-González, M.A., Paz-Pellat, F., Cruz-Gaistardo, C.O., Argumedo-Espinoza, J.A.., Romero-Benítez, V.M., DelaCruz-Cabrera, J.C., 2016.Mapa de erosión de los suelos de México y posibles implicaciones en el almacenamiento de carbono orgánico del suelo.Terra Latinoamericana., 34, 271–288.

Borrelli, P., Alewell, C., Alvarez, P., Anache, J.A.A., Baartman, J., Ballabio, C., Bezak, N., Biddoccu, M., Cerdà, A., Chalise, D., Chen, S., Chen, W., De Girolamo, A.M., Gessesse, G.D., Deumlich, D., Diodato, N., Efthimiou, N., Erpul, G., Fiener, P., Freppaz, M., Gentile, F., Gericke, A., Haregeweyn, N., Hu, B., Jeanneau, A., Kaffas, K., Kiani-Harchegani, M., Villuendas, I.L., Li, C., Lombardo, L., López-Vicente, M., Lucas-Borja, M.E., Märker, M., Matthews, F., Miao, C., Mikoš, M., Modugno, S., Möller, M., Naipal, V., Nearing, M., Owusu, S., Panday, D., Patault, E., Patriche, C.V., Poggio, L., Portes, R., Quijano, L., Rahdari, M.R., Renima, M., Ricci, G.F., Rodrigo-Comino, J., Saia, S., Samani, A.N., Schillaci, C., Syrris, V., Kim, H.S., Spinola, D.N., Oliveira, P.T., Teng, H., Thapa, R., Vantas, K., Vieira, D., Yang, J.E., Yin, S., Zema, D.A., Zhao, G., Panagos, P., 2021.Soil erosion modelling: A global review and statistical analysis.Science of the Total Environment., 780.

Bravo-Espinosa, M., Fregoso-Tirado, L.E., Medina-Orozco, L.E., 2006.Parámetros de erosionabilidad del modelo WEPP para andosoles con uso pecuario en la cuenca del Lago de Pátzcuaro , Michoacán WEPP erodibility parameters for Andisols under rangeland use in the Patzcuaro Lake Watershed, Michoacan, Mexico.Técnica Pecuaria en México., 44, 129–141.

Campbell, D., Berry, L., 2008.Land degradation in Mexico: its extent and impact.

Cao, P., Lu, C., Yu, Z., 2018.Historical nitrogen fertilizer use in agricultural ecosystems of the contiguous United States during 1850 – 2015 : application rate , timing , and fertilizer types.Earth System Science Data., 969–984.

Contreras-Hinojosa, J., Volke-Haller, V., Oropeza-Mota, J., Rodríguez-Franco, C., Martínez-Saldaña, T., Martínez-Garza, Á., 2005.REDUCCIÓN DEL RENDIMIENTO DE MAÍZ POR LA EROSIÓN DEL SUELO EN YANHUITLÁN , OAXACA , MÉXICO Reduction of Maize Yield by Erosion in Yanhuitlan , Oaxaca , Mexico.Terra Latinoamericana., 23, 399–408.

Cotler, H., Cuevas, M.L., 2019.Adoption of soil conservation practices through knowledge governance: the Mexican experience.Journal of Soil Science and Environmental Management., 10, 1–11.

Cotler, H., López, C.A., Martínez-Trinidad, S., 2011.¿Cuánto nos cuesta la erosión de suelos? Aproximación a una valoración económica de la pérdida de suelos agrícolas en México.Investigación Ambiental., 3, 31–43.

FAO, 2019.Soil erosion: the greatest challenge to sustainable soil management. Rome.

FAO, ITPS, 2015.Status of the World's Soil Resources (SWSR) - Main Report. Rome, Italy.

Figueroa, S.B., Amante, A.O., Cortés, G.H.T., Pimentel, L.J., Osuna, E.S.C., Rodriguez, J.M.O., Morales, F.J.F., 1991.Manual de Predicción de Pérdidas de Suelos por Erosión. SARH.

Flanagan, D.C., Ii, J.C.A., Nicks, A.D., Nearing, M.A., Laflen, J.M., 1995.OVERVIEW OF THE WEPP EROSION PREDICTION MODEL. In: USDA-Water Erosion Prediction Project. U.S. Department of Agriculture, West Lafayette, IN, pp. 1–12.

Flores-López, H.E., Martínez-Menes, M., Oropeza-Mota, J.L., Mejía-Saens, E., Carrillo-González, R., 2003.Integración De La Eups a Un Sig Para Estimar La Erosión Hídrica Del Suelo En Una Cuenca Hidrográfica De Tepatitlán, Jalisco, México.Terra Latinoamericana., 21, 233–244.

Foster, G.R., Flanagan, D.C., Nearing, M.A., Lane, L.J., Risse, L.M., Finkner, S.C., 1995.HILLSLOPE EROSION COMPONENT. In: USDA-Water Erosion Prediction Project (WEPP). National Soil Erosion Research Laboratory. NSERL Report No. 10, West Lafayette, IN, pp. 1–12.

Foster, G.R., McCool, D.K., Renard, K.G., Moldenhauer, W.C., 1981.Conversion of the universal soil loss equation to SI metric units.Journal of Soil and Water Conservation., 36, 355–359.

Foster, G.R., Toy, T.E., Renard, K.G., 2003.Comparison of the USLE, RUSLE1.06c, and RUSLE2 for application to highly disturbed lands. In: Proceedings of the First Interagency Conference on Research in the Watersheds, Benson, Arizona. USDA - Agricultural Research Service, Wahington, DC, pp. 154–160.

Foster, G.R., Weesies, G.A., Renard, K.G., Yoder, D.C., McCool, D.K., Porter, J.P., 1997.Support Practice Factor (P). In: Renard, K.G., Foster, G.R., Weesies, G.A., McCool, D.K., Yoder, D.C. (Eds.): Predicting Soil Erosion by Water: A Guide to

Conservation Planning With the Revised Universal Soil Loss Equation (RUSLE). U.S. Department of Agriculture, Wahington, DC, pp. 183–222.

Friedrich, T., Derpsch, R., Kassam, A., 2017.Overview of the global spread of conservation agriculture.Field Actions Science Reports [Online]., 8, 53–68.

Galindo, M.S., Reynoso, D.S.F., Menes, M.M., Granados, E.R., Berber, J.D.R., 2017.Modelo hidrológico de la cuenca del río Sordo, Oaxaca, México, con SWA.Tecnologia y Ciencias del Agua., 8, 141–156.

González-Arqueros, M.L., Mendoza, M.E., Vázquez-selem, L., 2017.Catena Human impact on natural systems modeled through soil erosion in GeoWEPP : A comparison between pre-Hispanic periods and modern times in the Teotihuacan Valley (Central Mexico).Catena., 149, 505–513.

González-Morales, S.B., Mayer, A., Ramírez-Marcial, N., 2018.Assessment of soil erosion vulnerability in the heavily populated and ecologically fragile communities in Motozintla de Mendoza, Chiapas, Mexico.Solid Earth., 9, 745–757.

Gutierrez-Lopez, R., MUCIÑO-PORRAS, J.J., ARELLANO-MONTERROSAS, J.L.L., GUICHARD-ROMERO, D.D.E.L.R., AGUILAR-SUÁREZ, M.Á., 2021.Estimation of Water Erosión and the Transportation of Sediments in the Upper Basin df Cuxtepeques River, Chiapas, Mexico. X1 - Estimación de la Erosión Hídrica y el Transporte de Sedimentos en la Cuenca Superior del Río Cuxtepeques, Chiapas, México.Revista EIA., 18, 173–186.

Jetten, V.G., Maneta, M.P., 2011.Calibration of Erosion Model. In: Morgan, R.P.C., Nearing, M.A. (Eds.): Handbook of Erosion Modelling. Blackwell Publishing Ltd.

Larose, M., Oropeza-Mota, J.L., Norton, D., Turrent-Fernández, A., Martínez-Menes, M., Pedraza-Oropeza, J.A., Francisco-Nicolás, N., 2004.Application of the WEPP model to hillside lands in the Tuxtlas, Veracruz, México.Agrociencia., 38, 155–163.

Lianes Revilla, E., 2008.Estudio del factor vegetación "C" de la ecuación universal de pérdidas de suelo revisada "RUSLE" en la cuenca del río Birrís (Costa Rica). Universidad Politécnica de Madrid.

López-García, E.M., Torres-Trejo, E., López-Reyes, L., Flores-Domínguez, Á.D., Peña-Moreno, R.D., López-Olguín, J.F., 2020.Estimation of soil erosion using USLE and GIS in the locality of Tzicatlacoyan , Puebla , México.Soil and Water Research., 15, 9–17.

Martínez-Rivera, L.M., 2004.Watershed management to control pollution in the Ayuquila river, Jalisco, México. Utah State University.

McCool, D.K., Foster, G.R., Weesies, G.A., 1997.Slope length and steepness factors (LS). In: Renard, K.G., Foster, G.R., Weesies, G.A., McCool, D.K., Yoder, D.C. (Eds.): Predicting Soil Erosion by Water: A Guide to Conservation Planning With the Revised Universal Soil Loss Equation (RUSLE). Agriculture Handbook No. 703. US Department of Agriculture, Wahington, DC, pp. 101–118.

Montes-León, M.A.L., Uribe-Alcántara, E.M., García-Celis, E., 2011.Mapa nacional de erosión potencial.Tecnologia y Ciencias del Agua., 2, 5–17.

Nearing, M.A., 2013.Soil erosion and conservation. In: Wainwright, J., Mullingan, M. (Eds.): Environmental Modelling: Findings Simplicity in Complexity. John Wiley & Sons, Ltd, pp. 365–378.

Panagos, P., Standardi, G., Borrelli, P., Emanuele, L., Montanarella, L., Bosello, F., 2018.Cost of agricultural productivity loss due to soil erosion in the European Union : From direct cost evaluation approaches to the use of macroeconomic models.Land Degradation & Development., 29, 471–484.

Pandey, A., Himanshu, S.K., Mishra, S.K., Singh, V.P., 2016.Physically based soil erosion and sediment yield models revisited.Catena., 147, 595–620.

Patil, R.J., 2018.Spatial techniques for soil erosion estimation: remote sensing and GIS approach. Springer, Cham.

Pedraza-Villafaña, A., 2015.Estimación de la erosión hídrica mediante dos métodos de la Ecuación Universal de Pérdida de Suelo (EUPS) de la cuenca del Río Chapingo, Texcoco. Universidad Atónoma del Estado de México.

Pimentel, D., Harvey, C., Resosudarmo, P., Sinclair, K., Kurz, D., Mcnair, M., Shpritz, L., Fitton, L., Saffouri, R., Blair, R., Pimentel, D., Harvey, C., Resosudarmo, P., Sinclair, K., Kurz, D., Mcnair, M., Crist, S., Shpritz, L., Fitton, L., Saffouri, R., Blair, R., 1995.Environmental and Economic Costs of Soil Erosion and Conservation Benefits.Science., 267, 1117–1123.

Prado-Hernández, J.V., Rivera-Ruiz, P., DeLeón-Mojarro, B., Carrillo-García, M., Martínez-Ruiz, A., 2017.Calibration of the USLE and MUSLE soil loss models in a mexican forest watershed: El Malacate case study.Agrociencia., 51, 265–284.

Rai, R.K., Singh, V.P., Upadhyay, A., 2017.Chapter 4 - Hydrologic Computations. In: Rai, R.K., Singh, V.P., Upadhyay, A. (Eds.): Planning and Evaluation of Irrigation Projects. Academic Press, pp. 83–229.

Ramírez-León, J.M., 2009.Producción de sedimentos en cuencas: revisión de criterios y aplicabilidad a la cuenca del rio Apulco. Universidad Nacional Autónoma de México.

Renard, K.G., Foster, G.R., Weesies, G.A., Porter, J.P., 1991.RUSLE: revised universal soil loss equation.Journal of Soil & Water Conservation., 46, 30–33.

Renard, K.G., McCool, D.K., Cooley, K.R., Foster, G.R., Istok, J.D., Mutchler, C.K., 1997.Rainfall-Runoff Erosivity Factor (R). In: Renard, K.G., Foster, G.R., Weesies, G.A., McCool, D.K., Yoder, D.C. (Eds.): Predicting Soil Erosion by Water: A Guide to Conservation Planning With the Revised Universal Soil Loss Equation (RUSLE). Agriculture Handbook No. 703. US Department of Agriculture., Washington, D.C., pp. 19–38.

Romkens, M.J.M., Young, R.. A., Poesen, J.W.A., McCool, D.K., El-Swaify, S.A., Bradford, J.M., 1997.Soil Erodibility Factor (K). In: Renard, K.G., Foster, G.R., Weesies, G.A., McCool, D.K., Yoder, D.C. (Eds.): Predicting Soil Erosion by Water: A Guide to Conservation Planning With the Revised Universal Soil Loss Equation

(RUSLE). Agriculture Handbook No. 703, US Department of Agriculture, Washington, D.C., pp. 65–99.

Sadeghi, S.H.R., Gholami, L., Khaledi Darvishan, A., Saeidi, P., 2014.A review of the application of the MUSLE model worldwide.Hydrological Sciences Journal., 59, 365–375.

SEMARNAT-CP, 2003.Memoria Nacional 2001- 2002. Evauación de la degradación del suelo causada por el hombre en la rapublica mexicana escala 1:250000.

Silva, A., Ponce de León, J., García, F., Durán, A., 1988.Aspectos metodológicos en la determinación de la capacidad de retener agua de los suelos de Uruguay.Boletín de investigación 10.

Simonian, L., 1995.Defending the Land of the Jaguar.

Smith, A., 1917.Relation of the mechanical analysis to the moisture equivalent of soils.Soil Science., 471–476.

Stott, D.E., Alberts, E.E., Weltz, M.A., 1995.RESIDUE DECOMPOSITION AND MANAGEMENT. In: USDA-Water Erosion Prediction Project (WEPP). National Soil Erosion Research Laboratory. NSERL Report No. 10, West Lafayette, IN, pp. 1–16.

Tetteh, E.N., Abunyewa, A.A., Tuffour, H.O., Berchie, J.N., Acheampong, P.P., Twum-Ampofo, K., Dawoe, E., Logah, V., Agbenyega, O., Ennin, S.A., Nunoo, I., Melenya, C., Danquah, E.O., Barnes, V.R., Partey, S.T., 2019.Rubber and plantain intercropping: Effects of different planting densities on soil characteristics.PLoS ONE., 14, 1–17.

Velásquez-Valle, M.A., Sánchez-Cohen, I., Esquivel-Arriaga, G., Bueno-Hurtado, P., Martínez-Burciaga, O.U., 2016.Aplicación de la MUSLE para predecir las pérdidas de suelo en una cuenca de pastizal al sur de Zacatecas, México. In: II Congreso Nacional de Riego y Drenaje COMEII. COMEII, Chapingo, Edo. de México, pp. 1–8.

Wang, B., Zheng, F., Guan, Y., 2016.Improved USLE- K factor prediction : A case study on water erosion areas in China.International Soil and Water Conservation Research., 4, 168–176.

Williams, J.R., 1975.Sediment-yield prediction with universal equation using runoff energy factor. In: Present and Prospective Technology for Predicting Sediment Yields and Sources. ARS, pp. 244–252.

Wischmeier, W.H., Smith, D.D., 1978.Predicting rainfall erosion losses - a guide to conservation planning.

Yoder, D.C., Porter, J.P., Laflen, J.M., Simanton, J.R., Renard, K.G., McCool, D.K., Foster, G.R., 1997.Cover-Management Factor (C). In: Renard, K.G., Foster, G.R., Weesies, G.A., McCool, D.K., Yoder, D.C. (Eds.): Predicting Soil Erosion by Water: A Guide YODER DC, PORTER JP, LAFLEN JM, SIMANTON JR, RENARD KG, MCCOOL DK and FOSTER GR (1997) Cover-Management Factor (C). In: RENARD KG, FOSTER GR, WEESIES GA, MCCOOL DK and YODER DC (Eds.) Predicting Soil Erosion by Wa. U.S. Department of Agriculture, Wahington, DC, pp. 143–167.

Zingg, A.W., 1940.Degree and length of land slope as it affects soil loss in run-off.Agric. Engng., 21, 59–64.